Supplementary Information (SI) for Inorganic Chemistry Frontiers.

Cationic Polypnictogen Complexes as Building Blocks for Novel Ferrocenes

Maximilian Widmann, Zihan Zhang, Anja Rehse, Dr. Gábor Balázs, Prof. Dr. Alexey Y. Timoshkin, Prof. Dr. Karsten Meyer, Prof. Dr. Rainer Winter and Prof. Dr. Manfred Scheer

Contents

1 Synthesis and Analytical Data

1.1 General Considerations

All manipulations were carried out using standard Schlenk techniques at a Stock apparatus under N_2 as an inert gas or in a glove box with Ar atmosphere. All glassware was dried with a heat gun (600 °C) for at least 30 minutes prior use. 1,2-Difluorobenzene (*o*-DFB) was distilled from P_4O_{10}, C_6D_6 and Tol-d^8 were distilled from NaK, CD_2Cl_2 was distilled from CaH_2 and other solvents were directly taken from an MSBraun SPS-800 solvent purification system and degassed at room temperature. Solution ^1H (400.130 MHz), ^{19}F (376.498 MHz), ^{31}P (161.976 MHz), NMR spectra were recorded at an Avance400 (Bruker) spectrometer using $(H_3C)_4Si$ (^1H), $CFCl_3$ (^{19}F), or 85% phosphoric acid (^{31}P), respectively, as external standards. Chemical shifts (δ) are provided in parts per million (ppm) and coupling constants (J) are reported in Hertz (Hz). Chemical shifts and coupling constants for all $^{31}P\{^1H\}$ and ^{31}P NMR spectra were derived from spectral simulation using the built-in simulation package of TopSpin4.1.4. The following abbreviations are used: s = singlet, d = doublet, dd = doublet of doublets, ddd = doublet of doublets of doublets, dddd = doublet of doublets of doublets of doublets, dt = doublet of triplets, t = triplet, m = multiplet, and br = broad. LIFDI, FD and ESI mass spectra were recorded at the internal mass spectrometry department using a Jeol AccuTOF GCX mass spectrometer (LIFDI, FD) or ThermoQuest Finnigan TSQ 7000 mass spectrometer (ESI) and peak assignment was performed using the Molecular weight calculator 6.50.[1] Elemental analysis of the products was conducted by the elemental analysis department at the University of Regensburg using an Elementar Vario EL. The starting materials [Cp*Fe(η^5-P_5)][2] and [[Cp*Fe(η^5-P_5Me)][OTf] (**A**)[3] and [Thia][FAl][4] ([FAl]$^-$ = [$C_{36}H_{46}AlO_3$]$^-$) were synthesised following literature procedures. All other chemicals were purchased from commercial vendors and used without further purification.

1.2 [Cp*Fe(η^4-P$_5$Me(C$_5$H$_4$^{t}Bu)] (1)

A Schlenk flask, equipped with an efficient stir bar, was loaded with [Cp*FeP$_5$Me][OTf] (0.20 g, 0.40 mmol, 1.00 equiv.) and NaCp´ (0.06 g, 0.40 mmol, 1.00 equiv.), suspended in Et$_2$O (approx. 15 mL). The suspension was stirred for 16 h at room temperature. Next, SiO$_2$ was added and the solvent was removed under reduced pressure. The preadsorbed reaction mixture was purified via column chromatography (SiO$_2$, *n*-hexane, 10 x 3 cm). Using *n*-hexane, **1** could be eluated as a brownish fraction. For further purification, **1** was crystallized from a concentrated solution of *n*-hexane at −30°C. **1** could be obtained as light green/brown crystals.

Yield: 50 mg (26 %).

Elemental Analysis: C$_{20}$H$_{31}$FeP$_5$.

calc (%) for C$_{20}$H$_{31}$FeP$_5$: C: 49.82, H: 6.48.

found (%): C: 49.90, H: 6.48.

FD-MS (Toluene): *m/z* (%) = 482.04 (100 %) [Cp*Fe(η^4-P$_5$Me(C$_5$H$_4$^{t}Bu)]$^+$ (M$^+$), 841.99 (19 %) unidentified decomposition/aggregation product.

1 shows significant isomerization. Neither by column chromatography nor by selective crystallization, **1** could be obtained as isomerically pure compound. Because of this isomerization, a detailed and exact analysis of the NMR spectroscopic data by simulation is not possible due to overlapping resonances.

^{1}H NMR (400 MHz, C$_6$D$_6$, 298 K): δ [ppm] = 0.75 (s, 9 H, ^{t}Bu), 1.66 (s, 15 H, Cp*), 1.97 (m, 3 H, Me), 2.56 (s, 2 H, Cp-H), 5.64 (s, 2 H, Cp-H).

^{31}P{^{1}H} NMR (162 MHz, C$_6$D$_6$, 298 K): δ [ppm] = −98.2 (m, 2 P, P$^{X/X´}$), 36.7 (m, 2 P, P$^{M/M´}$), 110.6 (m, 1 P, P^A).

^{31}P NMR (162 MHz, C$_6$D$_6$, 298 K): δ [ppm] = −98.2 (m, 2 P, P$^{X/X´}$), 36.7 (m, 2 P, P$^{M/M´}$), 110.6 (m, 1 P, P^A).

1.3 [Cp*Fe(η⁴-P₅Me(C₅H₃ᵗBu₂)] (2)

A Schlenk flask, equipped with an efficient stir bar, was loaded with [Cp*FeP$_5$Me][OTf] (0.10 g, 0.20 mmol, 1.00 equiv.) and NaCp´´ (0.4 g, 0.20 mmol, 1.00 equiv.), suspended in Et_2O (approx. 15 mL). The suspension was stirred for 16 h at room temperature. Next, the solvent was removed in vacuo, the product was extracted with warm *n*-hexane (60 °C), and filtered via a frit (P4). For further purification, **2** was crystallized from a concentrated *n*-hexane solution at −30°C. **2** could be obtained as light brown/green crystals.

Yield: 50 mg (47 %).

Elemental Analysis: $C_{24}H_{39}FeP_5$.

calc (%) for $C_{24}H_{39}FeP_5 \cdot (C_6H_{14})_{0.2}$: C: 54.48, H: 7.58.

found (%): C: 54.53, H: 7.71.

According to the X-ray structure, depicted in Figure S2.2, even after intensive drying of the product, 0.2 equivalents of *n*-hexane were found to be incorporated in the product.

FD-MS (Toluene): *m/z* (%) = 538.11 (100 %) [Cp*Fe(η⁴-P$_5$Me(C$_5$H$_3$^{t}Bu$_2$)]$^+$ (M$^+$), 358.20 (65 %), [Cp*Fe(η⁴-P$_5$C]$^+$.

^{1}H NMR (400 MHz, Tol-d$_8$, 298 K): δ [ppm] = 0.96 (s, 9 H, ^{t}Bu), 1.08 (s, 9 H, ^{t}Bu), 1.52 (dt, $^2J_{P\text{-}H}$ = 7.9 Hz, 3 H, Me), 1.60 (s, 15 H, Cp*), 3.27 (d, $^2J_{P\text{-}H}$ = 15.9 Hz, 1 H, Cp´´-H), 5.65 (br, 1 H, Cp´´-H), 6.04 (s, 1 H, Cp´´-H).

^{31}P{^{1}H} NMR (162 MHz, Tol-d$_8$, 298 K): δ [ppm] = −93.9 (ddd, $^1J_{PX\text{-}PA}$ = 374.9 Hz, $^1J_{PX\text{-}PL}$ = 400.5 Hz, $^2J_{PX\text{-}PM}$ = 32.8 Hz, $^2J_{PX\text{-}PT}$ = 3.5 Hz 1 P, P^X); −70.9 (dddd, $^1J_{PT\text{-}PM}$ = 400.5 Hz, $^1J_{PT\text{-}PA}$ = 400.8 Hz, $^2J_{PT\text{-}PL}$ = 33.4 Hz, $^2J_{PT\text{-}PX}$ = 3.5 Hz, 1 P, P^T); 24.3 (dddd, $^1J_{PM\text{-}PT}$ = 400.5 Hz, $^1J_{PM\text{-}PL}$ = 378.8 Hz, $^2J_{PM\text{-}PA}$ = 11.9 Hz, $^2J_{PM\text{-}PX}$ = 32.8 Hz, 1 P, P^M); 41.1 (ddd, $^1J_{PL\text{-}PX}$ = 400.5 Hz, $^1J_{PL\text{-}PM}$ = 378.8 Hz, $^2J_{PL\text{-}PA}$ = 10.2 Hz, $^2J_{PL\text{-}PT}$ = 33.4 Hz, 1 P, P^L); 115.8 (ddd, $^1J_{PA\text{-}PX}$ = 374.9 Hz, $^1J_{PA\text{-}PT}$ = 400.8 Hz, $^2J_{PA\text{-}PM}$ = 11.9 Hz, $^2J_{PA\text{-}PL}$ = 10.2 Hz, 1 P, P^A).

^{31}P NMR (162 MHz, Tol-d$_8$, 298 K): δ [ppm] = −93.9 (ddd, $^1J_{PX\text{-}PA}$ = 374.9 Hz, $^1J_{PX\text{-}PL}$ = 400.5 Hz, $^2J_{PX\text{-}PM}$ = 32.8 Hz, $^2J_{PX\text{-}PT}$ = 3.5 Hz 1 P, P^X); −70.9 (dddd, $^1J_{PT\text{-}PM}$ = 400.5 Hz, $^1J_{PT\text{-}PA}$ = 400.8 Hz, $^2J_{PT\text{-}PL}$ = 33.4 Hz, $^2J_{PT\text{-}PX}$ = 3.5 Hz, 1 P, P^T); 24.3 (dddd, $^1J_{PM\text{-}PT}$ = 400.5 Hz, $^1J_{PM\text{-}PL}$ = 378.8 Hz, $^2J_{PM\text{-}PA}$ = 11.9 Hz, $^2J_{PM\text{-}PX}$ = 32.8 Hz, 1 P, P^M); 41.1 (ddd, $^1J_{PL\text{-}PX}$ = 400.5 Hz, $^1J_{PL\text{-}PM}$ = 378.8 Hz, $^2J_{PL\text{-}PA}$ = 10.2 Hz, $^2J_{PL\text{-}PT}$ = 33.4 Hz, 1 P, P^L); 115.8 (ddd, $^1J_{PA\text{-}PX}$ = 374.9 Hz, $^1J_{PA\text{-}PT}$ = 400.8 Hz, $^2J_{PA\text{-}PM}$ = 11.9 Hz, $^2J_{PA\text{-}PL}$ = 10.2 Hz, $^2J_{PA\text{-}H}$ = 7.9 Hz, 1 P, P^A).

1.4 [Cp*Fe(η^4-$P_5Me(C_5H_2{}^tBu_3)$)] (3)

A Schlenk flask, equipped with an efficient stir bar, was loaded with [Cp*Fe(η^5-P_5Me)][OTf] (0.13 g, 0.25 mmol, 1.00 equiv.) and $NaC_5H_2(^tBu)_3$ (0.10 g, 0.25 mmol, 1.00 equiv.), suspended in Et_2O (approx. 15 mL). The solution was stirred for 16 h at room temperature. Next, the solvent was removed in vacuo and the product was extracted with warm *n*-hexane (60 °C) and filtered via a frit (P4). For further purification, **3** was crystallized from a concentrated solution in *n*-hexane at −30 °C. **3** could be obtained as light brown/green crystals.

Yield: 60 mg (40 %).

Elemental Analysis: $C_{28}H_{47}FeP_5$.

calc (%) for $C_{28}H_{47}FeP_5$: C: 56.58, H: 7.97.

found (%): C: 56.71, H: 8.33.

FD-MS (Toluene): *m/z* (%) = 594.18 (100 %) [Cp*Fe(η^4-$P_5Me(C_5H_2{}^tBu_3)$)]$^+$ (M^+), 538.10 (7 %) [Cp*Fe(η^4-$P_5Me(C_5H_3{}^tBu_2)$)]$^+$, 610.17 (33 %) [Cp*Fe(η^4-$P_5Me(C_5H_2{}^tBu_3)O$]$^+$, 626.17 (13 %) [Cp*Fe(η^4-$P_5Me(C_5H_2{}^tBu_3)O_2$]$^+$.

^{1}H NMR (400 MHz, C_6D_6, 298 K): δ [ppm] = 0.85 (s, 9 H, ^{t}Bu), 1.33 (s, 18 H, ^{t}Bu), 1.57 (s, 15 H, Cp*), 2.29 (dd, $^2J_{P\text{-}H}$ = 7.3 Hz, 3 H, Me), 5.59 – 6.01 (br, 2 H, Cp-H).

^{31}P{^{1}H} NMR (162 MHz, C_6D_6, 298 K): δ [ppm] = −51.9 (m, $^1J_{PX\text{-}PA}$ = 409.8 Hz, $^1J_{PX\text{-}PA}$ = 409.8 Hz, $^1J_{PX'\text{-}PA}$ = 409.5 Hz, $^1J_{PX\text{-}PM}$ = 403.0 Hz, $^1J_{PX'\text{-}PM'}$ = 419.6 Hz, $^2J_{PX\text{-}PM'}$ = −32.2 Hz, $^2J_{PX'\text{-}PM}$ = −46.4 Hz, $^2J_{PX\text{-}PX'}$ = −0.2 Hz, 2 P, $P^{X/X'}$), 48.3 (m, $^1J_{PM\text{-}PX}$ = 403.0 Hz, $^1J_{PM'\text{-}PX'}$ = 419.6 Hz, $^1J_{PM\text{-}PM'}$ = 387.7 Hz, $^2J_{PM\text{-}PA}$ = 13.1 Hz, $^2J_{PM'\text{-}PA}$ = 12.8 Hz, $^2J_{PM\text{-}PX'}$ = −46.4 Hz, $^2J_{PM'\text{-}PX}$ = −32.2 Hz, 2 P, $P^{M/M'}$), 125.3 (m, $^1J_{PA\text{-}PX}$ = 409.8 Hz, $^1J_{PA\text{-}PX'}$ = 409.5 Hz, $^2J_{PA\text{-}PM}$ = 13.1 Hz, $^2J_{PA\text{-}PM'}$ = 12.8 Hz, 1 P, P^A).

^{31}P NMR (162 MHz, C_6D_6, 298 K): δ [ppm] = −51.9 (m, $^1J_{PX\text{-}PA}$ = 409.8 Hz, $^1J_{PX\text{-}PA}$ = 409.8 Hz, $^1J_{PX'\text{-}PA}$ = 409.5 Hz, $^1J_{PX\text{-}PM}$ = 403.0 Hz, $^1J_{PX'\text{-}PM'}$ = 419.6 Hz, $^2J_{PX\text{-}PM'}$ = −32.2 Hz, $^2J_{PX'\text{-}PM}$ = −46.4 Hz, $^2J_{PX\text{-}PX'}$ = −0.2 Hz, 2 P, $P^{X/X'}$), 48.3 (m, $^1J_{PM\text{-}PX}$ = 403.0 Hz, $^1J_{PM'\text{-}PX'}$ = 419.6 Hz, $^1J_{PM\text{-}PM'}$ = 387.7 Hz, $^2J_{PM\text{-}PA}$ = 13.1 Hz, $^2J_{PM'\text{-}PA}$ = 12.8 Hz, $^2J_{PM\text{-}PX'}$ = −46.4 Hz, $^2J_{PM'\text{-}PX}$ = −32.2 Hz, 2 P, $P^{M/M'}$), 125.3 (m, $^1J_{PA\text{-}PX}$ = 409.8 Hz, $^1J_{PA\text{-}PX'}$ = 409.5 Hz, $^2J_{PA\text{-}PM}$ = 13.1 Hz, $^2J_{PA\text{-}PM'}$ = 12.8 Hz, $^2J_{PA\text{-}H}$ = 7.3 Hz, 1 P, P^A).

1.5 [Cp*Fe(η^4-P$_5$Me(C$_5$Me$_4$H)] (4)

A Schlenk flask, equipped with an efficient stir bar was loaded with [Cp*Fe(η^5-P$_5$Me)][OTf] (0.26 g, 0.50 mmol, 1.00 equiv.) and LiC$_5$Me$_4$H (0.06 g, 0.50 mmol, 1.00 equiv.), suspended in Et$_2$O (approx. 15 mL). The suspension was stirred for 16 h at room temperature. After stirring, the solvent was removed in the vacuum and the product was extracted with warm *n*-hexane (60 °C), filtered via a frit (P4) and dried on the vacuum. For further purification, **4** was crystallized from a concentrated solution of *n*-hexane at −30 °C. **4** could be obtained as light brown/green crystals.

Yield: 120 mg (50 %).

Elemental analysis: $C_{20}H_{31}FeP_5$.

calc. (%) for $C_{20}H_{31}FeP_5$: C: 49.82, H: 6.48.

found (%): C: 50.03, H: 6.91.

FD-MS (Toluene): *m/z* (%) = 482.04 (100 %) [Cp*Fe(η^4-P$_5$Me(C$_5$Me$_4$H)]$^+$ (M$^+$).

^{1}H NMR (400 MHz, C$_6$D$_6$, 298 K): δ [ppm] = 1.36 (s, 6 H, Me-Cp), 1.38 (br, 3 H, Me-P), 1.62 (s, 15 H, Cp*), 1.80 (s, 6 H, Me-Cp), 2.78 (d, $^2J_{P\text{-}H}$ = 14 Hz, 1 H, Cp-H).

^{31}P{^{1}H} NMR (162 MHz, C$_6$D$_6$, 298 K): δ [ppm] = −100.4 (m, $^1J_{PX\text{-}PA}$ = 392.9 Hz, $^1J_{PX'\text{-}PA}$ = 391.5 Hz, $^1J_{PX\text{-}PM}$ = 395.1 Hz, $^1J_{PX'\text{-}PM'}$ = 407.5 Hz, $^2J_{PX\text{-}PX'}$ = 1.4 Hz, $^2J_{PX\text{-}PM'}$ = −30.2 Hz, $^2J_{PX'\text{-}PM}$ = −45.8 Hz, 2 P, P$^{X/X'}$), 32.7 (m, $^1J_{PM\text{-}PX}$ = 395.1 Hz, $^1J_{PM'\text{-}PX'}$ = 407.5 Hz, $^2J_{PM\text{-}PA}$ = 10.3 Hz, $^2J_{PM'\text{-}PA}$ = 12.0 Hz, $^1J_{PM\text{-}PM'}$ = 379.7 Hz, $^1J_{PM\text{-}PX'}$ = −45.8 Hz, $^1J_{PM'\text{-}PX}$ = −30.2 Hz, 2 P, P$^{M/M'}$), 121.8 (tt, $^1J_{PA\text{-}PX}$ = 392.9 Hz, $^1J_{PA\text{-}PX'}$ = 391.5 Hz, $^2J_{PA\text{-}PM}$ = 10.3 Hz, $^2J_{PA\text{-}PM'}$ = 12.0 Hz, 2 P, P^A).

^{31}P NMR (162 MHz, C$_6$D$_6$, 298 K): δ [ppm] = −100.4 (m, $^1J_{PX\text{-}PA}$ = 392.9 Hz, $^1J_{PX'\text{-}PA}$ = 391.5 Hz, $^1J_{PX\text{-}PM}$ = 395.1 Hz, $^1J_{PX'\text{-}PM'}$ = 407.5 Hz, $^2J_{PX\text{-}PX'}$ = 1.4 Hz, $^2J_{PX\text{-}PM'}$ = −30.2 Hz, $^2J_{PX'\text{-}PM}$ = −45.8 Hz, 2 P, P$^{X/X'}$), 32.7 (m, $^1J_{PM\text{-}PX}$ = 395.1 Hz, $^1J_{PM'\text{-}PX'}$ = 407.5 Hz, $^2J_{PM\text{-}PA}$ = 10.3 Hz, $^2J_{PM'\text{-}PA}$ = 12.0 Hz, $^1J_{PM\text{-}PM'}$ = 379.7 Hz, $^1J_{PM\text{-}PX'}$ = −45.8 Hz, $^1J_{PM'\text{-}PX}$ = −30.2 Hz, 2 P, P$^{M/M'}$), 121.8 (t, $^1J_{PA\text{-}PX}$ = 392.9 Hz, $^1J_{PA\text{-}PX'}$ = 391.5 Hz, $^2J_{PA\text{-}PM}$ = 10.3 Hz, $^2J_{PA\text{-}PM'}$ = 12.0 Hz, $^2J_{PA\text{-}Cp\text{-}H}$ = 14.0 Hz, $^2J_{PA\text{-}PA\text{-}P}$ = 7.0 Hz, 2 P, P^A).

1.6 [{Cp*Fe(η⁴-P₅Me(C₅H₃ᵗBu₂)}₂Fe] (5)

A Schlenk flask, equipped with an efficient stir bar was loaded with **2** (0.26 g, 0.48 mmol, 1.00 euqiv.), dissolved in THF (approx. 20 mL). The mixture was cooled down to –80 °C. To the solution, $KN(SiMe_3)_2$ (0.01 g, 0.48 mmol, 1.00 equiv.) in THF (approx. 15 mL) was slowly added. After addition, the solution was allowed to warm up to room temperature and was then left stirring for 16 h at room temperature. Next, the solvent was removed and the brownish green residue was washed with *n*-hexane (1x 20 mL) and was afterwards dried on the vacuum.

Next, the residue was dissolved in THF and $FeBr_2$·dme (0.08 g, 0.24 mmol, 0.50 equiv.) in THF (approx. 15 mL) was added. The reaction mixture was stirred for 15 h at room temperature. Next, SiO_2 was added and the solvent was removed under reduced pressure. The pre-adsorbed reaction mixture was purified via column chromatography (SiO_2, *n*-hexane/toluene 1:1, 10 x 3 cm). Using *n*-hexane/toluene (1:1), **5** could be eluted as brownish fraction. By firstly using pure *n*-hexane, **6** could be obtained as a brown band (*vide infra*). To selectively crystallize an isomerically pure compound, **5** was crystallized from a concentrated solution of *n*-hexane at −30°C. **5** could be obtained as green/brown crystals.

Note: Owing to the nearly identical solubility of **5**, isomerically pure **5** could only once be obtained by column chromatographic purification. In all other attempts, only the isomeric mixture was isolated, from which, however, small amounts of isomerically pure **5** could be obtained by selective crystallization.

Yield: 87 mg (32 %); crystallized, isomerically pure: few milligrams.

Elemental analysis: $C_{48}H_{76}Fe_3P_{10}$

calc. (%) for $C_{48}H_{76}Fe_3P_{10}$: C: 51.00; H: 6.78.

found (%): C: 55.40, H: 7.44.

According to single-crystal analysis and after intensive drying, 1.8 equiv. of *n*-hexane were found in the product.

FD-MS (Toluene): *m/z* (%) = 1130.12 (100 %) [{Cp*Fe(η⁴-P₅Me(C₅H₃ᵗBu₂)}₂Fe] (M^+), 538.12 (100 %) [Cp*Fe(η⁴-P₅Me(C₅H₃ᵗBu₂)]⁺.

5 shows significant Cp´´ isomerization. The different isomers and their respective ratios are discussed in chapter 3.5.1. However, by selective crystallization, it was possible to isolate the main product of these isomers which is spectroscopically discussed in the following as well as in chapter 3.5.2 respectively.

¹H NMR (400 MHz, C_6D_6, 298 K): δ [ppm] = 1.23 (s, 9 H, ᵗBu), 1.31 (s, 9 H, ᵗBu), 1.60 (s, 15H, Cp*), 2.41 (br, 3 H, Me), 3.70 (s, 1 H, Cp´´-H), 4.12 (s, 1 H, Cp´´-H).

$^{31}P\{^{1}H\}$ NMR (162 MHz, C_6D_6, 298 K): δ [ppm] = −88.5 (br, 1 P, P^X), −49.9 (br, 1 P, P^T), 25.6 (br, 1 P, P^M), 41.9 (br, 1 P, P^L), 128.6 (br, 1 P, P^A).

^{31}P NMR (162 MHz, C_6D_6, 298 K): δ [ppm] = −88.5 (br, 1 P, P^X), −49.9 (br, 1 P, P^T), 25.6 (br, 1 P, P^M), 41.9 (br, 1 P, P^L), 128.6 (br, 1 P, P^A).

$^{31}P\{^{1}H\}$ NMR (162 MHz, Tol-d_8, 193 K): δ [ppm] = −93.9 (ddd, $^{1}J_{PX\text{-}PA}$ = 374.9 Hz, $^{1}J_{PX\text{-}PL}$ = 400.4 Hz, $^{2}J_{PX\text{-}PM}$ = 32.0 Hz, $^{2}J_{PX\text{-}PT}$ = 3.5 Hz 1 P, P^X); −53.9 (dddd, $^{1}J_{PT\text{-}PM}$ = 400.5 Hz, $^{1}J_{PT\text{-}PA}$ = 400.8 Hz, $^{2}J_{PT\text{-}PL}$ = 34.1 Hz, $^{2}J_{PT\text{-}PX}$ = 3.5 Hz, 1 P, P^T); 21.4 (dddd, $^{1}J_{PM\text{-}PT}$ = 400.5 Hz, $^{1}J_{PM\text{-}PL}$ = 378.7 Hz, $^{2}J_{PM\text{-}PA}$ = 10.1 Hz, $^{2}J_{PM\text{-}PX}$ = 32.0 Hz, 1 P, P^M); 35.8 (ddd, $^{1}J_{PL\text{-}PX}$ = 400.4 Hz, $^{1}J_{PL\text{-}PM}$ = 378.7 Hz, $^{2}J_{PL\text{-}PA}$ = 12.0 Hz, $^{2}J_{PL\text{-}PT}$ = 34.1 Hz, 1 P, P^L); 130.9 (ddd, $^{1}J_{PA\text{-}PX}$ = 374.9 Hz, $^{1}J_{PA\text{-}PT}$ = 400.8 Hz, $^{2}J_{PA\text{-}PM}$ = 10.1 Hz, $^{2}J_{PA\text{-}PL}$ = 12.0 Hz, 1 P, P^A).

^{31}P NMR (162 MHz, Tol-d_8, 193 K): δ [ppm] = −93.9 (ddd, $^{1}J_{PX\text{-}PA}$ = 374.9 Hz, $^{1}J_{PX\text{-}PL}$ = 400.4 Hz, $^{2}J_{PX\text{-}PM}$ = 32.0 Hz, $^{2}J_{PX\text{-}PT}$ = 3.5 Hz 1 P, P^X); −53.9 (dddd, $^{1}J_{PT\text{-}PM}$ = 400.5 Hz, $^{1}J_{PT\text{-}PA}$ = 400.8 Hz, $^{2}J_{PT\text{-}PL}$ = 34.1 Hz, $^{2}J_{PT\text{-}PX}$ = 3.5 Hz, 1 P, P^T); 21.4 (dddd, $^{1}J_{PM\text{-}PT}$ = 400.5 Hz, $^{1}J_{PM\text{-}PL}$ = 378.7 Hz, $^{2}J_{PM\text{-}PA}$ = 10.1 Hz, $^{2}J_{PM\text{-}PX}$ = 32.0 Hz, 1 P, P^M); 35.8 (ddd, $^{1}J_{PL\text{-}PX}$ = 400.4 Hz, $^{1}J_{PL\text{-}PM}$ = 378.7 Hz, $^{2}J_{PL\text{-}PA}$ = 12.0 Hz, $^{2}J_{PL\text{-}PT}$ = 34.1 Hz, 1 P, P^L); 130.9 (ddd, $^{1}J_{PA\text{-}PX}$ = 374.9 Hz, $^{1}J_{PA\text{-}PT}$ = 400.8 Hz, $^{2}J_{PA\text{-}PM}$ = 10.1 Hz, $^{2}J_{PA\text{-}PL}$ = 12.0 Hz, 1 P, P^A).

1.7 [{Cp*Fe(η⁴-P₅Me(C₅H₃ᵗBu₂)}FeCp´´] (6)

6 could be identified as decomposition product in the reaction forming **5**. **6** could be selectively isolated by purification of the crude reaction mixture by column chromatography (SiO_2, *n*-hexane 10 x 3 cm). By using *n*-hexane, **6** could be eluted as brown band. For further purification, **6** was crystallized from a concentrated solution of *n*-hexane at −30 °C. **6** could be isolated as greenish/brown crystals.

Yield: 54 mg (2 %)

Elemental analysis:

calc. (%) for $C_{37}H_{59}Fe_2P_5$: C: 57.68, H: 7.72.

found (%): C: 57.90, H: 7.87.

FD-MS (Toluene): *m/z* (%) = 770.22 (100 %) $[Cp^*Fe(\eta^4\text{-}P_5MeCp´´)FeCp´´]^+$ (M^+).

^{1}H NMR (400 MHz, Tol-d_8, 298 K): δ [ppm] = 1.12 (s, 9 H, ^{t}Bu), 1.21 (s, 9 H, ^{t}Bu), 1.34 (s, 9 H, ^{t}Bu), 1.35 (s, 9 H, ^{t}Bu), 1.67 (s, 15 H, Cp*), 2.67 (dt, $^2J_{P\text{-}H}$ = 8.7 Hz, 3 H, Me), 3.77 – 4.10 (br, 5 H, Cp-H).

^{31}P{^{1}H} NMR (162 MHz, Tol-d_8, 298 K): δ [ppm] = −89.6 (ddd, $^1J_{PX\text{-}PA}$ = 386.2 Hz, $^1J_{PX\text{-}PL}$ = 397.4 Hz, $^2J_{PX\text{-}PM}$ = 33.9 Hz, $^2J_{PX\text{-}PT}$ = 3.8 Hz 1 P, P^X); −57.4. (dddd, $^1J_{PT\text{-}PM}$ = 403.4 Hz, $^1J_{PT\text{-}PA}$ = 384.1 Hz, $^2J_{PT\text{-}PL}$ = 34.2 Hz, $^2J_{PT\text{-}PX}$ = 3.8 Hz, 1 P, P^T); 27.6 (dddd, $^1J_{PM\text{-}PT}$ = 403.4 Hz, $^1J_{PM\text{-}PL}$ = 386.2 Hz, $^2J_{PM\text{-}PA}$ = 10.8 Hz, $^2J_{PM\text{-}PX}$ = 33.9 Hz, 1 P, P^M); 41.8 (ddd, $^1J_{PL\text{-}PX}$ = 397.4 Hz, $^1J_{PL\text{-}PM}$ = 386.2 Hz, $^2J_{PL\text{-}PA}$ = 10.4 Hz, $^2J_{PL\text{-}PT}$ = 34.2 Hz, 1 P, P^L); 131.0 (ddd, $^1J_{PA\text{-}PX}$ = 386.2 Hz, $^1J_{PA\text{-}PT}$ = 384.1 Hz, $^2J_{PA\text{-}PM}$ = 10.8 Hz, $^2J_{PA\text{-}PL}$ = 10.4 Hz, 1 P, P^A).

^{31}P NMR (162 MHz, Tol-d_8, 298 K): δ [ppm] = −89.6 (ddd, $^1J_{PX\text{-}PA}$ = 386.2 Hz, $^1J_{PX\text{-}PL}$ = 397.4 Hz, $^2J_{PX\text{-}PM}$ = 33.9 Hz, $^2J_{PX\text{-}PT}$ = 3.8 Hz 1 P, P^X); −57.4. (dddd, $^1J_{PT\text{-}PM}$ = 403.4 Hz, $^1J_{PT\text{-}PA}$ = 384.1 Hz, $^2J_{PT\text{-}PL}$ = 34.2 Hz, $^2J_{PT\text{-}PX}$ = 3.8 Hz, 1 P, P^T); 27.6 (dddd, $^1J_{PM\text{-}PT}$ = 403.4 Hz, $^1J_{PM\text{-}PL}$ = 386.2 Hz, $^2J_{PM\text{-}PA}$ = 10.8 Hz, $^2J_{PM\text{-}PX}$ = 33.9 Hz, 1 P, P^M); 41.8 (ddd, $^1J_{PL\text{-}PX}$ = 397.4 Hz, $^1J_{PL\text{-}PM}$ = 386.2 Hz, $^2J_{PL\text{-}PA}$ = 10.4 Hz, $^2J_{PL\text{-}PT}$ = 34.2 Hz, 1 P, P^L); 131.0 (ddd, $^1J_{PA\text{-}PX}$ = 386.2 Hz, $^1J_{PA\text{-}PT}$ = 384.1 Hz, $^2J_{PA\text{-}PM}$ = 10.8 Hz, $^2J_{PA\text{-}PL}$ = 10.4 Hz, $^2J_{P\text{-}H}$ = 8.7 Hz, 1 P, P^A).

1.8 [{Cp*Fe(η^4-P$_5$Me(C$_5$H$_3$^{t}Bu$_2$)}$_2$Fe][FAl]$_2$ (7)

A Schlenk flask, equipped with an efficient stir bar was loaded with **5** (0.11 g, 0.09 mmol, 1.00 equiv.), dissolved in *o*-DFB and cooled to −30 °C. To the solution, [Thia][FAl] (0.30 g, 0.19 mmol, 1.95 equiv.) in *o*-DFB at −30 °C was slowly added. During addition, a color change from brown to dark red could be observed. The solution was stirred for 30 min at −30 °C, was then allowed to warm up to room temperature, and was afterwards stirred for 90 min at room temperature. Next, the solution was concentrated in vacuo and the product was precipitated by the addition of *n*-hexane. The crude compound was washed with toluene (1x approx. 5 mL) and then with *n*-hexane (2x approx. 5 mL) and was afterwards dried under vacuum. For further purification, the product was dissolved in *o*-DFB, carefully layered with *n*-hexane, and crystallized at room temperature. The product could be obtained as brown crystalline needles/blocks.

Yield: 160 mg (42 %); single crystalline: few crystals.

Elemental analysis:

calc. (%) for $C_{120}H_{76}Fe_2Al_2O_6P_{10}F_{92}$: C: 37.02; H: 1.97.

found (%): C: 37.23, H: 2.20.

ESI-MS (*o*-DFB): *m/z* (%) = 565.07 (32 %) [{Cp*Fe(η^4-P$_5$Me(C$_5$H$_3$^{t}Bu$_2$)}$_2$Fe]$^{2+}$ (M^{2+}), 1130.14 (16 %) [{Cp*Fe(η^4-P$_5$Me(C$_5$H$_3$^{t}Bu$_2$)}$_2$Fe]$^+$ (M^+) and decomposition products.

^{1}H NMR (400 MHz, CD_2Cl_2, 298 K): δ [ppm] = broad signals between −15 ppm and 4 ppm.

^{31}P{^{1}H} NMR (162 MHz, CD_2Cl_2, 298 K): δ [ppm] = no signals visible.

^{31}P NMR (162 MHz, CD_2Cl_2, 298 K): δ [ppm] = no signals visible.

^{19}F{^{1}H} NMR (376 MHz, CD_2Cl_2, 298 K): δ [ppm] = −172.0 (s, 1 F, Al−F), −165.0 (t, J_{F-F} = 19 Hz, 6 F, *m*-C_6F_5), −154.3 (t, J_{F-F} = 20 Hz, 3 F, *p*-C_6F_5), −141.4 (d, J_{F-F} = 275 Hz, 3 F), −137.3 (d, J_{F-F} = 282 Hz, 6 F), −130.6 (d, J_{F-F} = 286 Hz, 6 F), −128.0 (s, 6 F), −121.9 (d, J_{F-F} = 277 Hz, 3 F), −117.1 (d, J_{F-F} = 279 Hz, 3 F), −112.7 (d, J_{F-F} = 279 Hz, 6 F).

2 X-Ray Crystallography

Crystallographic data for all synthesized compounds were collected on an XtaLAB Synergy R, DW System with a HyPix-Arc 150 detector using Cu-Kα radiation from a rotating anode (**1 – 7**). All measurements were performed at 123 K. Data collection, data reduction, and absorption correction were performed with the CrysAlisPro software package.[5] Structure solution and refinement was conducted in Olex2 (1.5-alpha)[6] with ShelXT[7] (solution) and ShelXL-2018/3[8] (least squares refinement (F^2)). All non-H atoms were refined with anisotropic displacement parameters and H-atoms were treated as riding models with isotropic displacement parameters and fixed C-H bond lengths (sp^3: 0.96 (CH_3), 0.97 (CH_2); sp^2: 0.93 (CH)). Visualization of the crystal structures was performed with Olex2 (1.5-alpha).[6]

CIF files with comprehensive information on the details of the diffraction experiments and full tables of bond lengths and angles for the compounds **1** − **7** are deposited in the Cambridge Crystallographic Data Centre under the deposition codes CCDC 2481358 – 2481364.

Table S2.1*:* X-ray crystallographic data of all crystallographically characterized compounds.

Compound	**1**	**2**	**3**	**4**
Formula	$C_{20}H_{31}FeP_5$	$C_{27}H_{46}FeP_5$	$C_{28}H_{47}P_5Fe$	$C_{20}H_{31}FeP_5$
$D_{calc.}$/ g cm^{-3}	1.358	1.255	1.281	1.378
μ/mm^{-1}	8.348	6.480	6.481	8.473
Formula Weight	482.15	581.34	594.35	482.15
Colour	clear light green	clear light green	dark brown	clear light green
Shape	plate-shaped	plate-shaped	stick-shaped	block-shaped
Size/mm^3	0.16×0.11×0.06	0.46×0.28×0.16	0.36×0.10×0.08	0.10×0.06×0.03
T/K	122.99(10)	123.01(10)	123.00(10)	123.00(10)
Crystal System	triclinic	triclinic	monoclinic	triclinic
Space Group	$P\bar{1}$	$P\bar{1}$	$P2_1/c$	$P\bar{1}$
a/Å	8.0632(2)	9.13670(10)	8.79081(5)	8.6885(3)
b/Å	11.5785(3)	13.2398(2)	11.63930(8)	8.7404(5)
c/Å	12.8280(3)	13.7436(2)	30.1311(2)	15.8005(8)
a/°	80.536(2)	77.0440(10)	90	87.841(4)
b/°	86.535(2)	71.8410(10)	90.2686(5)	85.946(4)
g/°	89.747(2)	84.4000(10)	90	76.133(4)
V/Å^3	1179.14(5)	1538.83(4)	3082.95(3)	1161.75(10)
Z	2	2	4	2
Z'	1	1	1	1
Wavelength/Å	1.54184	1.54184	1.54184	1.54184
Radiation type	CuK_a	CuK_a	Cu K_a	CuK_a
Q_{min}/°	3.499	3.427	2.933	2.804
Q_{max}/°	73.730	73.606	75.352	73.626
Measured Refl's.	16617	19533	61370	13935
Indep't Refl's	4610	6019	6313	4490
Refl's I≥2 s(I)	4109	5789	5825	3795
R_{int}	0.0287	0.0201	0.0353	0.0263
Parameters	353	283	418	245
Restraints	262	0	35	0
Largest Peak	0.377	0.375	0.432	0.703
Deepest Hole	-0.269	-0.354	-0.304	-0.587
GooF	1.070	1.102	1.097	1.057
wR_2 (all data)	0.0771	0.0776	0.0866	0.1149
wR_2	0.0751	0.0772	0.0849	0.1107
R_1 (all data)	0.0355	0.0296	0.0338	0.0517
R_1	0.0308	0.0287	0.0310	0.0432

Compound	**5**	**6**	**7**

Formula	$C_{111}H_{187}Fe_6P_{20}$	$C_{37}H_{59}Fe_2P_5$	$C_{126}H_{80}Al_2F_{94}Fe_3O_6P_{10}$
$D_{calc.}$/ g cm^{-3}	1.288	1.277	1.783
μ/mm^{-1}	8.007	7.863	5.018
Formula Weight	2476.09	770.39	4007.11
Colour	clear light green	clear light green	clear light green
Shape	plate-shaped	needle-shaped	needle-shaped
Size/mm^3	0.35×0.10×0.05	0.15×0.09×0.04	0.46×0.21×0.10
T/K	123.01(10)	123.00(10)	123.00(10)
Crystal System	triclinic	monoclinic	monoclinic
Space Group	$P\bar{1}$	$P2_1$	$P2_1/n$
a/Å	19.0268(2)	9.4774(2)	17.94321(10)
b/Å	19.6771(3)	15.2109(2)	41.3799(3)
c/Å	20.1768(3)	13.9922(2)	20.19446(12)
a/°	115.436(2)	90	90
b/°	96.5270(10)	96.671(2)	95.4565(5)
g/°	104.5600(10)	90	90
V/Å^3	6386.89(18)	2003.46(6)	14926.22(16)
Z	2	2	4
Z'	1	1	1
Wavelength/Å	1.54184	1.54184	1.54184
Radiation type	CuK_a	CuK_a	CuK_a
Q_{min}/°	2.507	3.180	2.444
Q_{max}/°	73.776	75.242	73.275
Measured Refl's.	78802	21704	160191
Indep't Refl's	24716	6560	29016
Refl's I≥2 s(I)	18617	6356	26068
R_{int}	0.0391	0.0426	0.0306
Parameters	1819	824	2476
Restraints	2794	976	1323
Largest Peak	1.073	0.472	0.617
Deepest Hole	-0.449	-0.564	-0.447
GooF	1.077	1.103	1.052
wR_2 (all data)	0.1430	0.1091	0.0908
wR_2	0.1342	0.1084	0.0888
R_1 (all data)	0.0713	0.0403	0.0381
R_1	0.0520	0.0392	0.0338

2.1 [Cp*Fe(η^4-P$_5$Me(C$_5$H$_4$^{t}Bu)] (1)

Single crystals of **1** were obtained by preparing a concentrated solution of **1** in *n*-hexane and subsequent crystallization at −30 °C for several days. **1** crystallizes as light green plates in a triclinic unit cell with the space group $P\bar{1}$ with one molecule of **1** per asymmetric unit. Disorders within the Cp* ligand were refined by using adequate restraints. The molecular solid-state structure of **1** is depicted in Figure S2.1.

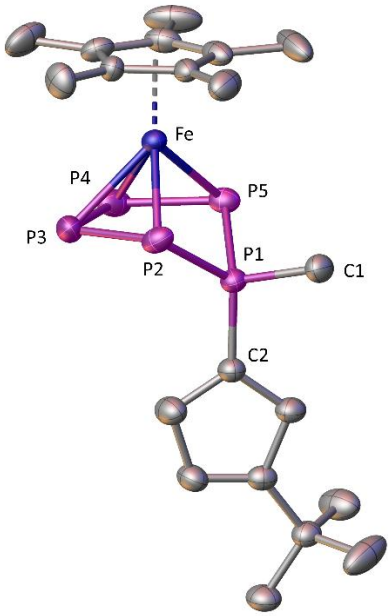

Figure S2.1: Solid-state structure of **1**. Shown is the asymmetric unit containing one molecule; thermal ellipsoids are drawn at the 50% probability level and H atoms are omitted for clarity.

2.2 [Cp*Fe(η^4-P$_5$Me(C$_5$H$_3$^{t}Bu$_2$)] (2)

Single crystals of **2** were obtained by preparing a concentrated solution of **2** in *n*-hexane and subsequent crystallization at −30 °C for several days. **2** crystallizes as light green blocks in a triclinic unit cell in the space group $P\bar{1}$, which could be solved without using any disorders. The asymmetric unit contains one molecule of **2** and one equivalent of *n*-hexane. The molecular solid-state structure of **2** is depicted in Figure S2.2.

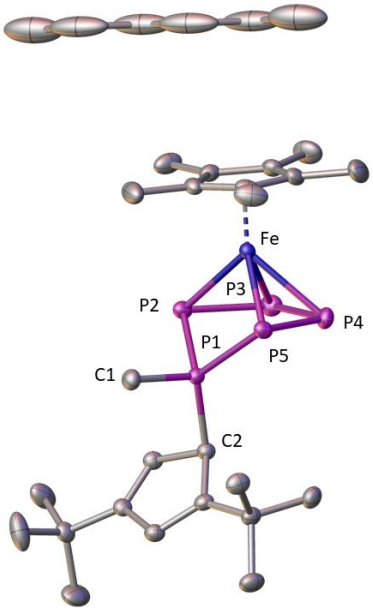

Figure S2.2: Solid-state structure of **2**. Shown is the asymmetric unit containing one molecule; thermal ellipsoids are drawn at the 50% probability level and H atoms are omitted for clarity.

2.3 [Cp*Fe(η^4-P$_5$Me(C$_5$H$_2$^{t}Bu$_3$)] (3)

Single crystals of **3** were obtained by preparing a concentrated solution of **3** in *n*-hexane and subsequent crystallization at −30 °C for several days. **3** crystallizes as light green plates in a monoclinic space group with the space group $P2_1/c$ with one molecule of **3** per asymmetric unit. Disorders within the Cp* ligand were refined by using adequate restraints. The molecular solid-state structure of **3** is depicted in Figure S2.3.

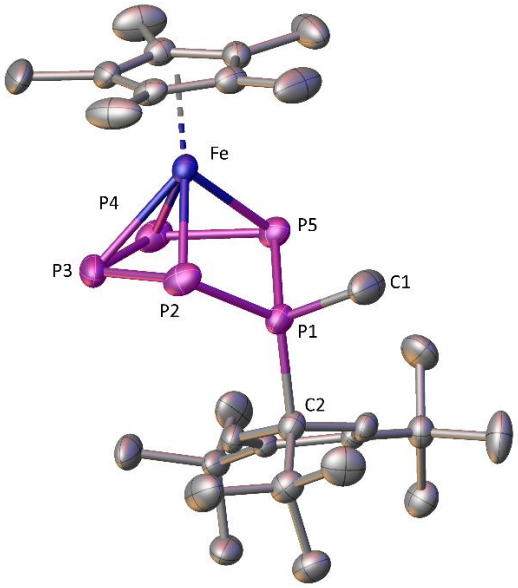

Figure S2.3: Solid-state structure of **3**. Shown is the asymmetric unit containing one molecule; thermal ellipsoids are drawn at the 50% probability level and H atoms are omitted for clarity.

2.4 [Cp*Fe(η^4-P$_5$Me(C$_5$Me$_4$H)] (4)

Single crystals of **4** were obtained by preparing a concentrated solution of **4** in *n*-hexane and subsequent crystallization at −30 °C for several days. **4** crystallizes as light green plates in a triclinic unit cell with the space group $P\bar{1}$, with one molecule of **4** per asymmetric unit, which could be solved without any disorder. The molecular solid-state structure of **4** is shown in Figure S2.4.

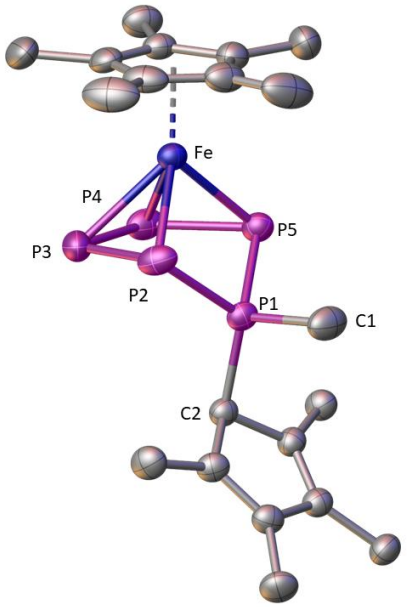

Figure S2.4: Solid-state structure of **4**. Shown is the asymmetric unit containing one molecule; thermal ellipsoids are drawn at the 50% probability level and H atoms are omitted for clarity.

2.5 [{Cp*Fe(η^4-P$_5$Me(C$_5$H$_3$^{t}Bu$_2$)}$_2$Fe] (5)

Single crystals of **5** were obtained by preparing a concentrated solution of **5** in *n*-hexane and subsequent crystallization at −30 °C for several days. **5** crystallizes as green plates in a triclinic unit cell with the space group $P\bar{1}$. The asymmetric unit contains two molecules of **5** and 2.5 molecules of *n*-hexane. Disorders within the *cyclo*-P$_5$ ligand as well as within the Cp* ligand were refined by using adequate restraints. The molecular solid-state structure of **5** is depicted in Figure S2.5.

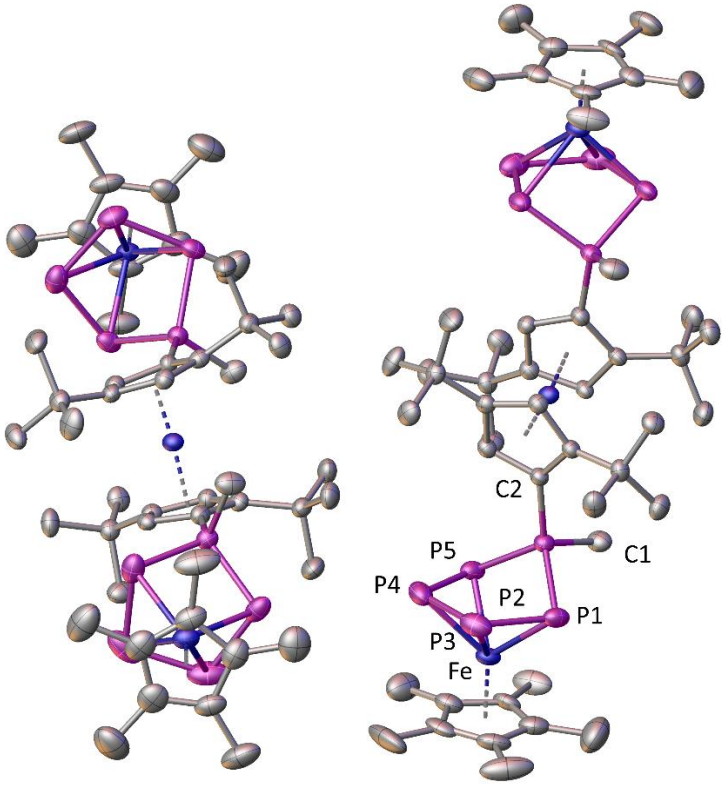

Figure S2.5: Solid-state structure of **5**. Shown is the asymmetric unit containing two molecules; thermal ellipsoids are drawn at the 50% probability level and H atoms are omitted for clarity.

2.6 [{Cp*Fe(η⁴-P₅Me(C₅H₃ᵗBu₂)}FeCp´´] (6)

Single crystals of **6** were obtained by preparing a concentrated solution of **6** in *n*-hexane and subsequent crystallization at –30 °C for several days. **6** crystallizes as light green needles in a monoclinic unit cell with the space group $P2_1$. Disorders within the *cyclo*-P_5 moiety and the ferrocene core were refined by using adequate restraints. The asymmetric unit contains one molecule of **6**. The molecular solid-state structure of **6** is depicted in Figure S2.6.

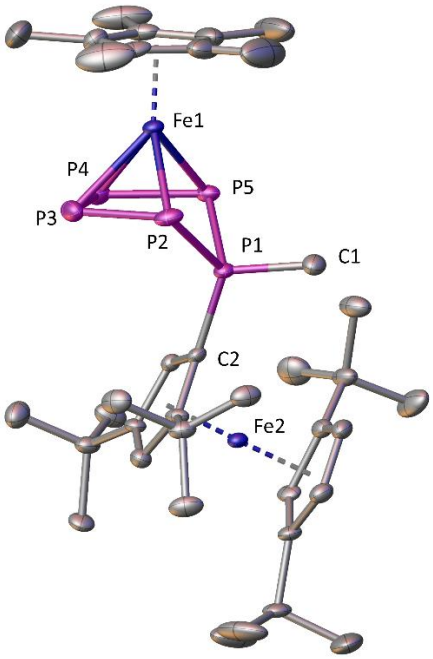

Figure S2.6: Solid-state structure of **6**; Shown is the asymmetric unit containing one molecule; thermal ellipsoids are drawn at the 50% probability level and H atoms are omitted for clarity.

2.7 [{Cp*Fe(η^4-$P_5Me(C_5H_3{}^tBu_2)$}$_2$Fe][FAl]$_2$ (7)

Single crystals of **7** were obtained by layering a concentrated solution of **7** in *o*-DFB with *n*-hexane and subsequent crystallization at room temperature for several days. **7** crystallizes as green needles in a monoclinic unit cell with the space group $P2_1/n$. The asymmetric unit contains one dication of $[\mathbf{5}]^{2+}$, two $[FAl]^-$ counteranions, as well as one molecule of *o*-DFB. Disorders within the *cyclo*-P_5 ligand as well as within the Cp* ligand were refined by using adequate restraints. The solid-state structure of **7** is depicted in Figure S2.7.

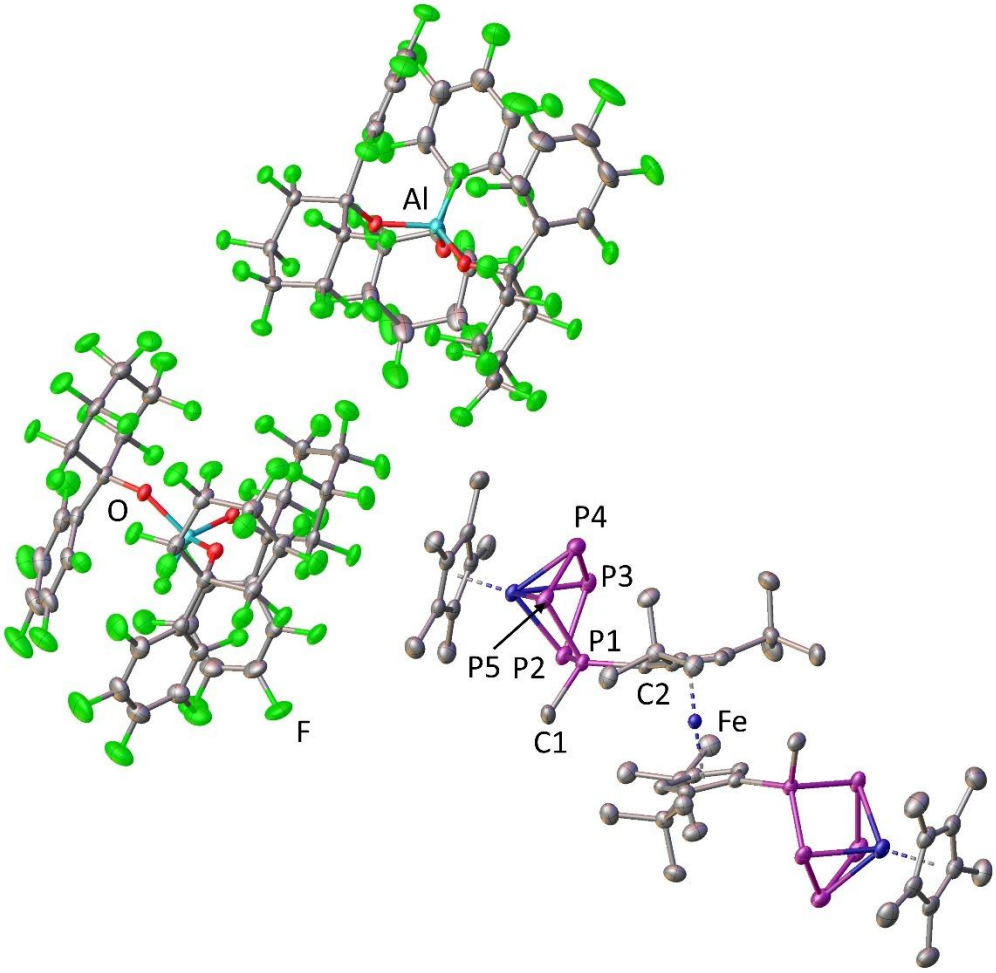

Figure S2.7: Solid-state structure of **7**; Shown is the asymmetric unit containing one molecule; thermal ellipsoids are drawn at the 50% probability level and H atoms are omitted for clarity.

3 NMR Spectroscopic Investigations

3.1 [Cp*Fe(η⁴-P₅Me(C₅H₄ᵗBu)] (1)

1 is well soluble in C_6D_6, enabling the NMR spectra to be recorded with ease. **1** shows a significant proportion of isomerisation products, which prevents an exact and clear assignment of the signals as well as a detailed analysis by simulation due to numerous overlapping signals. The ^{1}H NMR spectrum of **1** (Figure S3.1) shows several signals for the ^{t}Bu substituents between δ = 0.69 ppm and 0.94 ppm. Furthermore, signals for the Cp* ligand can be detected between δ = 1.59 and 1.66 ppm. The signal for the Me group, detectable at δ = 1.97 ppm shows significant overlap of the resonances of different isomerization products, which also distorts the determined integral value. The signals for the residual Cp-H atoms (also showing signals, referred to isomers) can be detected between δ = 2.26 ppm and 6.39 ppm. The ^{31}P{^{1}H} (Figure S3.2) and ^{31}P NMR spectra (Figure S3.3) show an AMM´XX´ spin system which also shows several isomers, which could be partially assigned via ^{31}P–^{31}P−COSY (Figure S3.4) measurements. Due to the massive overlap of signals, no simulation and detailed spin system analysis by simulation could be performed.

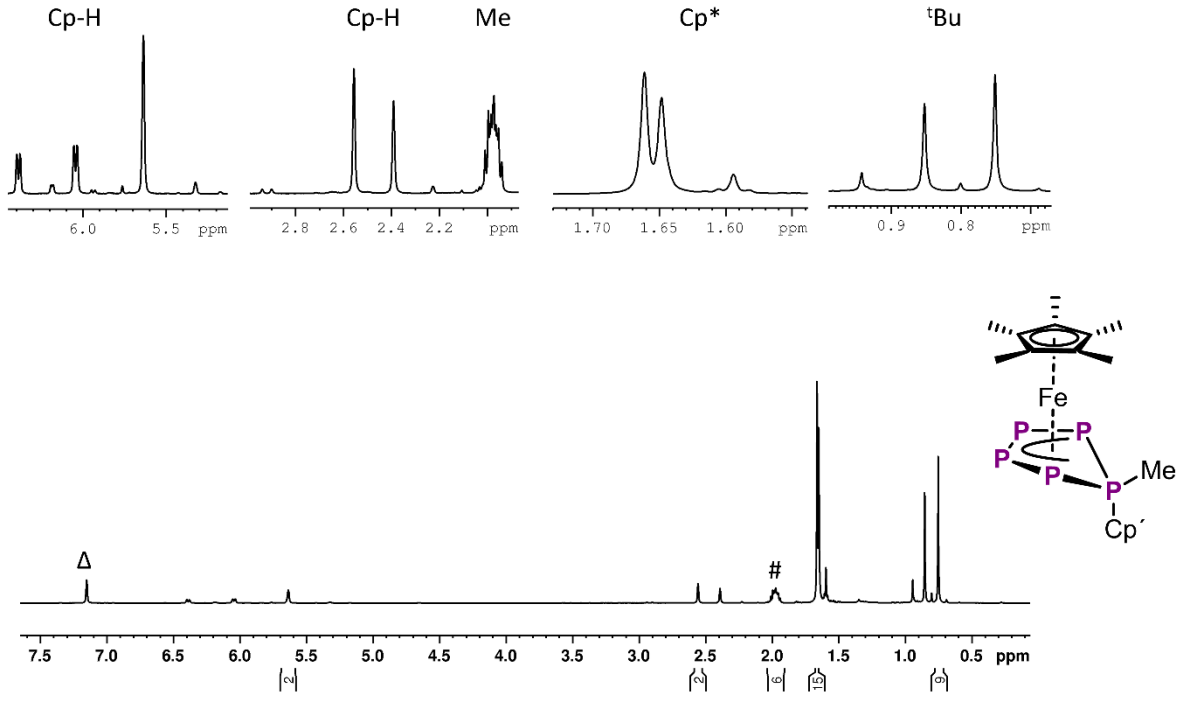

Figure S3.1: ^{1}H NMR spectrum of **1**. Measured in C_6D_6 at 298 K. Δ marks the signal for the residual solvent signal of C_6D_6. # marks the too high integral value of the Me substituent, caused by the massive overlap of signals belonging to different isomers.

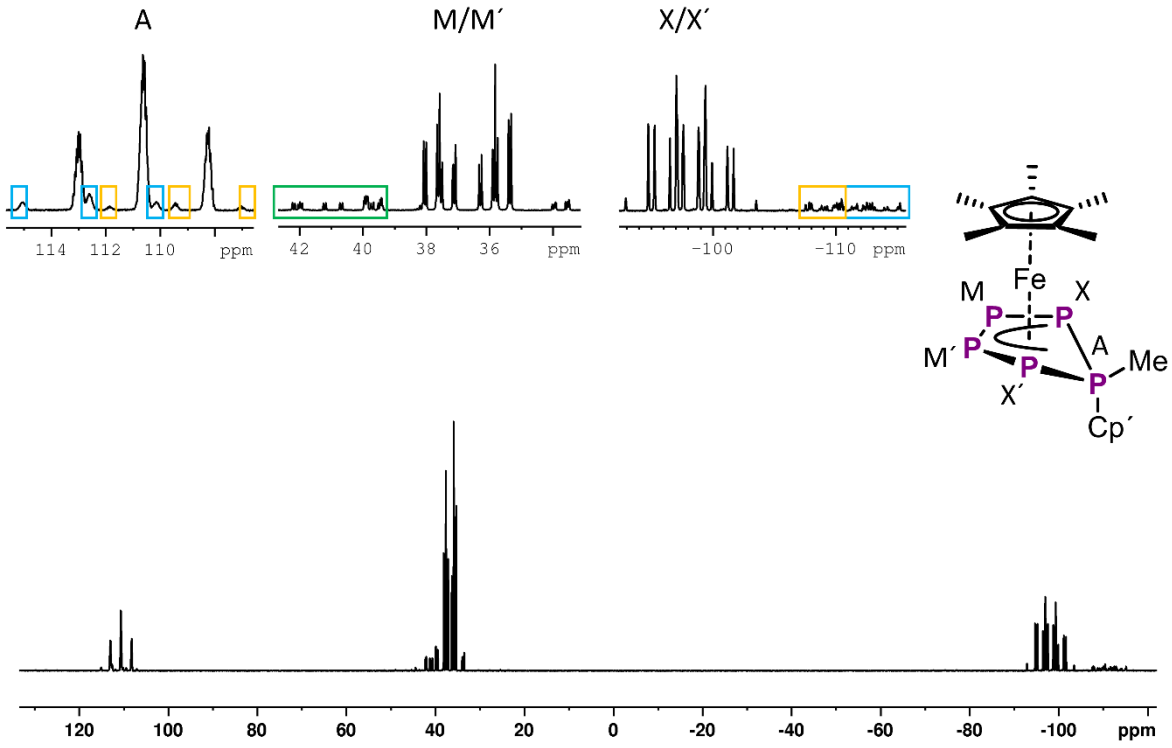

Figure S3.2: $^{31}P\{^{1}H\}$ NMR spectrum of **1**, measured in C_6D_6 at 298 K. The greenly marked signal for the isomerization product in the signal $P^{M/M´}$ shows in ^{31}P-^{31}P-COSY measurements coupling to both yellow and blue marked signals next to signal $P^{X/X´}$, indicating the presence of two products within the identified signal.

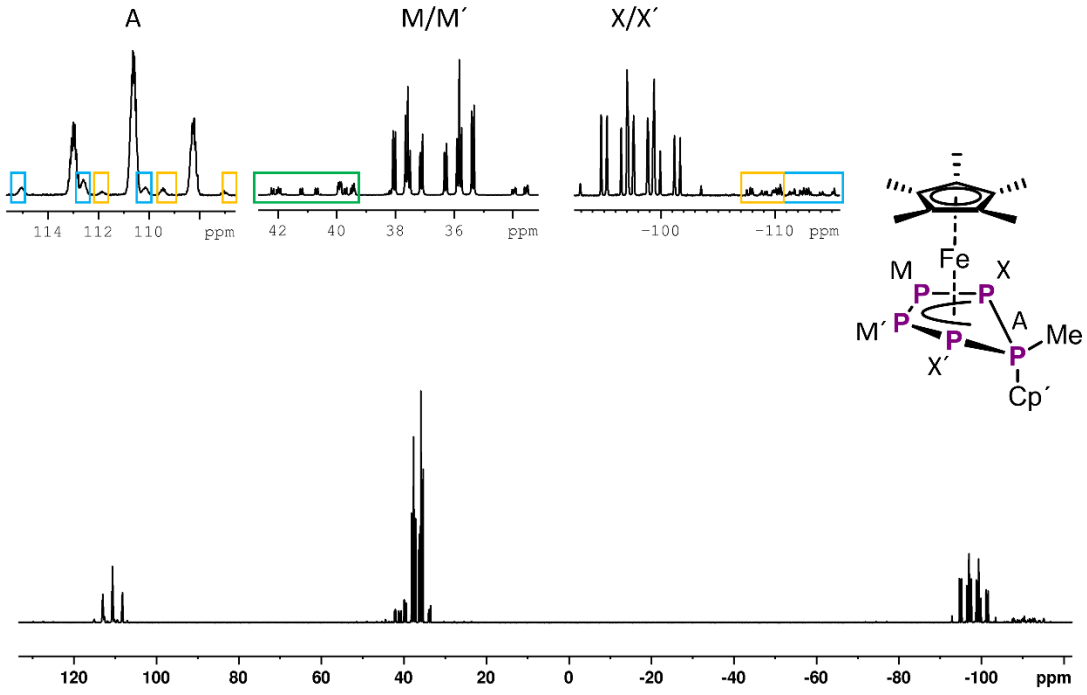

Figure S3.3: ^{31}P NMR spectrum of **1**, measured in C_6D_6 at 298 K. The greenly marked signal for the isomerization product in the signal $P^{M/M´}$ shows in ^{31}P–^{31}P–COSY measurements coupling to both yellow

and blue marked signals next to signal $P^{X/X'}$, indicating the presence of two products within the identified signal.

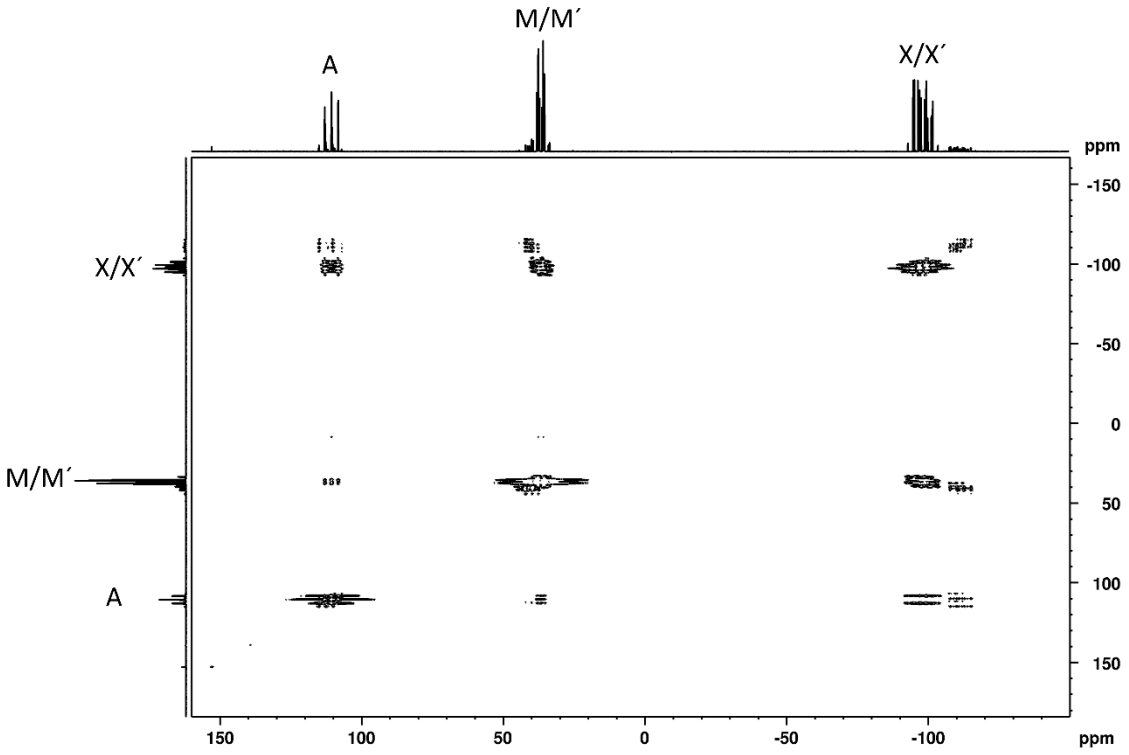

Figure S3.4: ^{31}P-^{31}P-COSY of **1**, measured in C_6D_6 at 298 K.

3.2 [Cp*Fe(η⁴-P₅Me(C₅H₃ᵗBu₂)] (2)

2 is well soluble in Tol-d_8. The ^{1}H NMR spectrum (Figure S3.5), recorded at room temperature shows two singlets for the ^{t}Bu groups at δ = 0.96 ppm and δ = 1.08 ppm, one sharp singlet at δ = 1.60 ppm for the Cp* ligand, and one doublet of triplets at δ = 1.52 ppm for the Me group. The signals for the residual Cp´´ protons are located at δ = 3.27 ppm, 5.65 ppm, and 6.04 ppm. The ^{31}P{^{1}H} (Figure S3.6) and ^{31}P NMR spectra (Figure S3.7) surprisingly show, in contrast to the AMM´XX´ spin systems usually observed for these systems, an ALMTX spin system, with chemical shifts and coupling constants provided in Table S3.1. A higher-order AMM´XX´ spin system could also not be obtained by using more polar solvents or higher temperatures. The signal P^A shows an additional coupling in the ^{31}P NMR spectrum. To gain deeper insight into the connectivity of the respective nuclei a ^{31}P–^{31}P–COSY was performed (Figure S3.8).

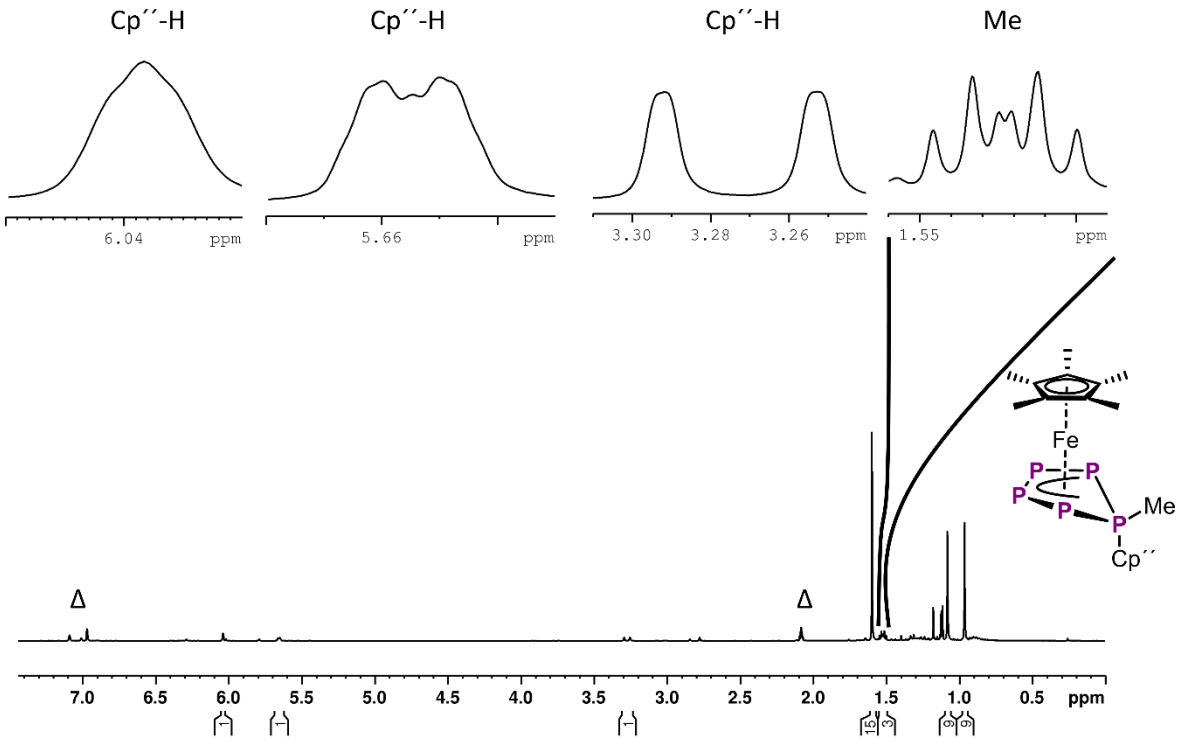

Figure S3.5: ^{1}H NMR spectrum of **2**, measured in Tol-d_8 at 298 K. Δ marks the signal for the residual solvent signal of Tol-d_8.

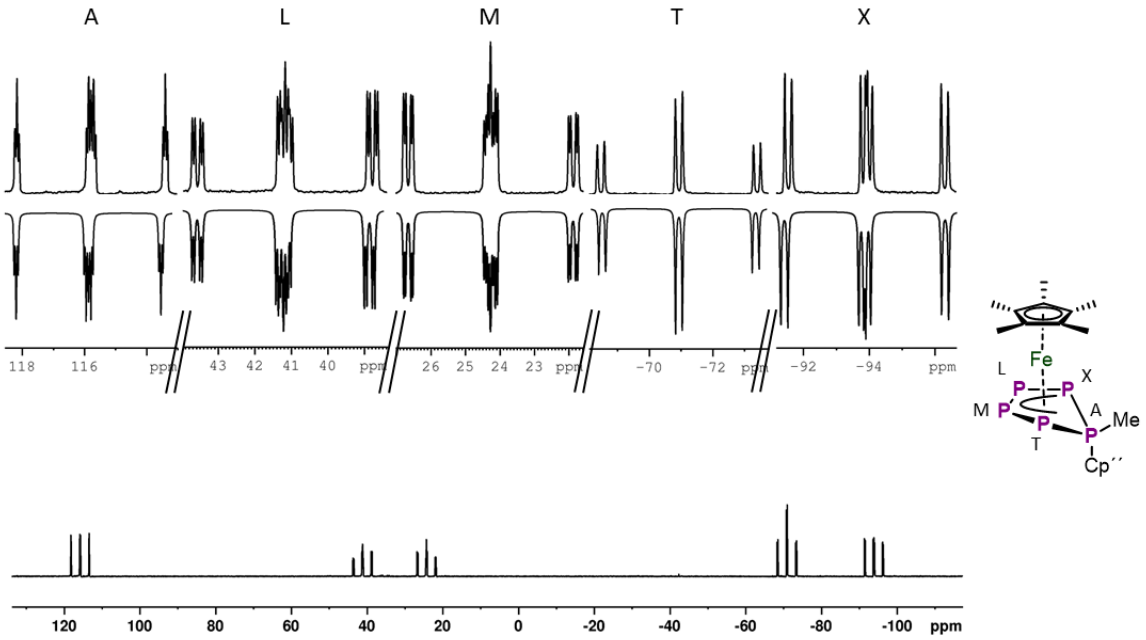

Figure S3.6: Experimental (top) and simulated (bottom) $^{31}P\{^{1}H\}$ NMR spectrum of **2** in C_6D_6 at 298 K.

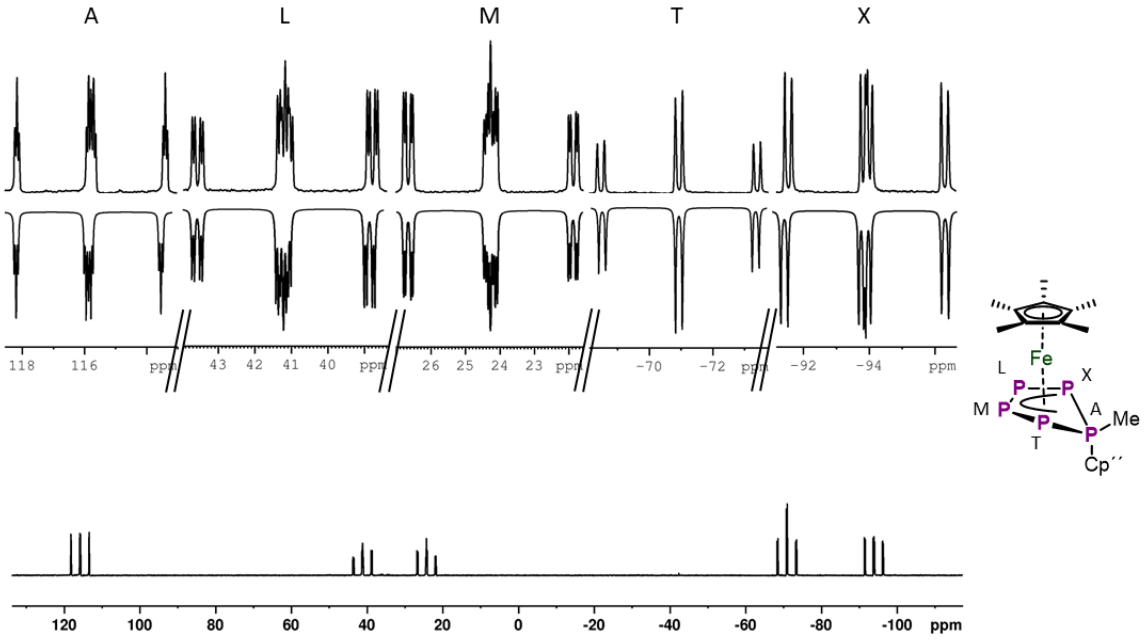

Figure S3.7: Experimental (top) and simulated (bottom) ^{31}P NMR spectrum of **2** in C_6D_6 at 298 K.

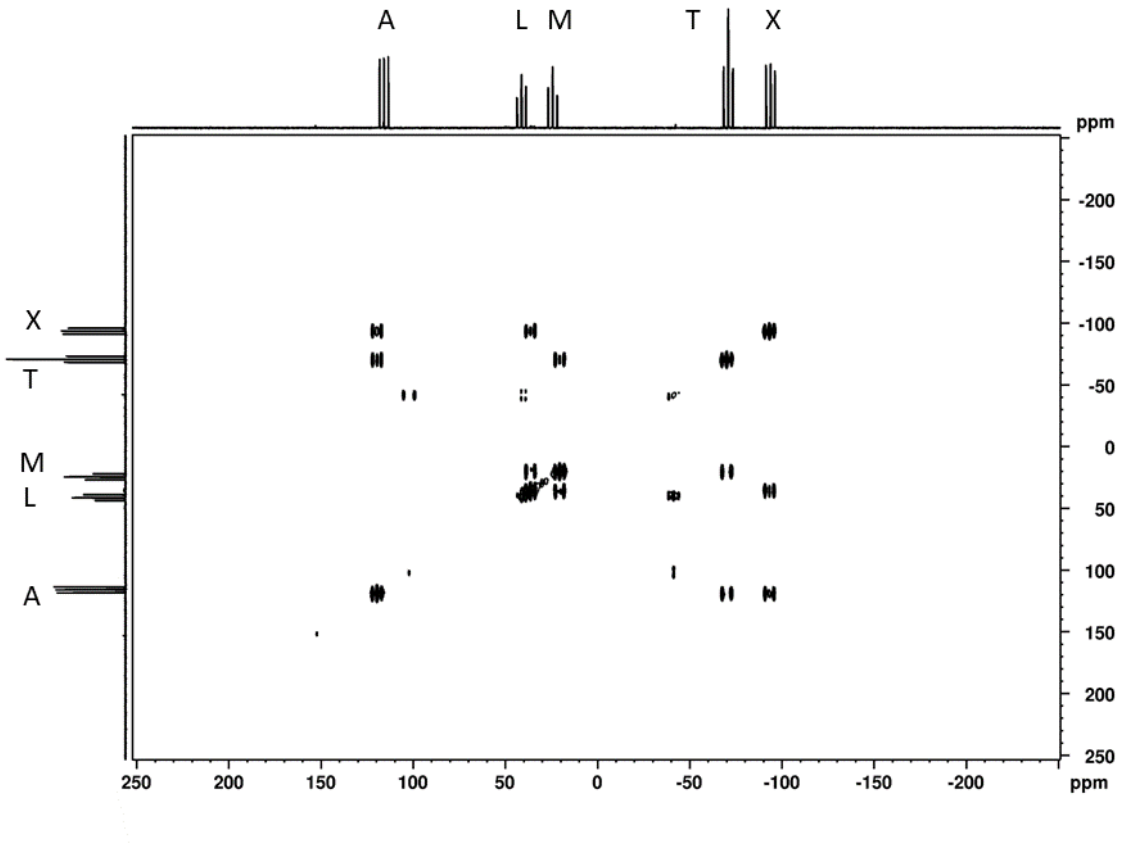

Figure S3.8: ^{31}P-^{31}P-COSY spectrum of **2** in CD_2Cl_2 at 298 K.

Table S3.1: Chemical shifts and coupling constants of **2**, extracted from the simulated ^{31}P NMR spectrum of **2**, measured in Tol-d_8.

***J* (Hz)**		**δ (ppm)**	
$^1J_{PA-PX}$	374.9	115.8	P^A
$^1J_{PA-PT}$	400.8	41.2	P^L
$^1J_{PX-PL}$	400.5	24.3	P^M
$^1J_{PT-PM}$	400.5	−71.0	P^T
$^1J_{PL-PM}$	378.8	−93.9	P^X
$^2J_{PA-PM}$	11.9		
$^2J_{PA-PL}$	10.2		
$^2J_{PX-PM}$	32.8		

$^{2}J_{PL\text{-}PT}$	33.4
$^{2}J_{PX\text{-}PT}$	3.5
$^{2}J_{PA\text{-}H}$	7.9

3.3 [Cp*Fe(η⁴-P₅Me(C₅H₂ᵗBu₃)] (3)

3 is well soluble in C_6D_6, allowing the NMR spectra to be recorded with ease. The ^1H NMR (Figure S3.9) spectrum of **3** shows two different signals for the ^{t}Bu groups at δ = 0.85 ppm and δ = 1.33 ppm and one sharp singlet for the Cp* ligand at δ = 1.57 ppm. Furthermore, the signal for the Me group as well as the residual C-H atoms can be detected at δ = 2.29 ppm as well as δ = 5.59 – 6.01 ppm respectively. Additionally, **3** shows signals for suspected Cp´´´ isomers, which show a signal for the Me group at δ = 1.98 ppm as well as smaller signals between δ = 5.59 to 6.01 ppm respectively. By integration of the distinguishable Me signals of the two isomers, the ratio between these isomers could be determined to 1 : 0.23. The $^{31}P\{^1H\}$ (Figure S3.10), as well as the ^{31}P NMR spectra (Figure S3.11) respectively show an AMM´XX´ spin system with chemical shifts and coupling constants provided in Table S3.2. The signal P^A shows an additional coupling to the Me-substituent. Furthermore, similar to **1**, the presence of Cp´´´ isomers could be shown by ^{31}P-^{31}P-COSY (Figure S3.12) measurements. The signals of the isomers are marked within the respective spectra.

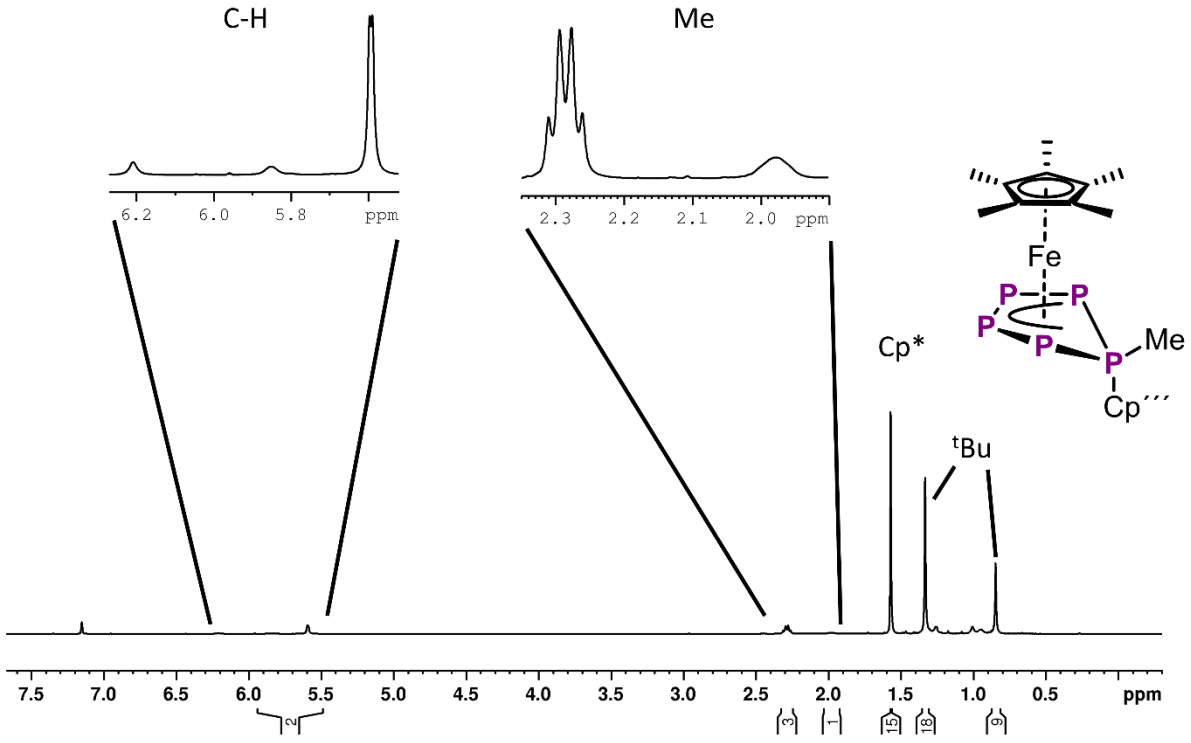

Figure S3.9: ^1H NMR spectrum of **3**, measured in C_6D_6 at 298 K. Δ marks the signal for the residual solvent signal of C_6D_6.

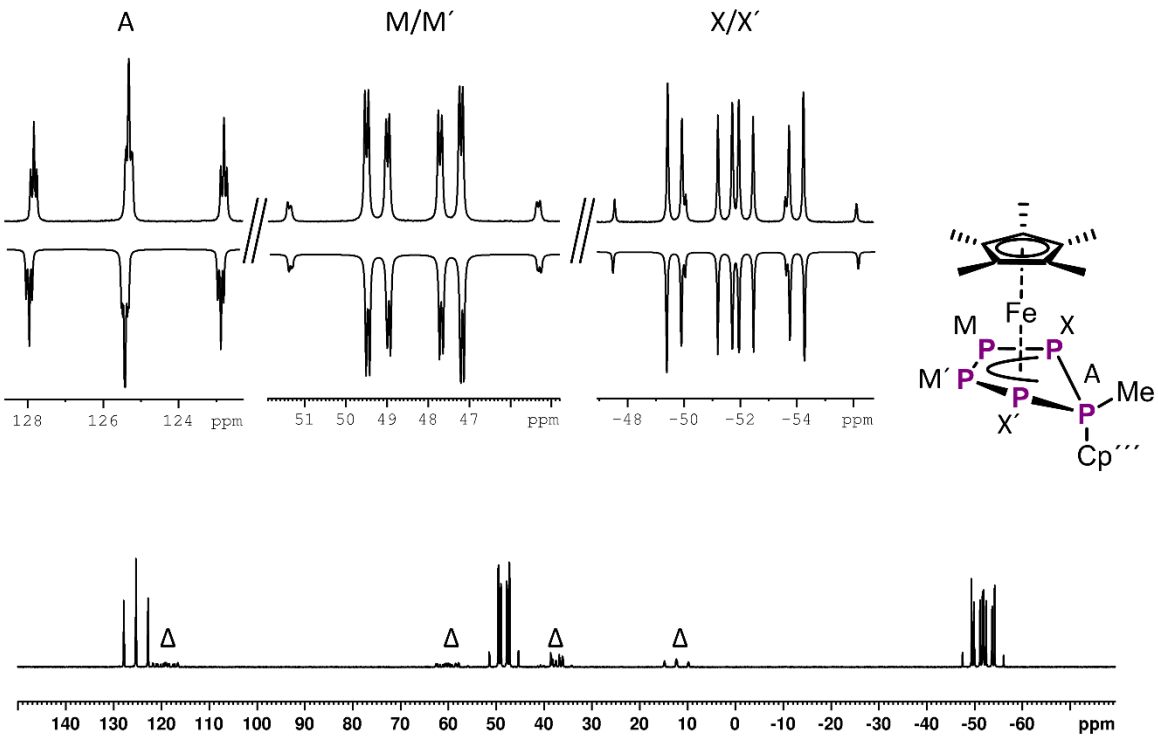

Figure S3.10: Experimental (top) and simulated (bottom) $^{31}P\{^{1}H\}$ NMR spectrum of **3,** measured in C_6D_6 at 298 K. Δ marks the signals for the suspected isomers of Cp´´´.

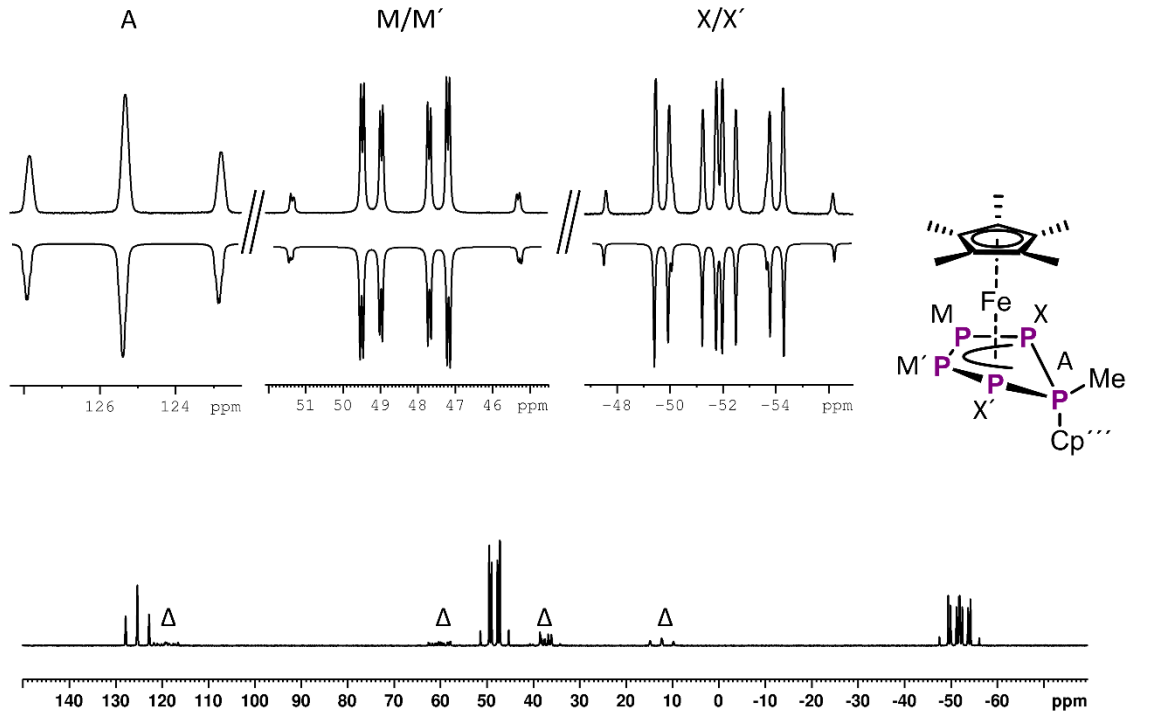

Figure S3.11: Experimental (top) and simulated (bottom) ^{31}P NMR spectrum of **3,** measured in C_6D_6 at 298 K. Δ marks the signals for the suspected isomers of Cp´´´.

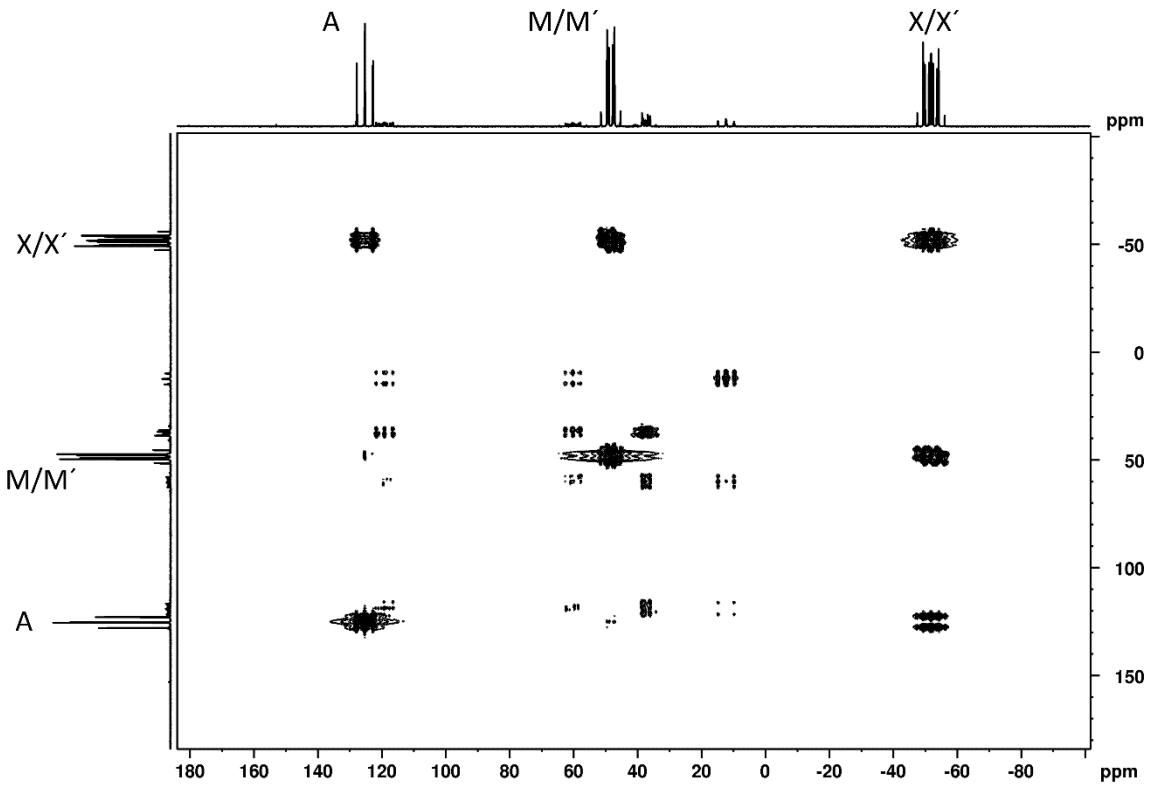

Figure S3.12: ^{31}P-^{31}P-COSY of **3**. Measured in C_6D_6 at 298 K.

Table S3.2: Chemical shifts and coupling constants of **3**, extracted from the simulated ^{31}P NMR spectrum of **3**, measured in C_6D_6.

***J* (Hz)**		**δ (ppm)**	
$^{1}J_{PA\text{-}PX/X´}$	409.8/409.5	125.3	P^{A}
$^{1}J_{PM/M´\text{-}PX/X´}$	403.0/419.6	48.3	$P^{M/M´}$
$^{2}J_{PA\text{-}PM/PA\text{-}PM´}$	13.1/12.8	−51.9	$P^{X/X´}$
$^{1}J_{PM\text{-}PM´}$	387.7		
$^{2}J_{PX\text{-}PX´}$	−0.2		
$^{2}J_{PM\text{-}PX´/PM´\text{-}PX}$	−46.4/−32.2		
$^{2}J_{PA\text{-}P\text{-}H/PA\text{-}Cp\text{-}H}$	7.3		

3.4 [Cp*Fe(η⁴-P₅Me(C₅Me₄H)] (4)

4 is well soluble in C_6D_6. The ^1H NMR spectrum of **4** (Figure S3.13) shows one broad signal at δ = 1.36 ppm for the Me groups of the C_5Me_4H substituent, overlapping with the signals of the Me group binding in 1-position at δ = 1.38 ppm. To further prove this assumption, a $^1H\{^{31}P\}$ NMR spectrum of **4** (Figure S3.14) was recorded, showing an uncoupled singlet at δ = 1.38 ppm for the Me group. The $^{31}P\{^1H\}$ (Figure S3.15) and ^{31}P NMR spectra (Figure S3.16) respectively show a symmetrical AMM´XX´ spin system with chemical shifts and coupling constants provided in Table S3.3. The signal P^A shows an additional coupling to the Me-group.

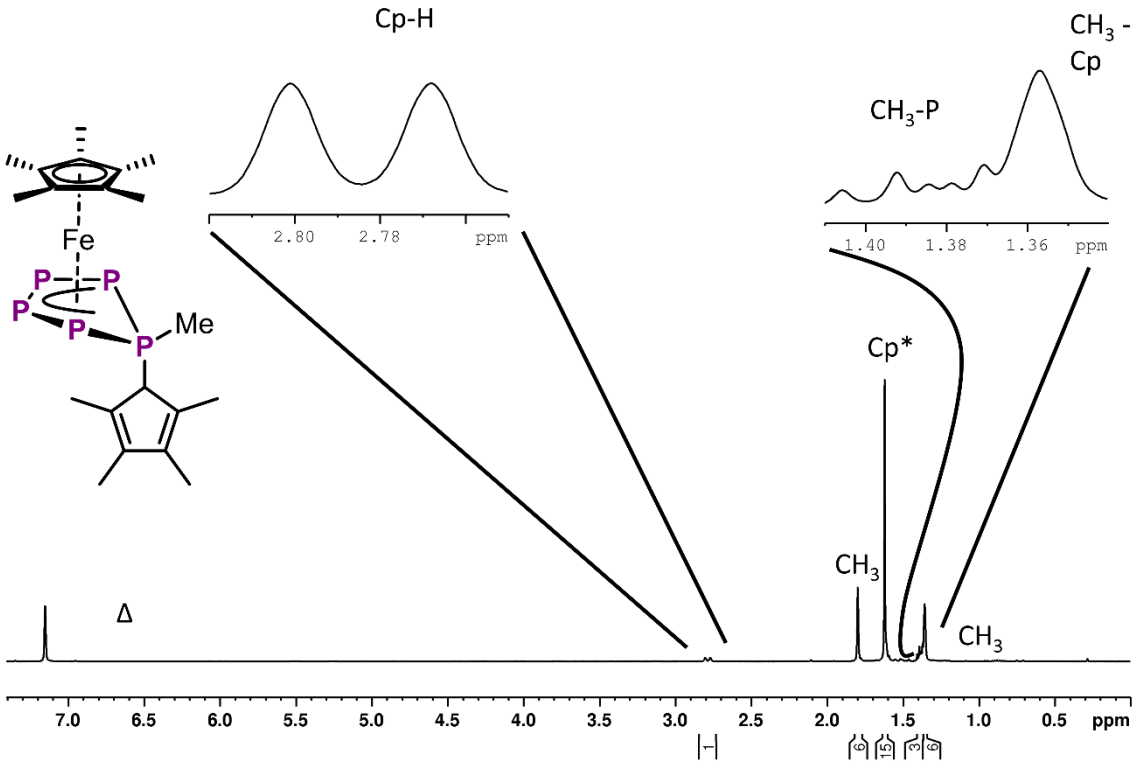

Figure S3.13: ^1H NMR spectrum of **4**, measured in C_6D_6 at 298 K. Δ marks the signal for the residual solvent signal for C_6D_6.

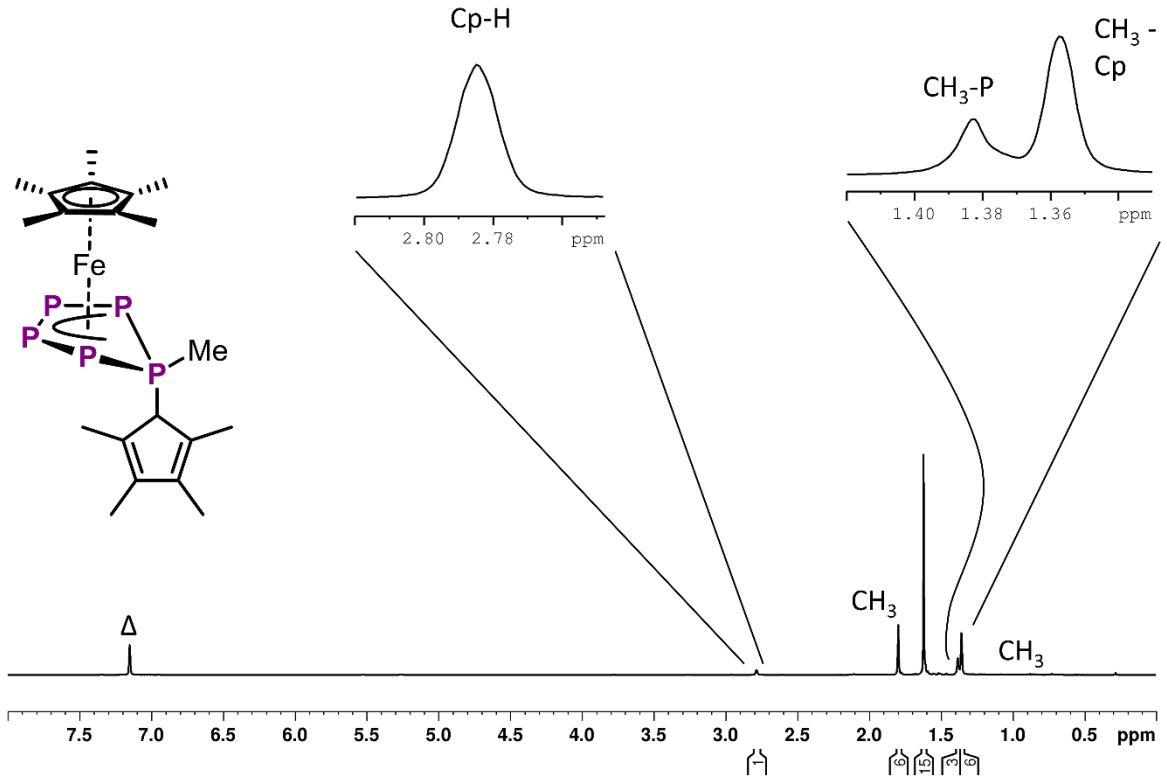

Figure S3.14: $^{1}H\{^{31}P\}$ NMR spectrum of **4**, measured in C_6D_6 at 298 K. Δ marks the signal for the residual solvent signal for C_6D_6.

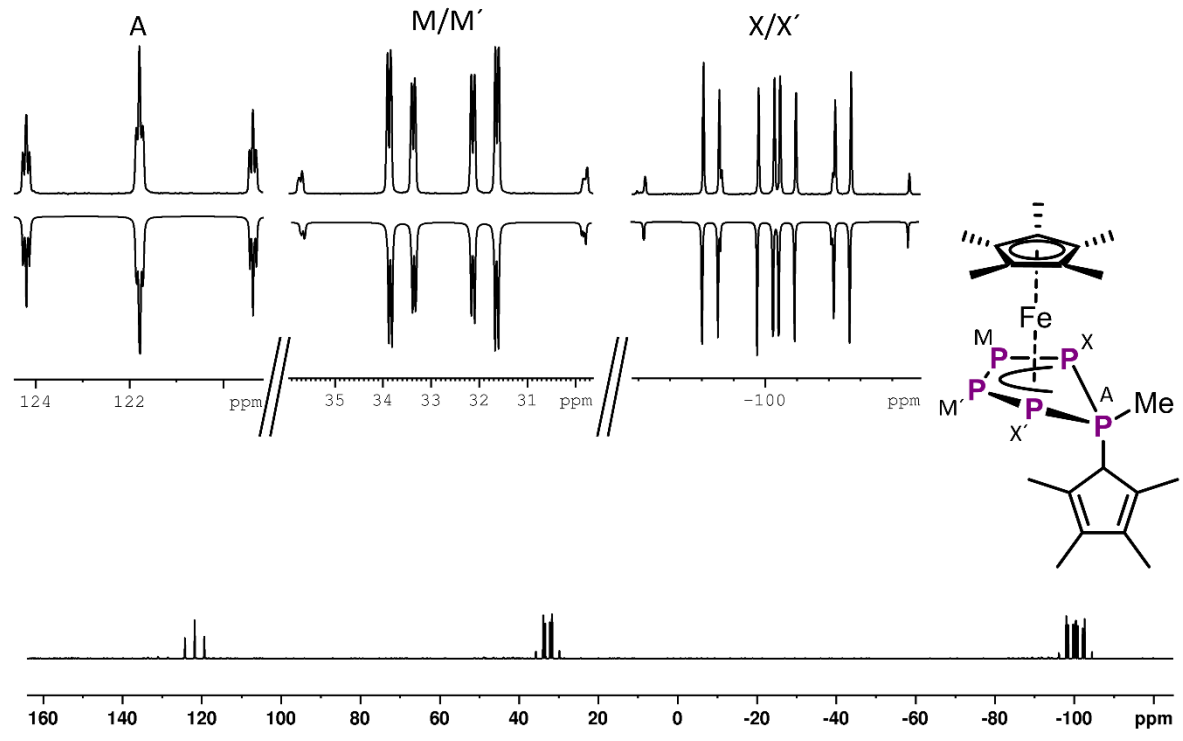

Figure S3.15: Experimental (top) and simulated (bottom) $^{31}P\{^{1}H\}$ NMR spectrum of **4**, measured in C_6D_6 at 298 K.

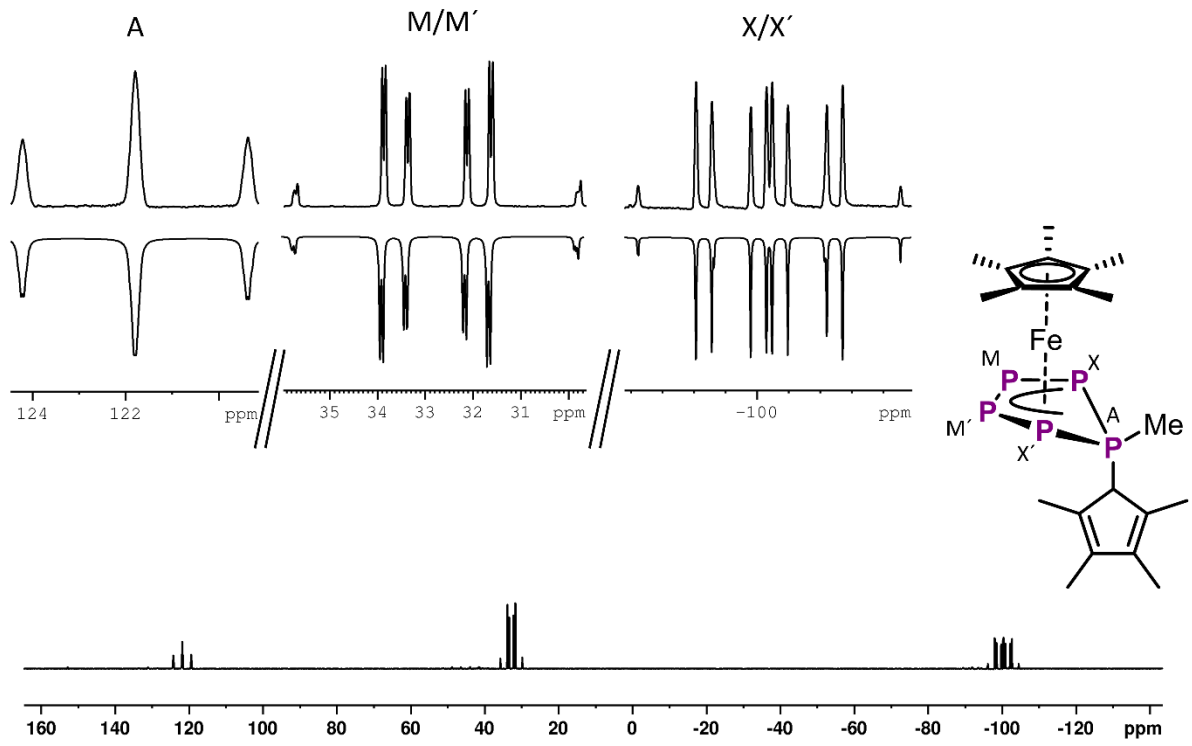

Figure S3.16: Experimental (top) and simulated (bottom) ^{31}P NMR spectrum of **4**, measured in C_6D_6 at 298 K.

Table S3.3: Chemical shifts and coupling constants of **4**, extracted from the simulated ^{31}P NMR spectrum of **4**, measured in C_6D_6.

***J* (Hz)**		**δ (ppm)**	
$^{1}J_{PA\text{-}PX/X´}$	392.9/391.5	121.8	P^{A}
$^{1}J_{PM/M´\text{-}PX/X´}$	395.1/407.5	32.7	$P^{M/M´}$
$^{2}J_{PA\text{-}PM/PA\text{-}PM´}$	10.3/12.0	−100.4	$P^{X/X´}$
$^{1}J_{PM\text{-}PM´}$	379.7		
$^{2}J_{PX\text{-}PX´}$	1.4		
$^{2}J_{PM\text{-}PX´/PM´\text{-}PX}$	−45.8/−30.2		
$^{2}J_{PA\text{-}P\text{-}H/PA\text{-}Cp\text{-}H}$	7.0/14.0		

3.5 [{Cp*Fe(η⁴-P₅Me(C₅H₂ᵗBu₂)}₂Fe] (5)

3.5.1 Isomerization

5 shows significant isomerization. Therefore, several signals for the P-scaffold and the Cp´´ fragments can be detected. The ^{1}H NMR spectrum of **5** (Figure S3.17) shows several signals for the Me- and ^{t}Bu-substituents as well as the Cp-H protons, respectively. The ^{31}P{^{1}H} NMR (Figure S3.18) spectrum in addition shows the expected signals of different isomers. With the help of ^{1}H-^{31}P HMBC (Figure S3.19) as well as ^{31}P-^{31}P-COSY (Figure S*3.20*) experiments, the identity of the respective signals could be further examined. Via integration of the identified Me-signals, the ratio of the isomers could be determined to be 1 : 0.2 : 0.2. Via column chromatographic workup or via selective crystallization, the main product of these isomers could be successfully isolated and spectroscopically characterized further.

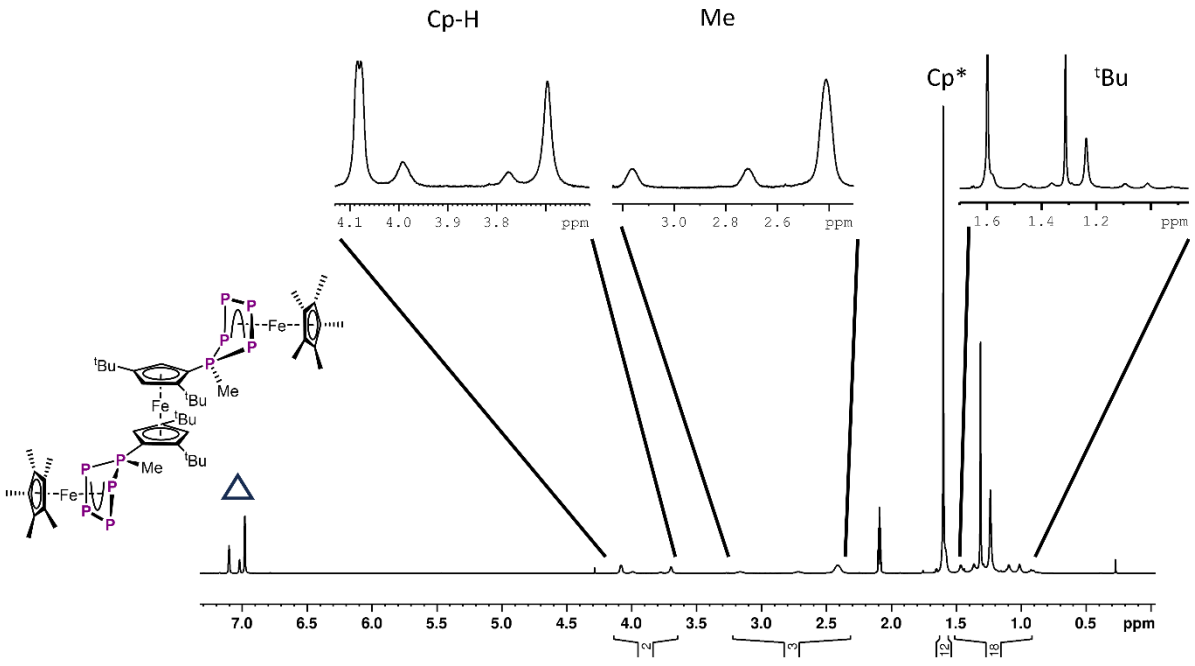

Figure S3.17*:* ^{1}H NMR spectrum of **5**, measured in Tol-d_8 at 298 K. Δ marks the signal for the residual solvent signal of Tol-d_8.

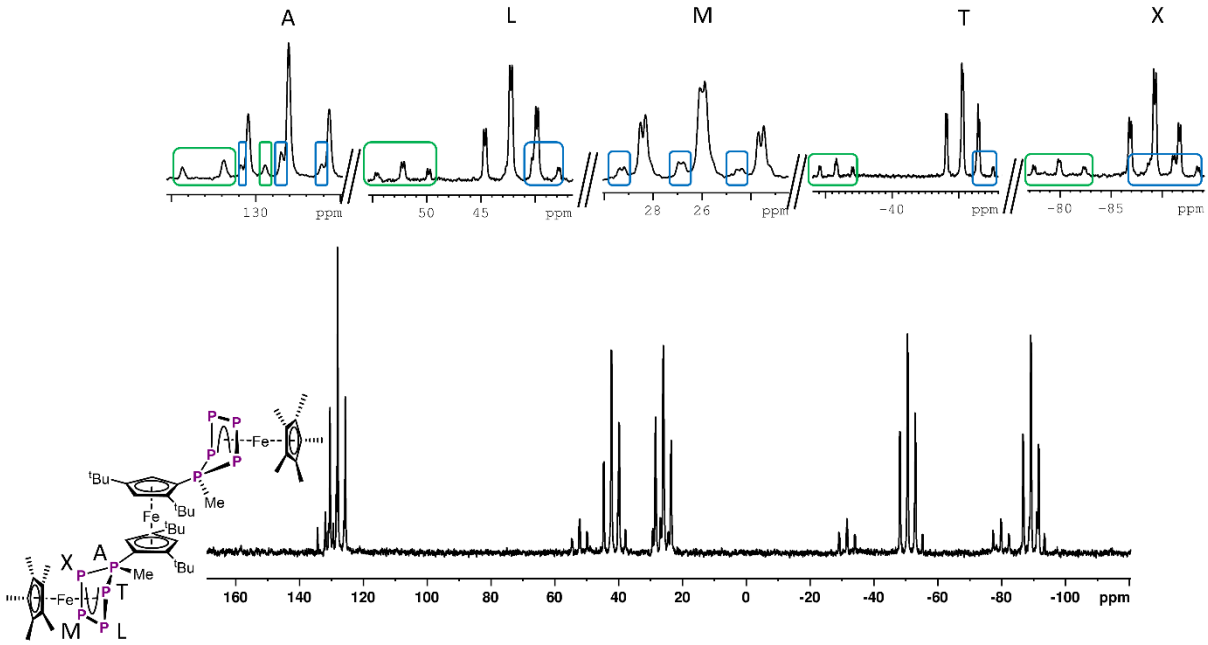

Figure S3.18: $^{31}P\{^{1}H\}$ NMR spectrum of **5**, measured in Tol-d_8 at 293 K.

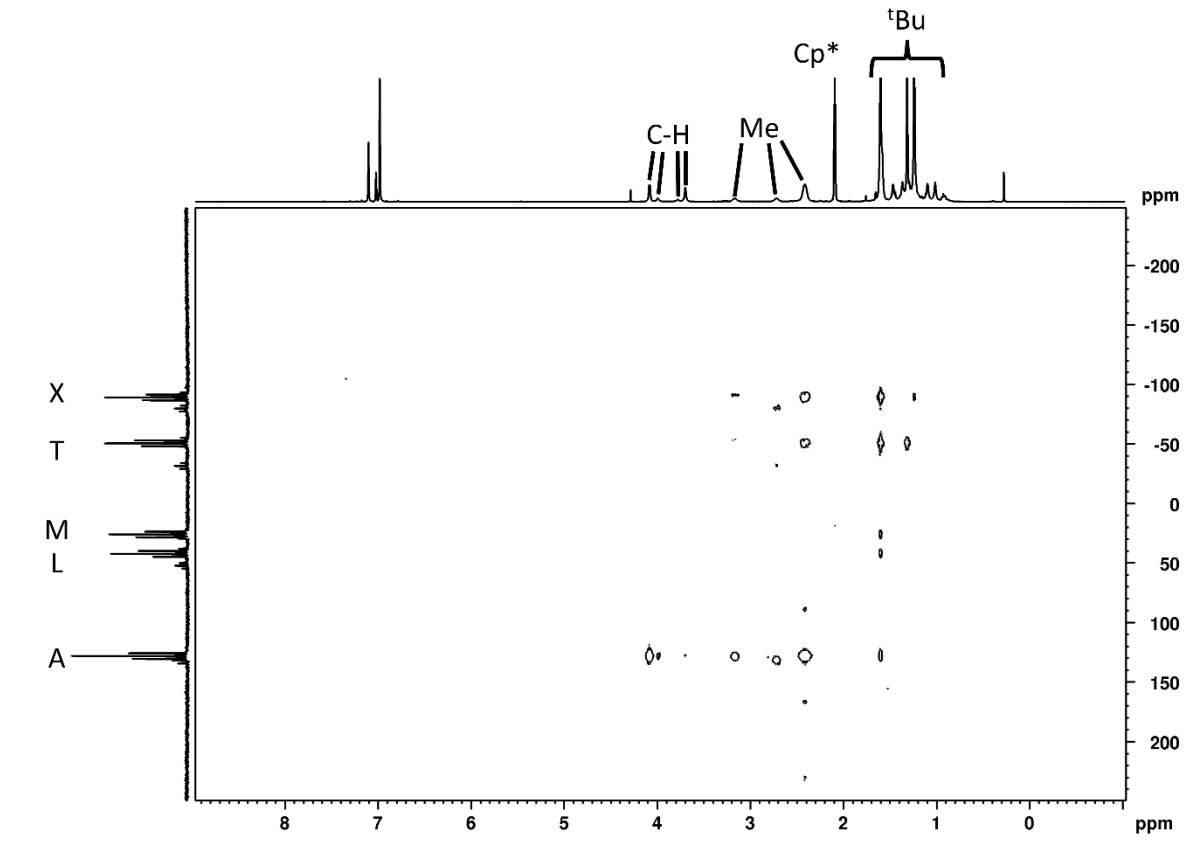

Figure S3.19: ^{1}H-^{31}P-HMBC. Measured in Tol-d_8 at 298 K.

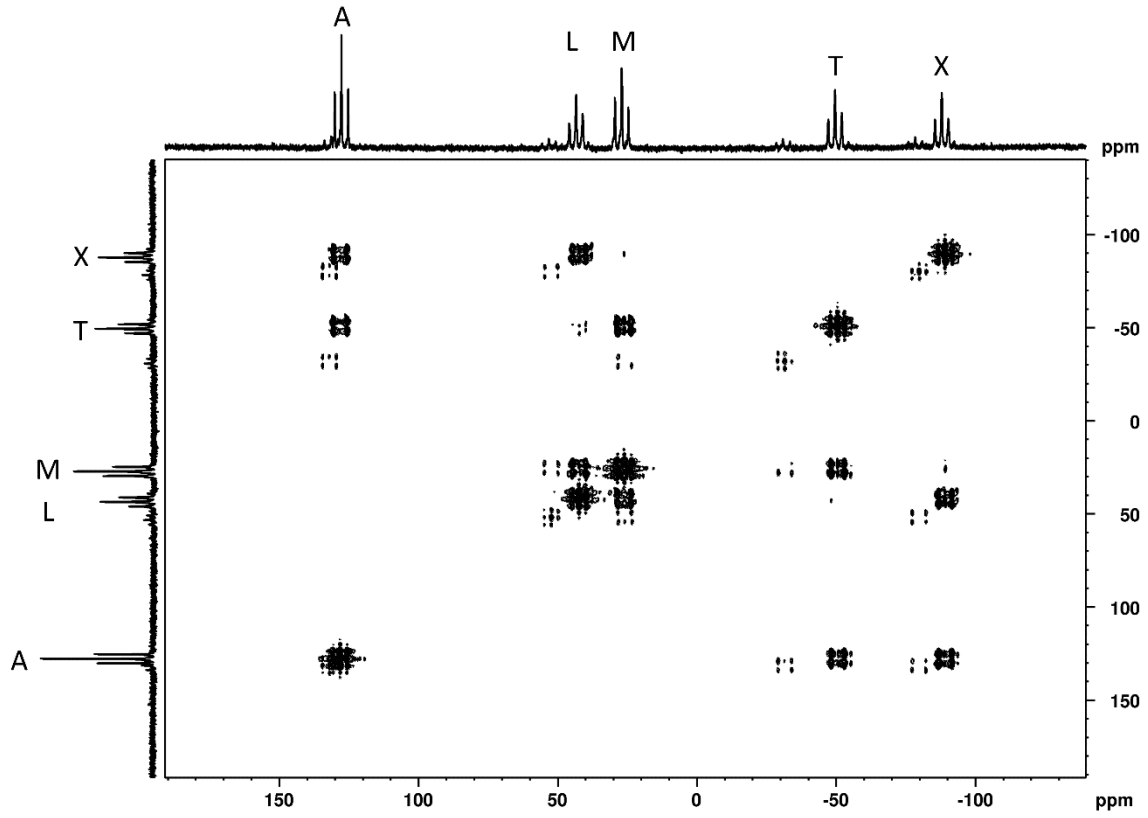

Figure S3.20: ^{31}P-^{31}P-COSY of **5**. Measured in Tol-d_8 at 298 K.

It should be mentioned that the isomer mixture of **5** shows three distinguishable isomers. It is assumed that the sterically demanding environment causes discrimination of the different enantiomers, which makes detection by NMR spectroscopy possible. In the computational part (see Table S8.2), possible conformers with their respective relative energies were calculated, which attempt to theoretically rationalize this circumstance.

3.5.2 Purified [{Cp*Fe(η⁴-P₅Me(C₅H₂ᵗBu₂)}₂Fe]

Purification of the isomeric mixture of **5** can be either performed by selective crystallization of the isomeric mixture of **5** or by column chromatography. However, due to the nearly identical solubilities of all isomers, purification of isomerically pure **5** by column chromatography could up to this point only achieved once. **5** is well soluble in C_6D_6, enabling the recording of the NMR spectra with ease. The ^1H NMR spectrum at room temperature (Figure S3.21) shows two separate signals for the ^{t}Bu substituents of the Cp´´ at δ = 1.23 ppm and δ = 1.31 ppm, a sharp singlet at δ = 1.31 ppm, for the Cp* ligand, one broad signal at δ = 2.41 ppm for the Me group

and two singlet at δ = 3.70 ppm and δ = 4.12 ppm for the residual H-atoms in the Cp´´ fragment. The $^{31}P\{^{1}H\}$ (Figure S3.22) as well as the ^{31}P NMR (Figure S3.23) show similar to **2** an ALMTX spin system. However, at room temperature a determination of the coupling constants by simulation is not possible due to significant broadening of the signals. For better resolution, the respective $^{31}P\{^{1}H\}$ (Figure S3.25) as well as the ^{31}P NMR (Figure S3.26) spectra were recorded at –80 °C. Chemical shifts and coupling constants are provided in Table S3.4. Despite the better resolution of the ^{31}P NMR spectra, the ^{1}H NMR spectrum of **5**, measured at – 80 °C (Figure S3.24) did not exhibit sharper resonance signals.

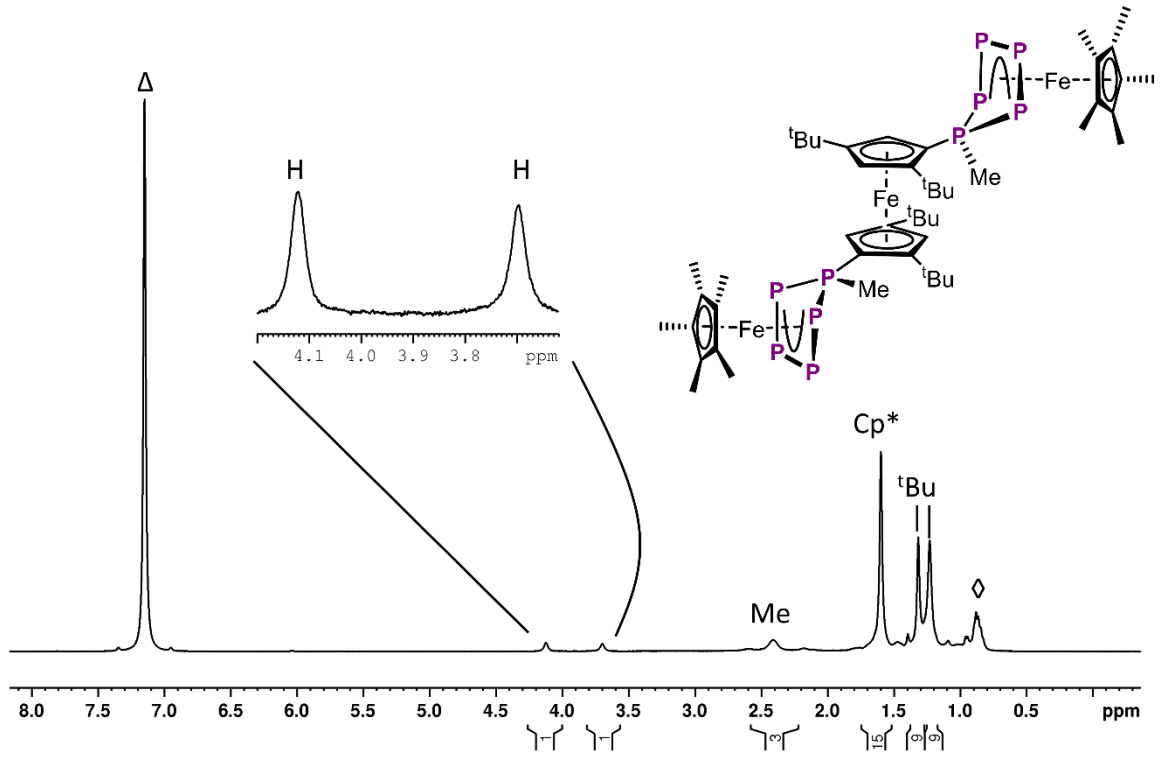

Figure S3.21: ^{1}H NMR spectrum of **5**, measured in C_6D_6 at 298 K. Δ marks the signal for the residual solvent signal for C_6D_6. ◊ marks the solvent signal for *n*-hexane, contained in the asymmetric unit cell, according to single crystal analysis.

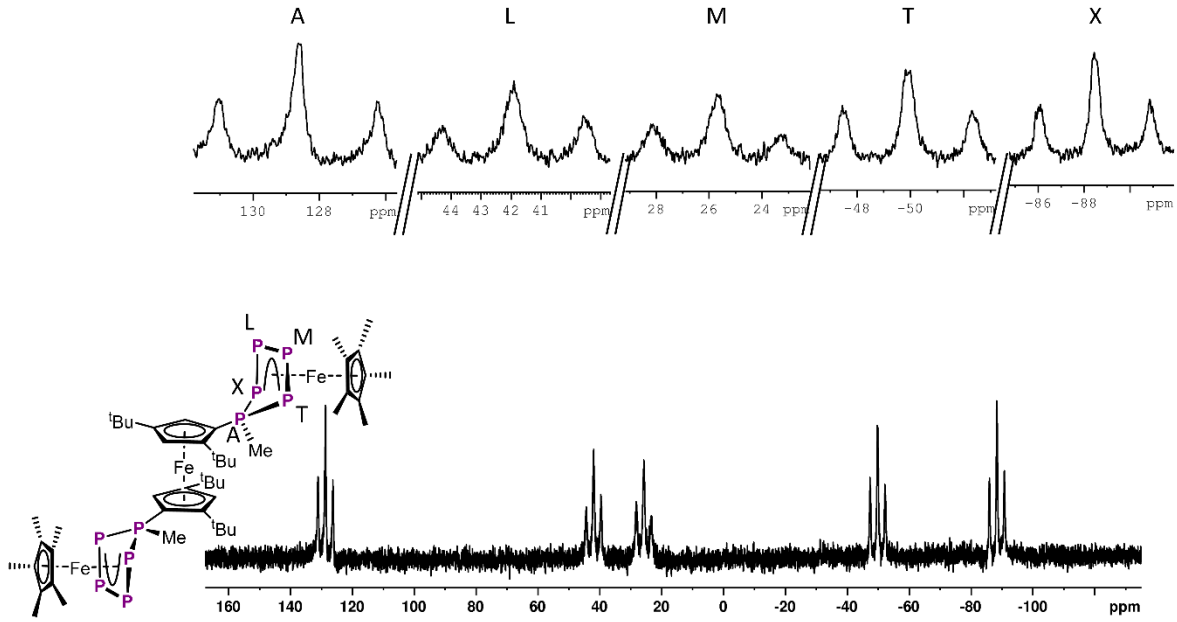

Figure S3.22: $^{31}P\{^{1}H\}$ NMR spectrum of **5**, measured in C_6D_6 at 298 K.

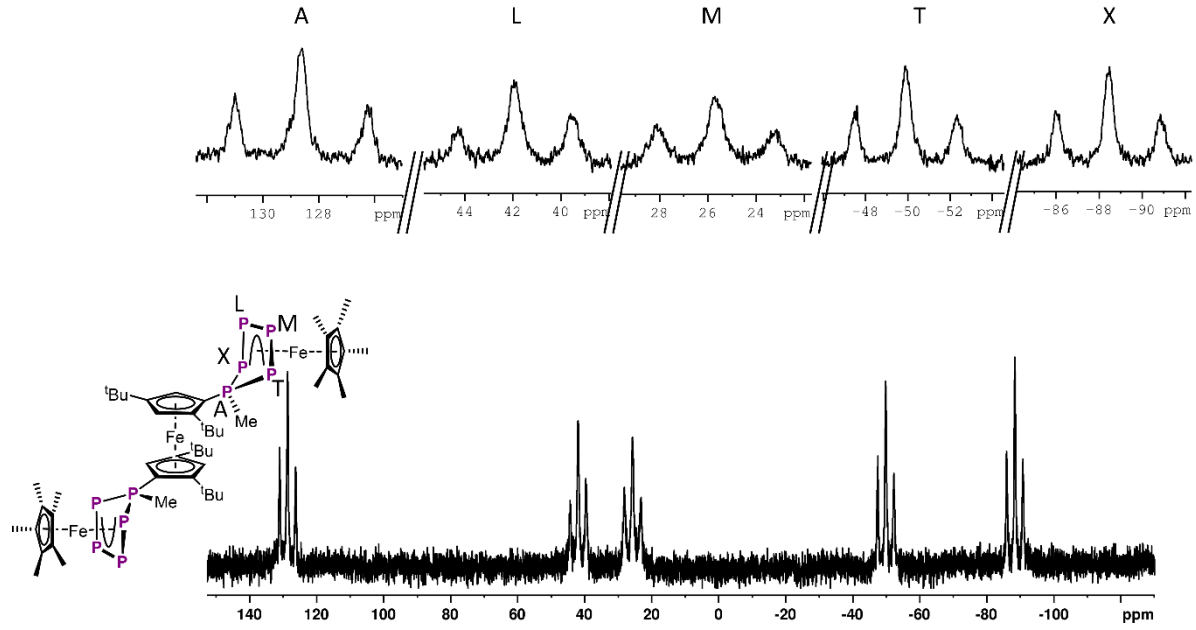

Figure S3.23: ^{31}P NMR spectrum of **5**, measured in C_6D_6 at 298 K.

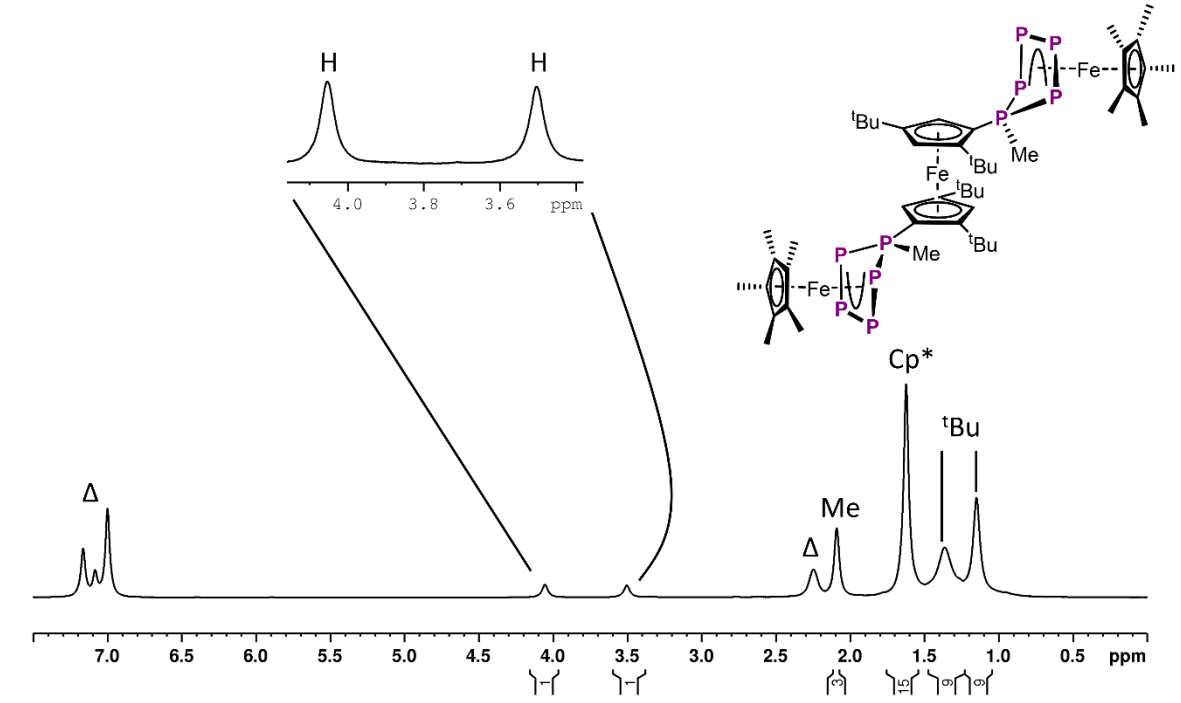

Figure S3.24: ^{1}H NMR spectrum of **5**, measured in Tol-d_8 at 193 K. Δ marks the signal for the residual solvent signal of Tol-d_8.

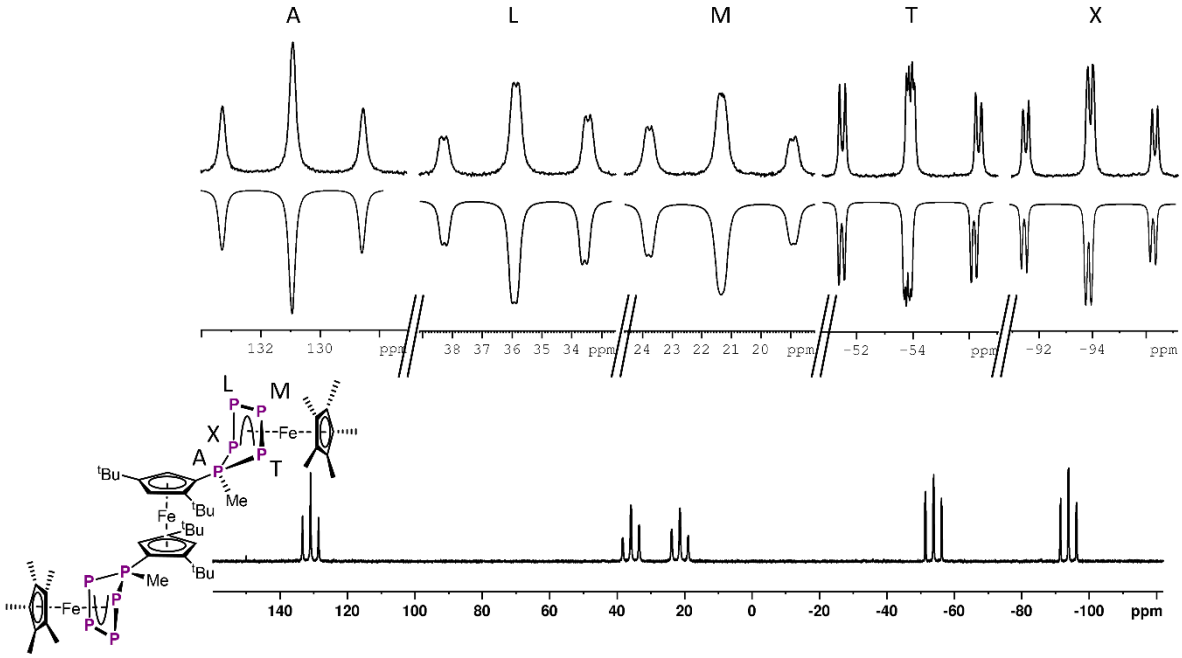

Figure S3.25: ^{31}P{^{1}H} NMR spectrum of **5**, measured in Tol-d_8 at 193 K.

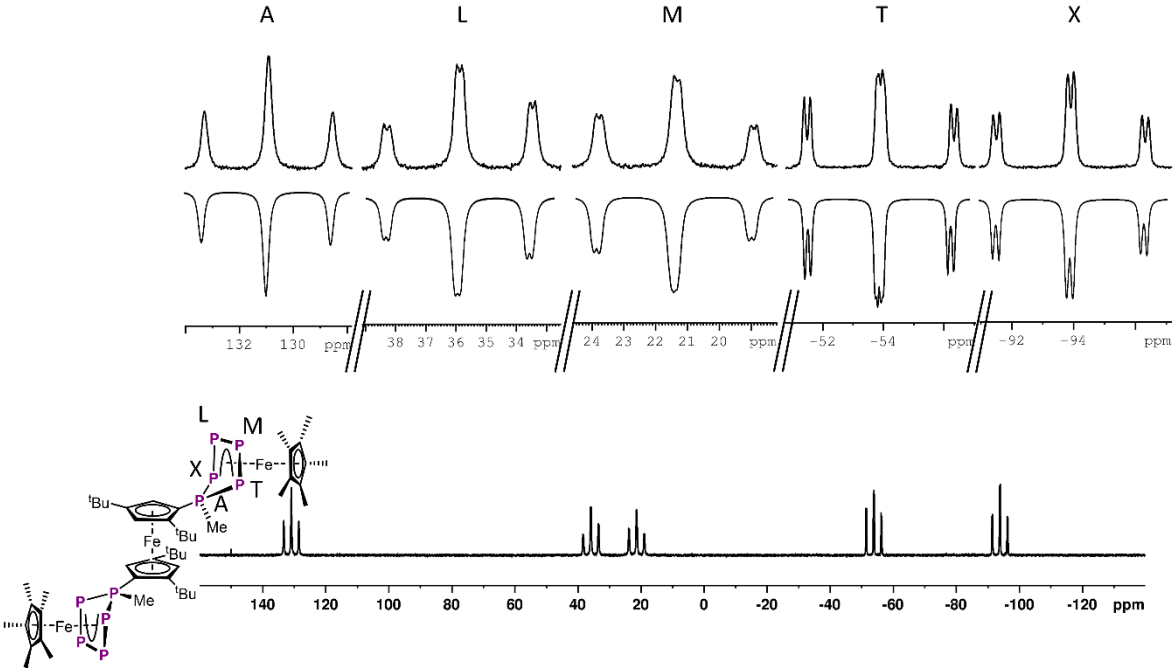

Figure S3.26: ^{31}P NMR spectrum of **5**, measured in Tol-d_8 at 193 K.

Table S3.4: Chemical shifts and coupling constants of **5**, extracted from the simulated ^{31}P NMR spectrum of **5**, measured in Tol-d_8 at 193 K.

***J* (Hz)**		**δ (ppm)**	
$^1J_{PA-PX}$	374.9	130.9	P^A
$^1J_{PA-PT}$	400.8	35.8	P^L
$^1J_{PX-PL}$	400.4	21.4	P^M
$^1J_{PT-PM}$	400.5	−53.9	P^T
$^1J_{PL-PM}$	378.7	−93.9	P^X
$^2J_{PA-PM}$	10.1		
$^2J_{PA-PL}$	12.0		
$^2J_{PX-PM}$	32.0		
$^2J_{PL-PT}$	34.1		
$^2J_{PX-PT}$	3.5		

$^{2}J_{PA-H}$	Not determinable

3.6 [{Cp*Fe(η⁴-P₅Me(C₅H₂ᵗBu₂)}FeCp´´] (6)

Compound **6** shows excellent solubility in C_6D_6. The ^{1}H NMR spectrum of **6** (Figure S3.27) shows four separate signals for the ^{t}Bu groups which can be detected at δ = 1.12 ppm, 1.21 ppm, 1.34 ppm and 1.35 ppm. Furthermore, the signal for the Cp* ligand can be detected at δ = 1.67 ppm. The Me-group, bound at the 1-position, shows a signal at δ = 2.67 ppm. The remaining signals for the hydrogen atoms on the Cp´´ ligand can be detected between δ = 3.77 and 4.10 ppm. The ^{31}P{^{1}H} (Figure S3.28) as well as the ^{31}P NMR spectrum (Figure S3.29) respectively, show, similarly to **2** and **5**, a ALMTX spin system with chemical shifts and coupling constants provided in Table S3.5. The signal P^A shows an additional coupling to the Me-group.

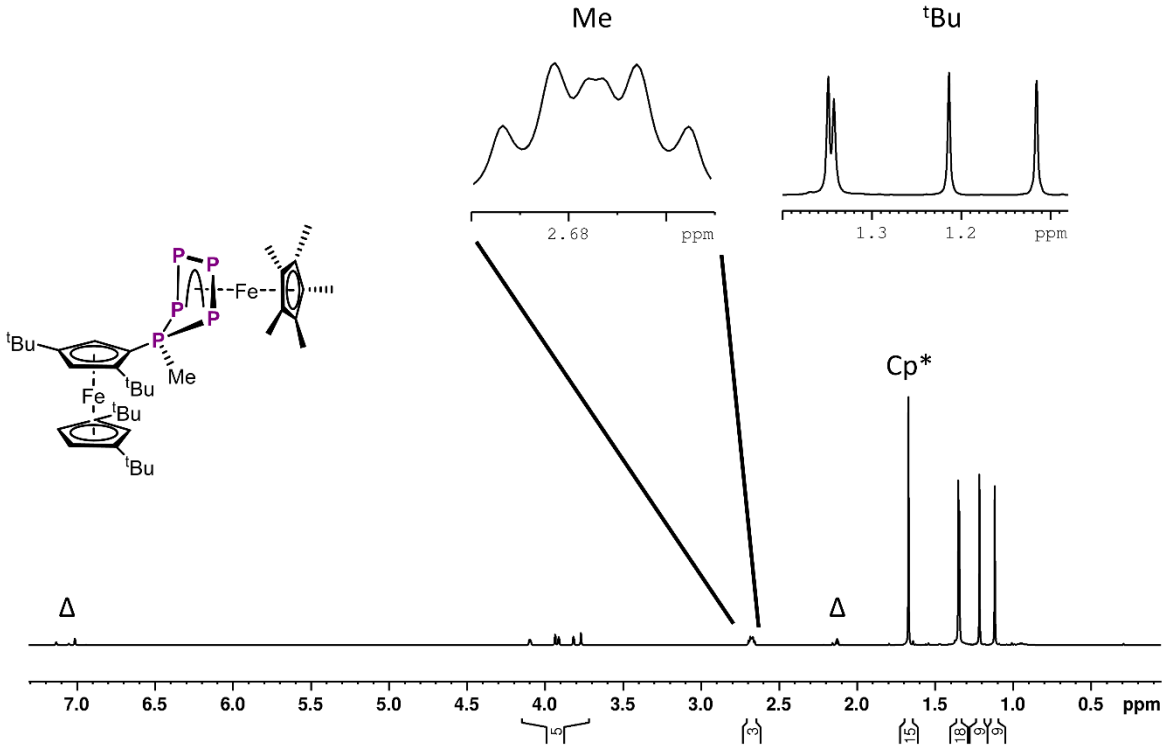

Figure S3.27: ^{1}H NMR spectrum of **6**, measured in Tol-d_8 at 298 K. Δ marks the signal for the residual solvent signal of Tol-d_8.

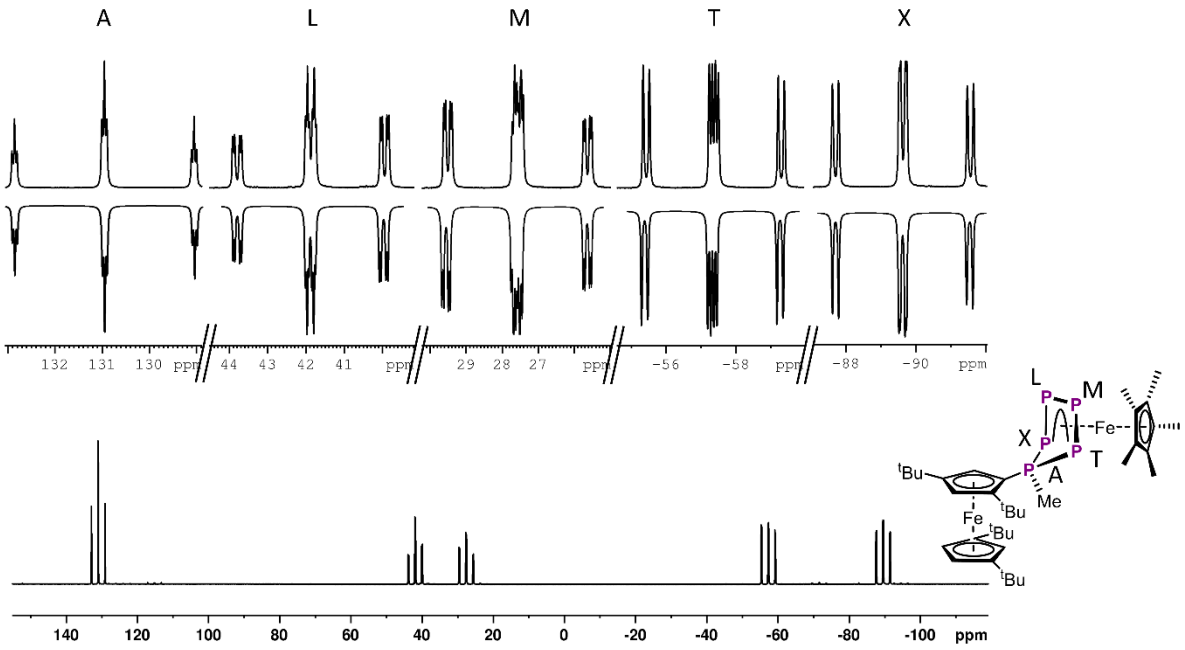

Figure S3.28: $^{31}P\{^{1}H\}$ NMR spectrum of **6**, measured in Tol-d_8 at 298 K.

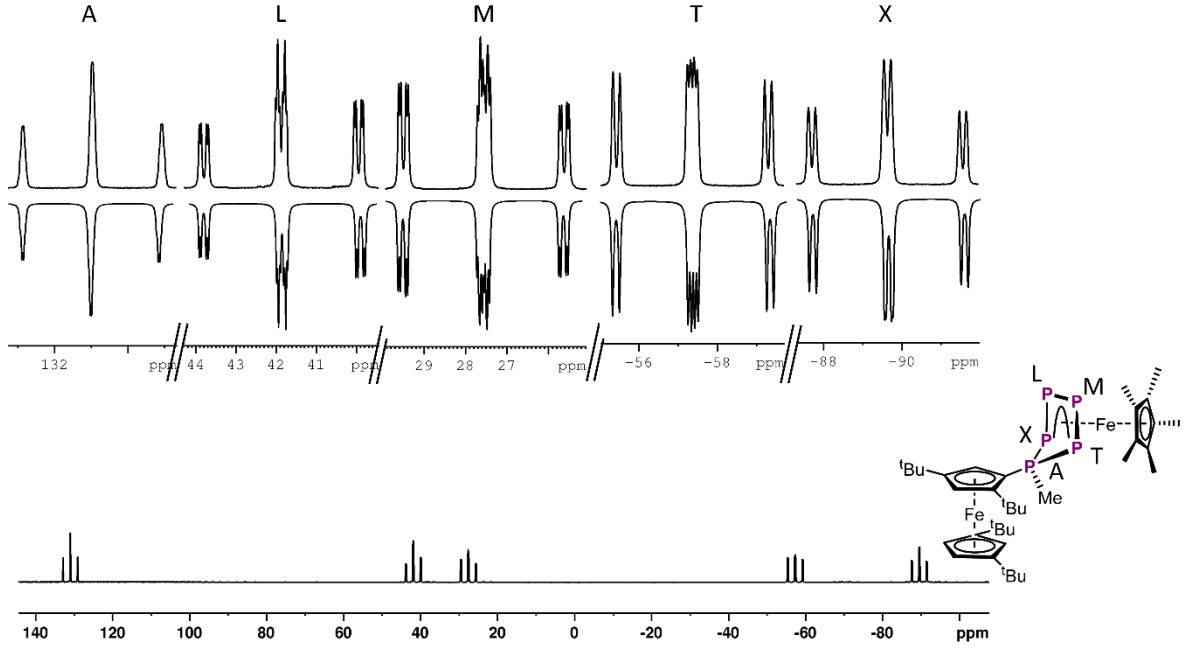

Figure S3.29: ^{31}P NMR of **6**, measured in Tol-d_8 at 298 K.

Table S3.5: Chemical shifts and coupling constants of **6**, extracted from the simulated ^{31}P NMR spectrum of **6**, measured in Tol-d_8 at 298 K.

***J* (Hz)**		**δ (ppm)**	
$^{1}J_{PA-PX}$	386.2	131.0	P^{A}

$^{1}J_{PA-PT}$	384.1	41.8	P^{L}
$^{1}J_{PX-PL}$	397.4	27.6	P^{M}
$^{1}J_{PT-PM}$	403.4	−57.4	P^{T}
$^{1}J_{PL-PM}$	386.2	−89.6	P^{X}
$^{2}J_{PA-PM}$	10.8		
$^{2}J_{PA-PL}$	10.4		
$^{2}J_{PX-PM}$	33.9		
$^{2}J_{PL-PT}$	34.2		
$^{2}J_{PX-PT}$	3.8		
$^{2}J_{PA-H}$	8.7		

3.7 [{Cp*Fe(η⁴-P₅Me(C₅H₂ᵗBu₂)}₂Fe][FAl]₂ (7)

7 shows excellent solubility in CD_2Cl_2, enabling the NMR spectra to be recorded with ease. The ^1H NMR spectrum of **7** (Figure S3.30) shows several broad signals between −15 ppm and 4 ppm. The ^{31}P as well as the $^{31}P\{^1H\}$ NMR spectra both show no detectable signals. The $^{19}F\{^1H\}$ NMR spectrum of **7** (Figure S3.31) shows several signals for the $[FAl]^-$ anions, which are in line with literature reports. To determine the number of unpaired electrons of **7**, an additional ^1H NMR spectrum was measured via the Evans method (Figure S3.32).

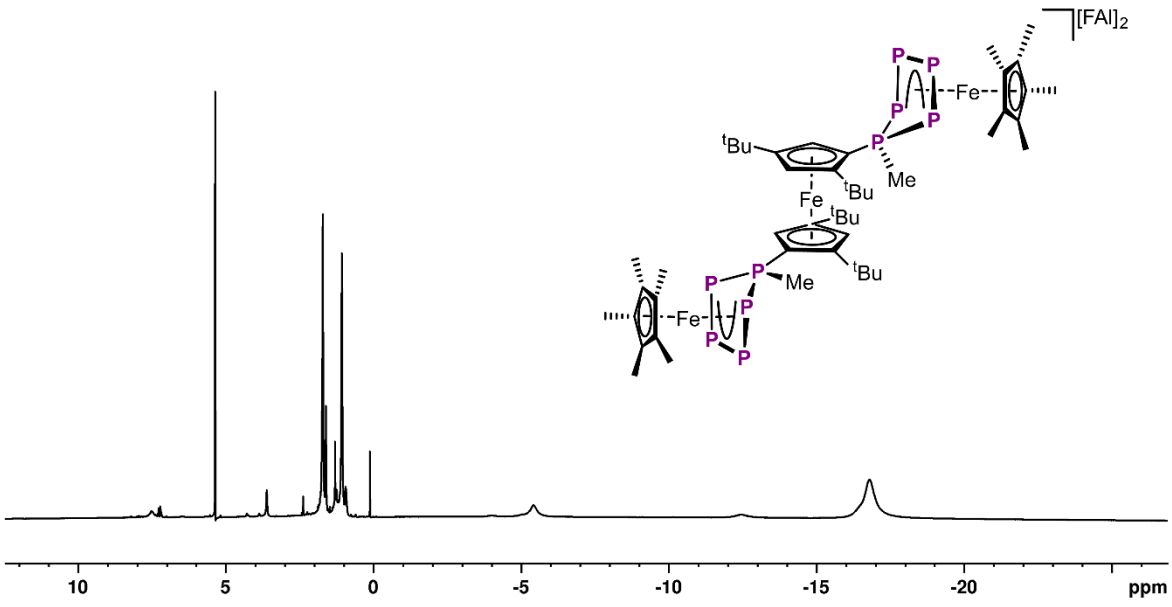

Figure S3.30: ^1H NMR spectrum of crystalline **7**, measured in CD_2Cl_2 at 298 K.

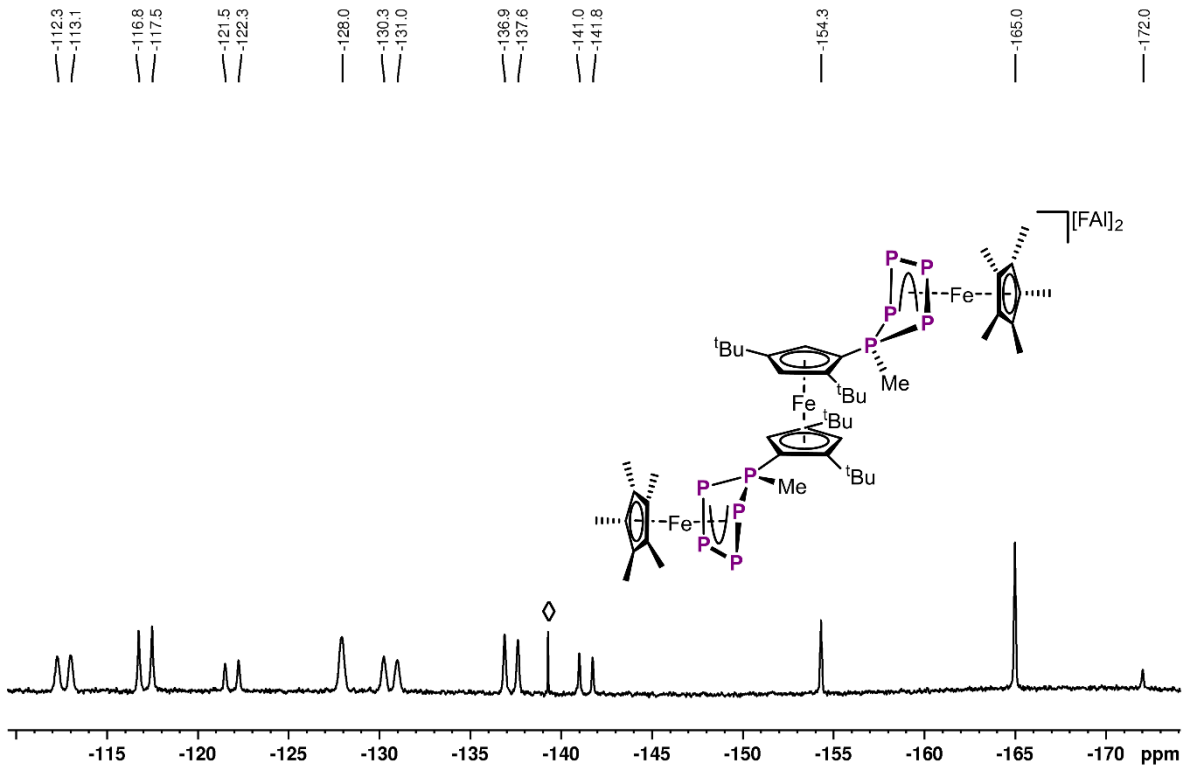

Figure S3.31: $^{19}F\{^{1}H\}$ NMR spectrum of crystalline **7**, measured in CD_2Cl_2 at 298 K. The diamond symbol (◊) marks the signal for the residual solvent signal of *o*-DFB, contained in the asymmetric unit cell.

The number of the unpaired electrons, present in **7**, was determined by the Evans-Method.[9] The contribution of the counteranions ($[FAl]^- = [C_{36}F_{46}AlO_3]^-$) to the diamagnetic molar susceptibility χ_D was calculated as the sum of the covalently bound atoms. Furthermore, the Cp* ligands are modelled according to tabulated values for $[C_5H_5]^-$.[10] Taking all those factors into account, a total effective magnetic moment μ_{eff} of $\mu_{eff} = 2.40\ \mu_B$ was calculated. This results in a number of 1.60 unpaired electrons for **7**. This value provides, as a first rough estimate, a value that agrees with the expected dicationic compound $\mathbf{5}^{2+}$ (**7**).

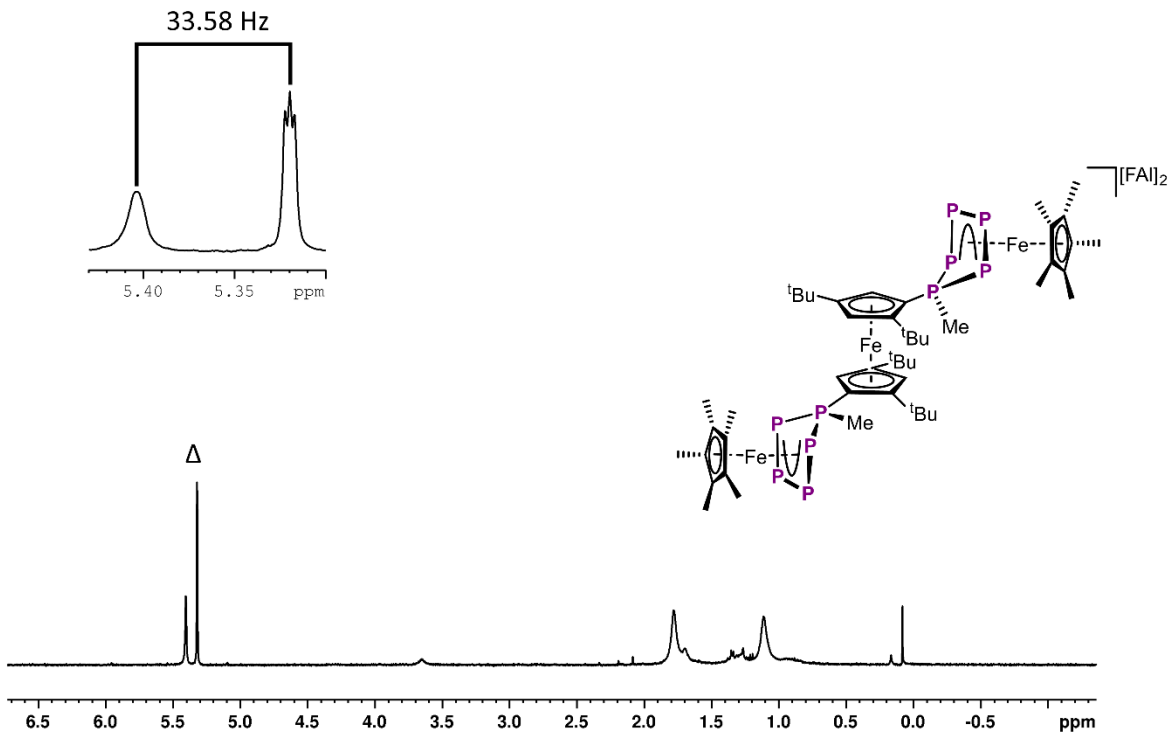

Figure S3.32: ^{1}H NMR spectrum of **7**, measured in CD_2Cl_2 at 298 K. 18 mg of substance were dissolved in 0.7 mL of CD_2Cl_2 inside the NMR tube and a coaxial capillary filled with CD_2Cl_2 was added to determine the number of unpaired electrons in **7** via the Evans NMR method.

4 Electrochemical Investigations

Electrochemical measurements were conducted under argon atmosphere in a custom-built cell with a Pt working, a Pt counter and a Ag/AgCl (pseudo)reference electrode in CH_2Cl_2/ $^nBu_4N^+[BAr^{F24}]^-$ (0.1 M) and THF/ $^nBu_4N^+PF_6^-$ (0.1 M), respectively, as the supporting electrolyte. The working electrode was polished with diamond pastes prior to use (Buehler&Wirtz, 1.0 µm and 0.25 µm). The data was acquired with a computer-controlled BASi Epsilon potentiostat. The cyclic voltammograms were referenced to the $FeCp_2/FeCp_2^+$ redox couple by adding ca. equimolar amounts of decamethylferrocene ($E_{1/2}^{0/+}$ = −540 mV vs. FcH/FcH$^+$) as internal reference.

Quantification of the number of electrons under the oxidation wave in the cyclic voltammograms of compound **5** was done using linear sweep voltammetry and chronoamperometry as published by Baranski, Fawcett and Gilbert.[11] Decamethylferrocene was used as reference substance. The linear sweep voltammograms were recorded with a Pt microelectrode (diameter 50 µm, BASi) as working electrode. The starting potential was chosen so as to keep the faradaic current at a negligibly small level. The potential was varied with a scan rate v of 10 and 20 mV/s, respectively, to a potential sufficiently positive of the wave (> 200 mV), where oxidation occurs under diffusion-control. The height of the potential step then equals i_∞. For chronoamperometric measurements, a glassy carbon working electrode with a diameter of 3 mm was used. The current $i(t)$ was plotted against $t^{-1/2}$ and a linear regression of the diffusion-controlled region was performed to determine the slope S. With the known concentration of the substance c_S and the reference substance c_{ref}, the measured limiting currents from linear sweep voltammetry ($i_{\infty,S}$; $i_{\infty,ref}$) and the slopes of the $i(t)$ vs $t^{-1/2}$ plots from chronoamperometry for substance **5** (S_S) and the decamethylferrocene reference (S_{ref}), equation (1) yields the number of transferred electrons n_S for the redox wave of the substance:

$$n_S = n_{ref} \cdot \frac{S_S^2}{S_{ref}^2} \cdot \frac{i_{\infty,ref}}{i_{\infty,S}} \cdot \frac{c_{ref}}{c_S} \qquad (1)$$

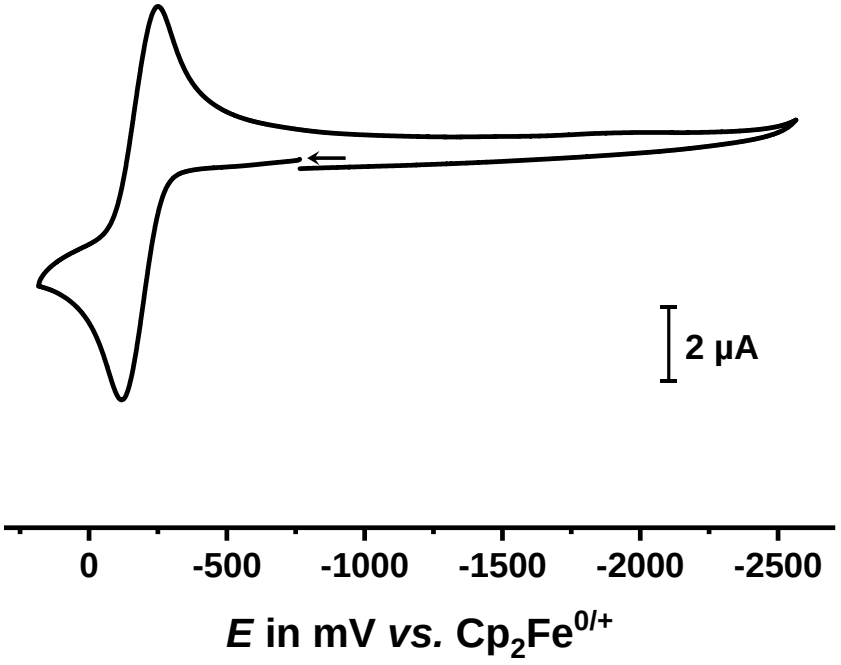

Figure S4.1: Full cyclic voltammogram of **5** in THF/ $^{n}Bu_4N^+$ PF_6^- at a scan rate of 100 mV/s.

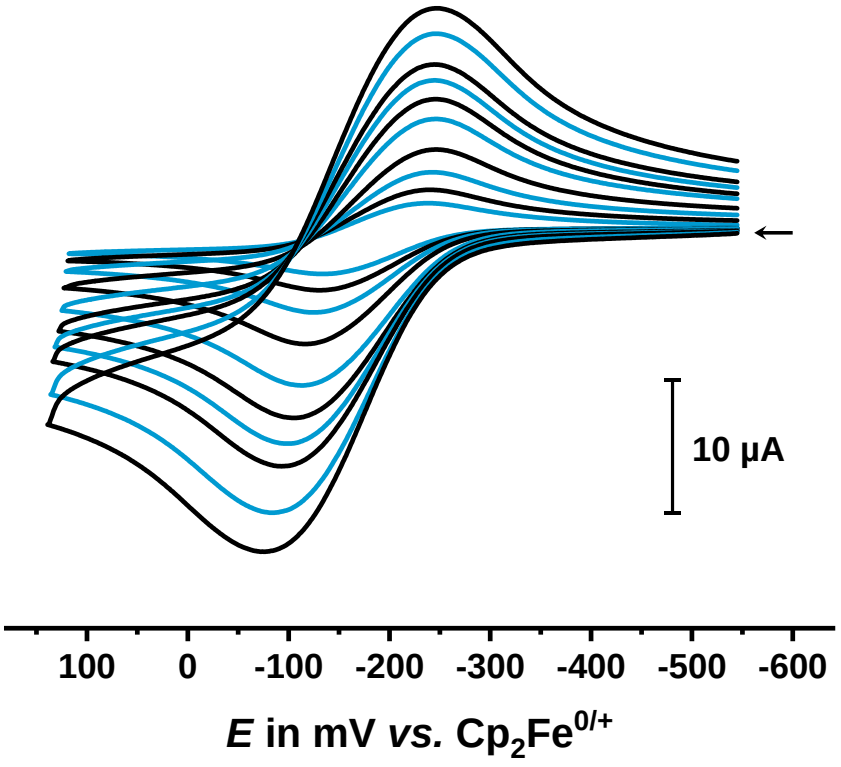

Figure S4.2: Cyclic voltammograms of the first oxidation wave of **5**, measured in THF/ $^{n}Bu_4N^+$ PF_6^- at different scan rates between 25 and 2000 mV/s.

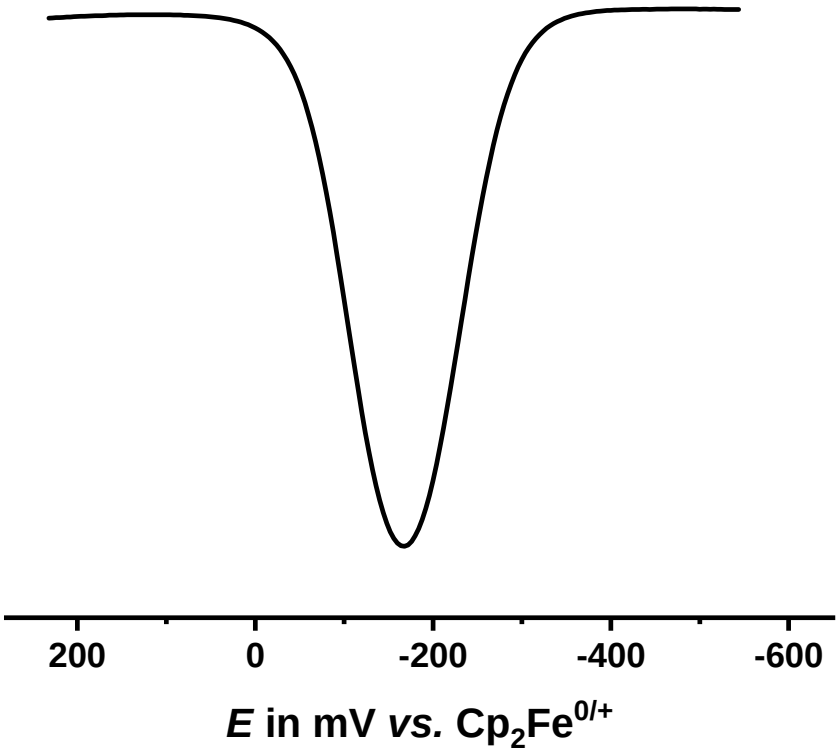

Figure S4.3: Square wave voltammogram of **5** measured in THF/ $^{n}Bu_4N^+ PF_6^-$.

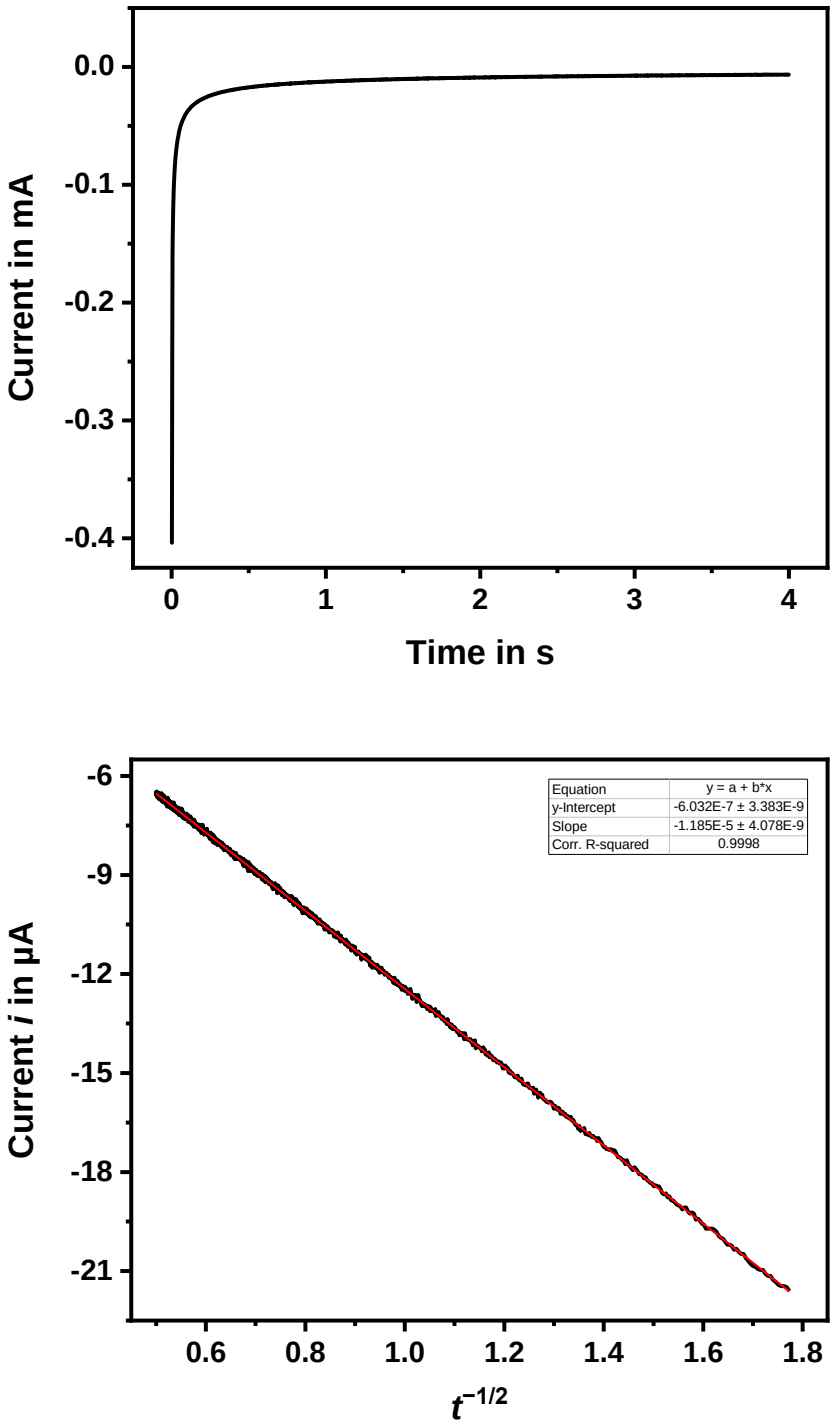

Figure S4.4: (Top) Chronoamperogram of decamethylferrocene in THF/ $^{n}Bu_4N^+$ PF_6^-. (Bottom) Plot of current *i* vs. $t^{-1/2}$.

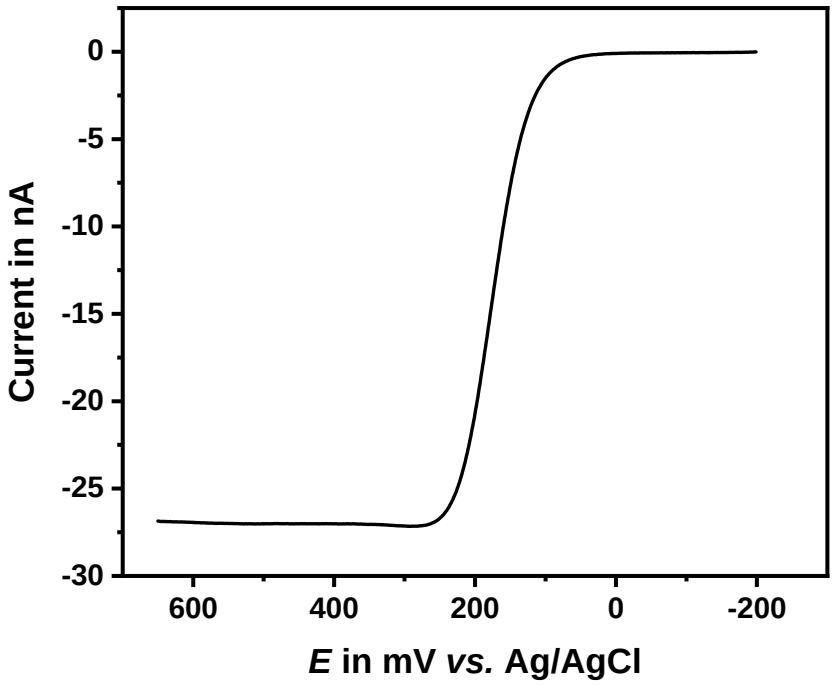

Figure S4.5: Linear sweep voltammogram of decamethylferrocene in THF/ $^{n}Bu_4N^{+}PF_6^{-}$ at a scan rate *v* of 20 mV/s. Limiting current $i_{\infty,S}$ = 26.96 nA.

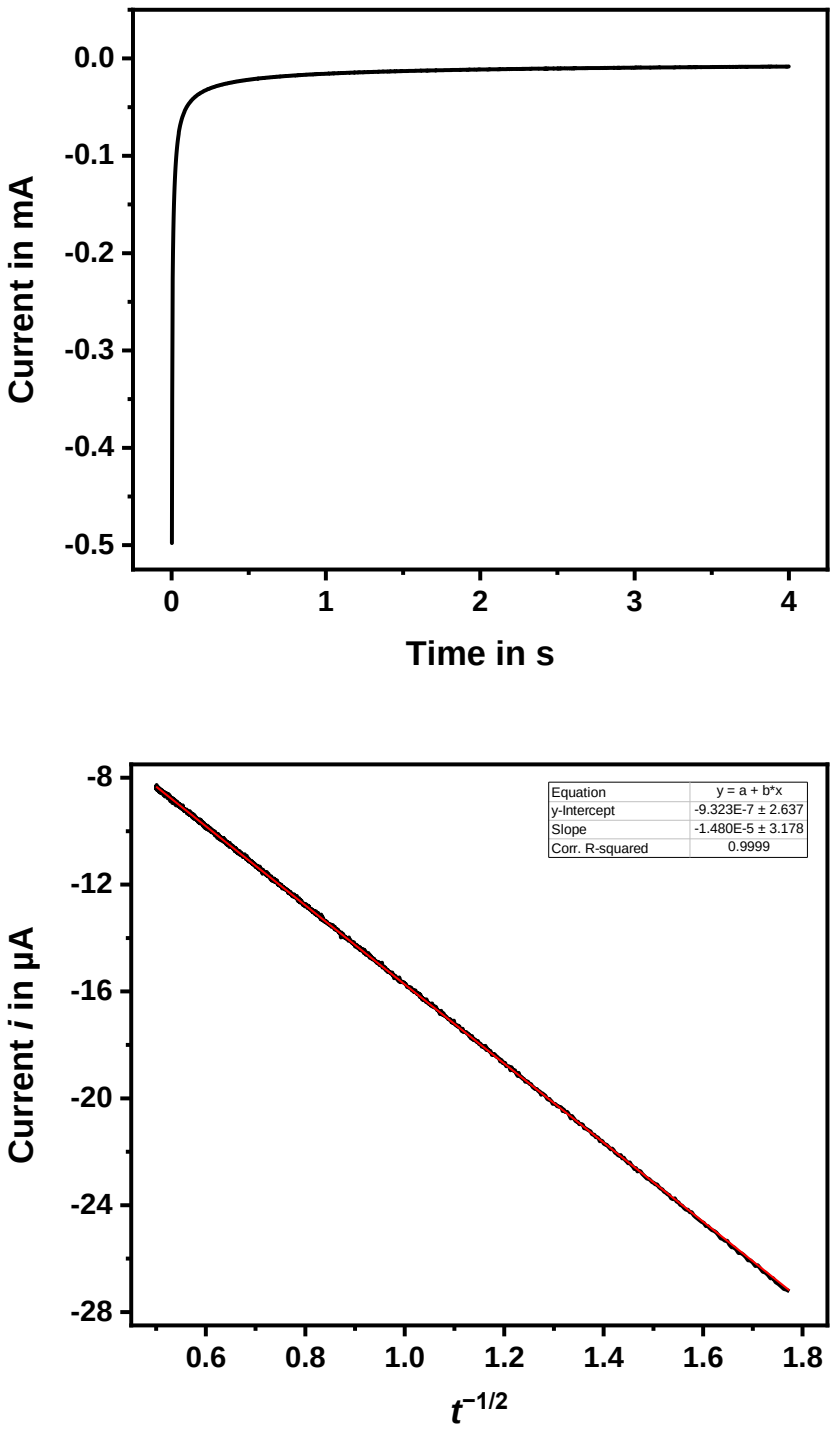

Figure S4.6: (Top) Chronoamperogram of **5** in THF/ $^{n}Bu_4N^+$ PF_6^-. (Bottom) Plot of current *i* vs. $t^{-1/2}$.

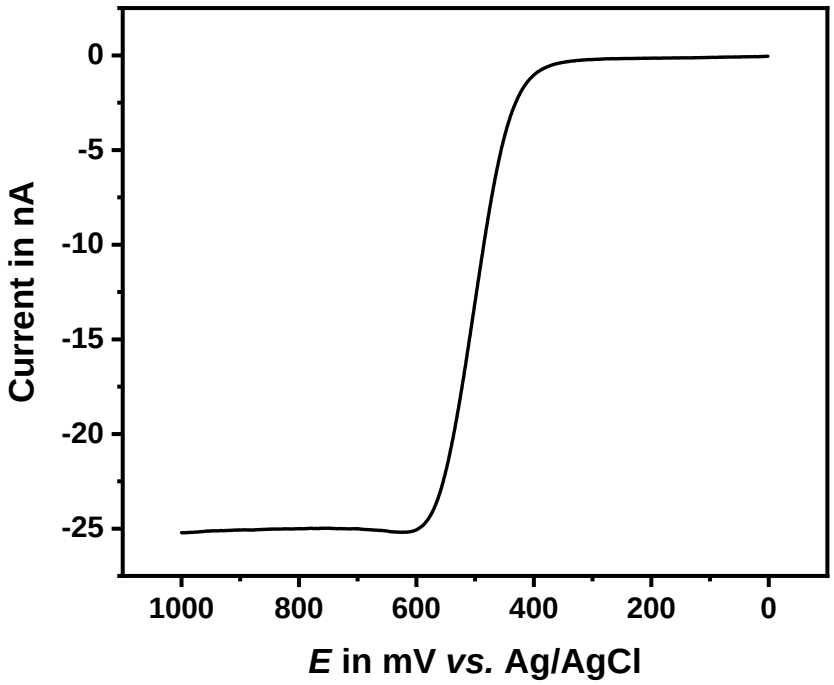

Figure S4.7: Linear sweep voltammogram of **5** in THF/ $^{n}Bu_4N^+$ PF_6^- at a scan rate *v* of 20 mV/s. Limiting current $i_{\infty,S}$ = 24.96 nA.

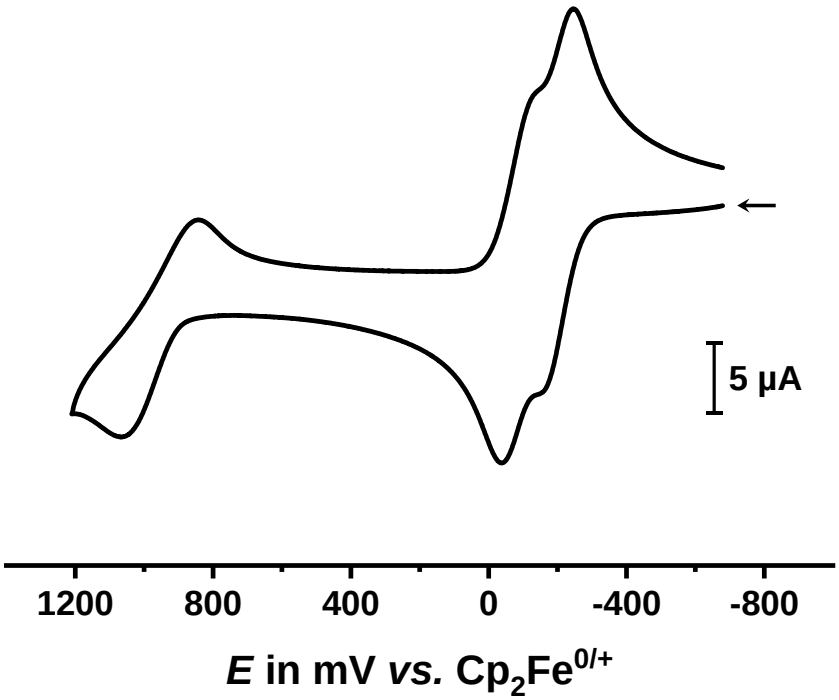

Figure S4.8: Full cyclic voltammogram of **5** in CH_2Cl_2/ $^{n}Bu_4N^+$ $[BAr^{F24}]^-$ at a scan rate of 100 mV/s showing three oxidation waves.

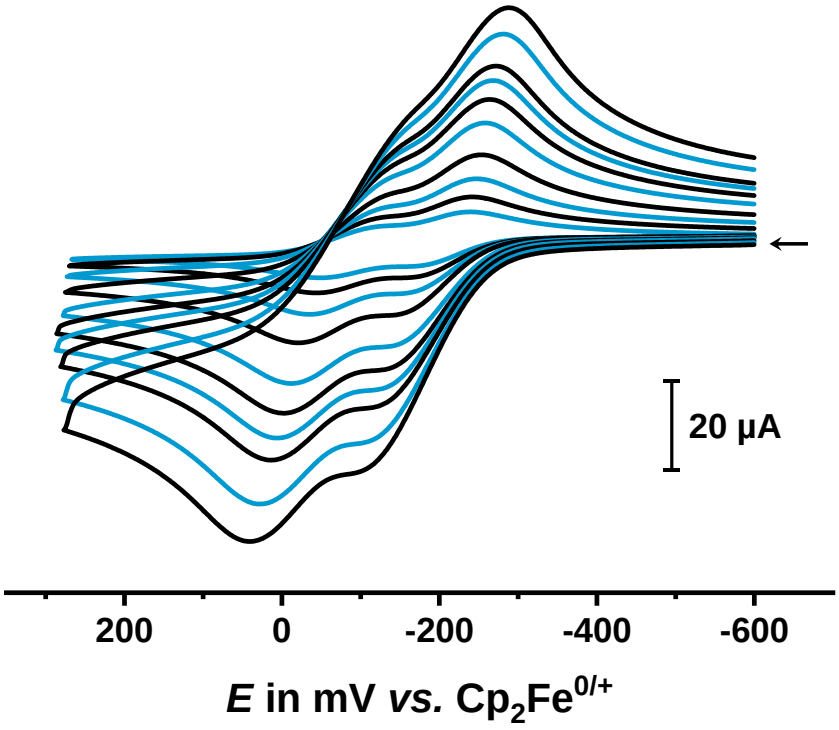

Figure S4.9: Cyclic voltammograms of the first two oxidations of **5**, measured in CH_2Cl_2/ $^nBu_4N^+$ $[BAr^{F24}]^-$ at different scan rates between 25 and 2000 mV/s.

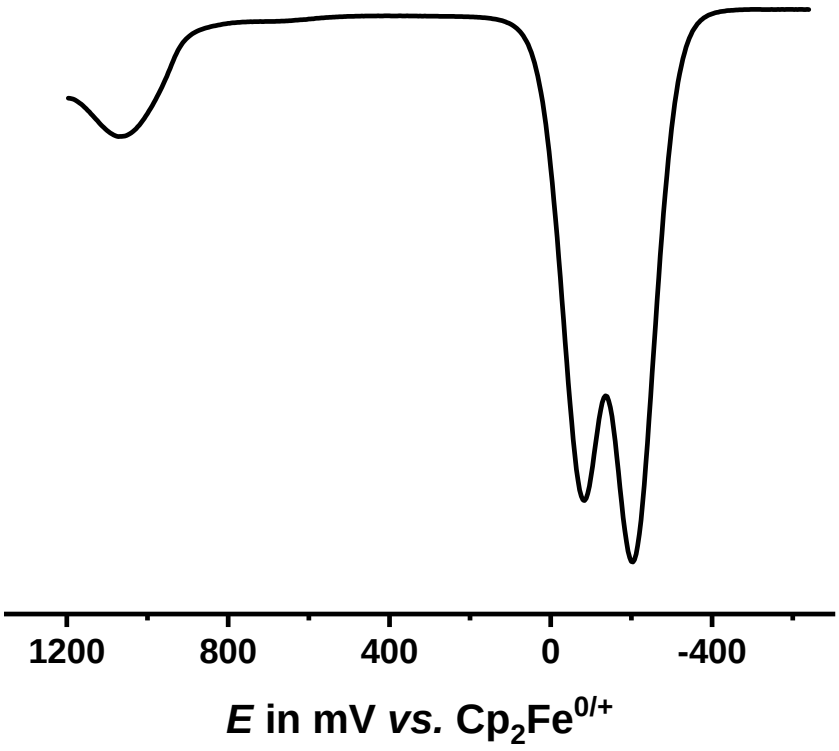

Figure S4.10: Square wave voltammogram of **5** measured in CH_2Cl_2/ $^nBu_4N^+$ $[BAr^{F24}]^-$.

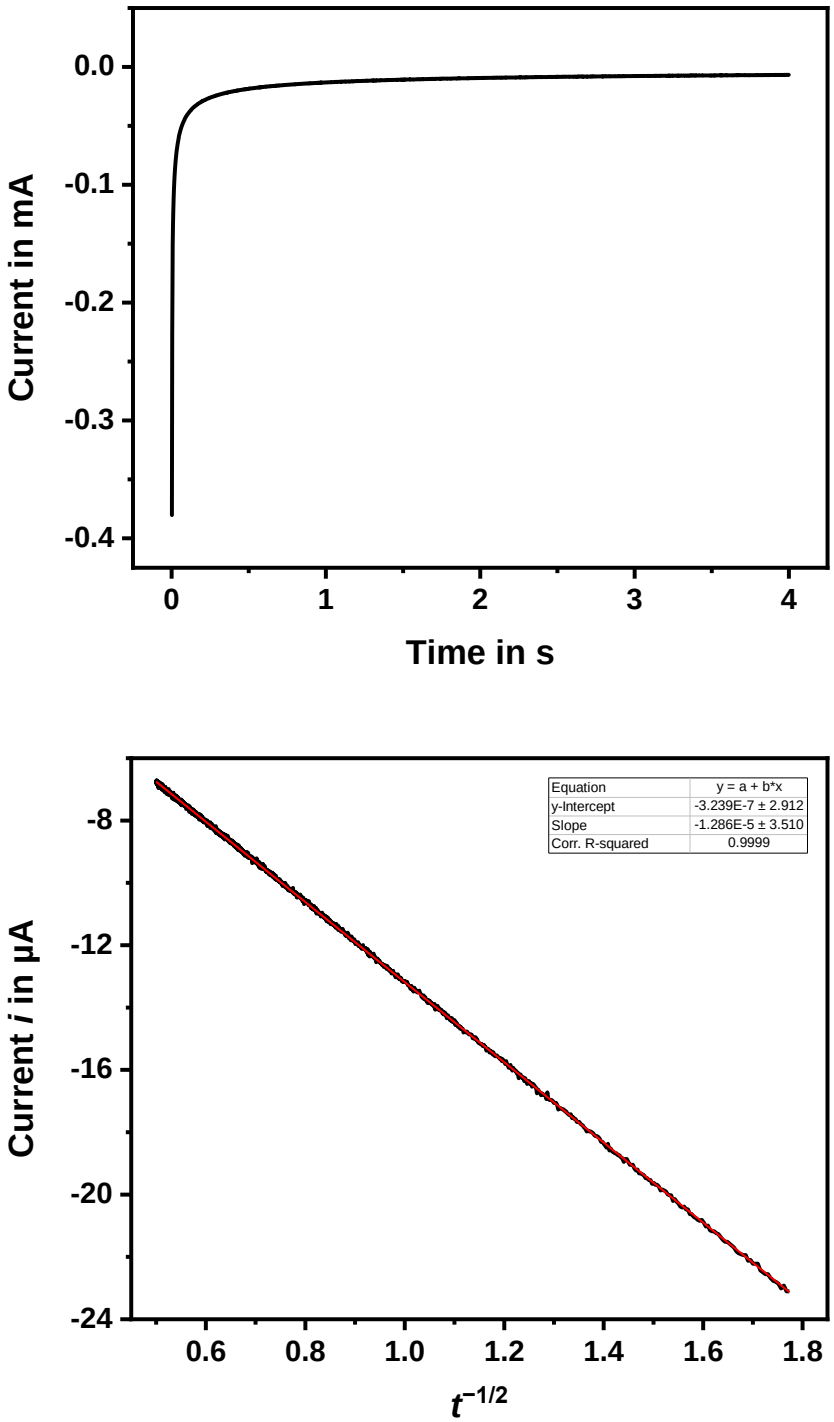

Figure S4.11: (Top) Chronoamperogram of decamethylferrocene in DCM/ $^{n}Bu_4N^+$ $[BAr^{F24}]^-$. (Bottom) Plot of *i* vs. $t^{-1/2}$.

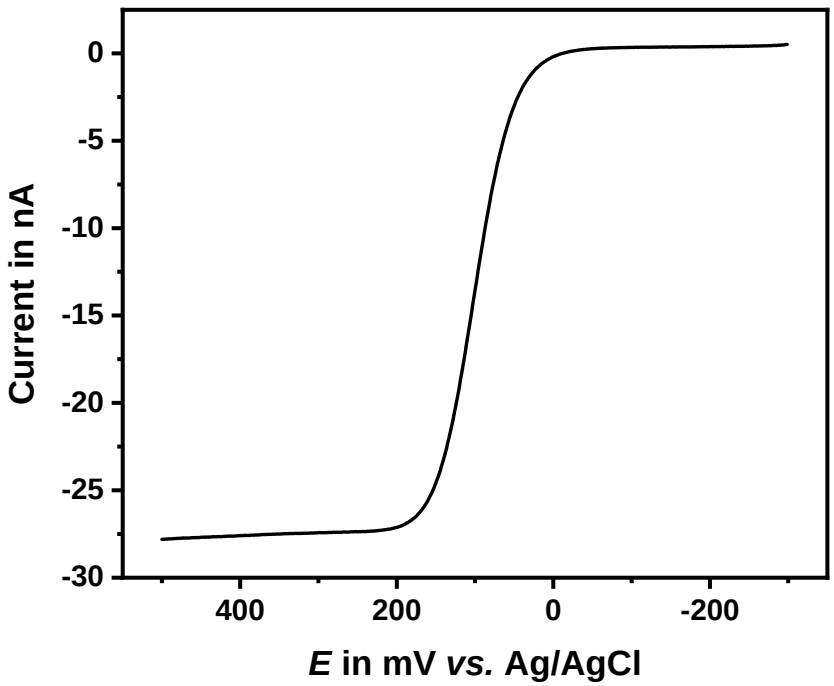

Figure S4.12: Linear sweep voltammogram of decamethylferrocene in DCM/ $^{n}Bu_4N^+$ $[BAr^{F24}]^-$ at a scan rate v of 10 mV/s. Limiting current $i_{\infty,ref}$ = 28.07 nA.

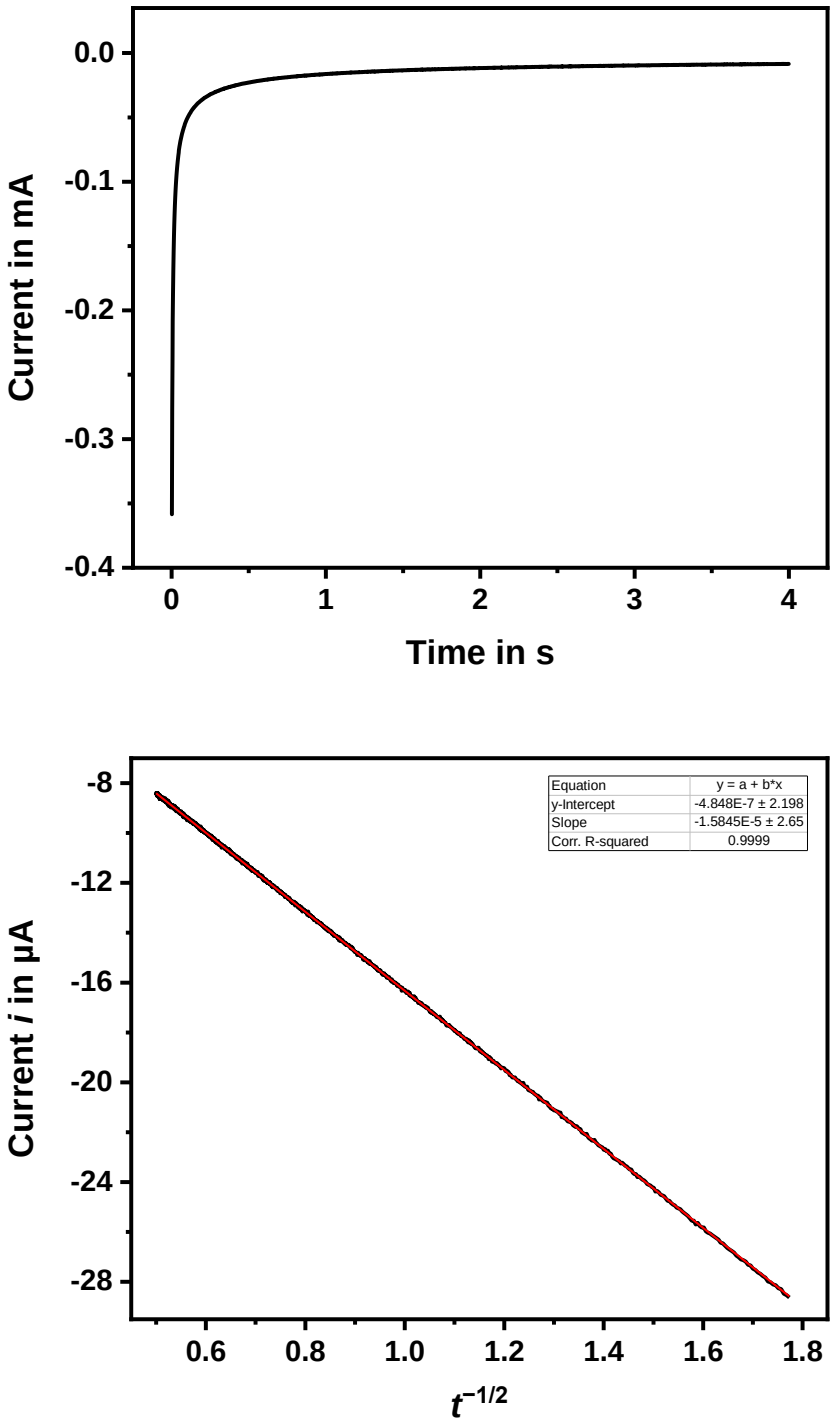

Figure S4.13: (Top) Chronoamperogram of **5** in DCM/ $^{n}Bu_4N^+$ $[BAr^{F24}]^-$. (Bottom) Plot of i vs. $t^{-1/2}$.

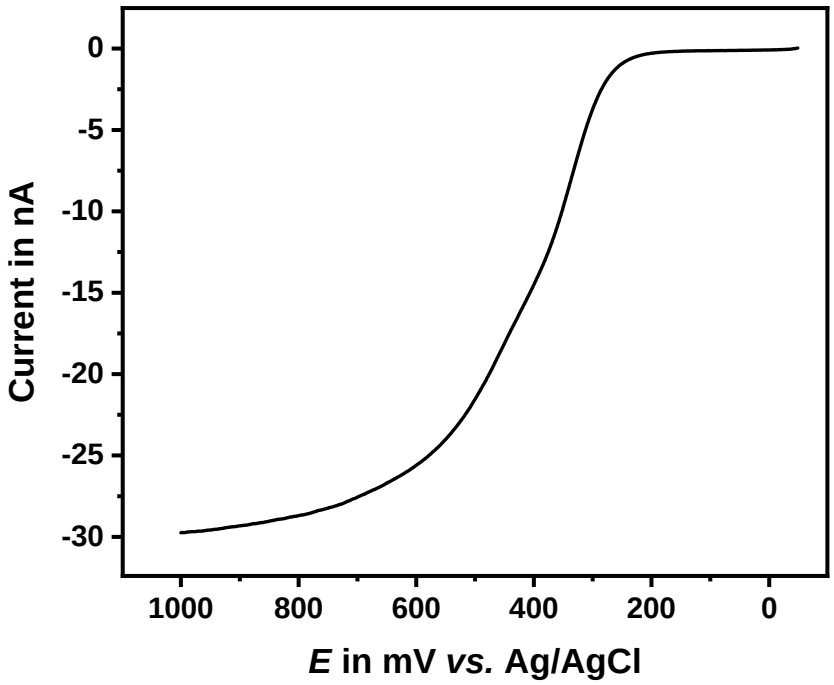

Figure S4.14: Linear sweep voltammogram of **5** in DCM/ $^{n}Bu_4N^+$ $[BAr^{F24}]^-$ at a scan rate v of 10 mV/s. Limiting current $i_{\infty,S}$ = 29.40 nA.

Cyclic and square wave voltammograms of **5** in THF / $^{n}Bu_4N^+PF_6^-$ exhibit just one quasireversible oxidation wave at $E_{1/2}$ = −0.17 V (see Figures S4.1–S4.3) within the accessible potential window of this electrolyte. At first glance, this seems to hint at primary oxidation of the inner ferrocene unit. However, it is also possible that the oxidation occurs at the peripheral Cp*FeP_4 units, their simultaneous oxidation being due to a lack of electronic as well as electrostatic interactions, i. e. complete decoupling. Further analysis of the process via the method published by Baranski et al.[11] (see Section 4 of the Supporting Information for more details and Figures S4.4 – S4.7) shows that the oxidation wave is indeed a two-electron process (n_{app} = 1.8). The deviation from the expected value of n = 2 for a two-electron process can be explained by somewhat sluggish electron transfer kinetics of **5** and inaccuracies in the concentrations. We therefore recorded cyclic voltammograms of **5** also in the very weakly coordinating electrolyte CH_2Cl_2 / $^{n}Bu_4N^+$ BAr^{F24-}, which exhibits a particularly low tendency to ion pair formation. This maximizes electrostatic repulsion between positively charged, adjacent redox sites in the dioxidized state and thereby increases the half-wave potential splitting of redox waves of closely spaced redox systems.[12] In this electrolyte, cyclic voltammograms of **5** (Figure S4.8–S4.9) show indeed two consecutive one-electron redox waves separated by 120 mV ($E_{1/2}^{0/+}$ = −0.20 V mV, $E_{1/2}^{+/2+}$ = −0.08 V mV), as determined by square wave voltammetry (see Figure S4.10). Quantitative analysis of the oxidation waves provides a value of n = 1.8 electrons as determined by linear sweep voltammograms and chronoamperograms according to the method of Baranski (see Figures S4.7–S4.10 for the corresponding data), which equals the value obtained for the THF / $^{n}Bu_4N^+$ PF_6^- electrolyte. This substantiates that the oxidation

wave in THF / $^{n}Bu_4N^+PF_6^-$ is indeed a two-electron process. As the much wider anodic discharge limit of the CH_2Cl_2 / $^{n}Bu_4N^+BAr^{F24-}$ electrolyte extends the accessible potential window to distinctly more positive values compared to THF, we could even detect a third one-electron oxidation ($E_{1/2}^{2+/3+}$ ca. 1.07 V), which is then ascribed to oxidation of the inner ferrocene unit. The large anodic shift compared with 1,1'-bis(dialkyl- or -arylphosphino)ferrocenes (η^5-$C_5H_4PR_2)_2Fe$ (e. g. $E_{1/2}$ = 0.06 V for R = ^{t}Bu,[13] 0.05 V for R = ^{i}Pr,[14] or ca. +0.18 V for R = Ph[15]) being due to electrostatic repulsion by the adjacent, positively charged Cp*FeP_4 units.

For additional reasons of clarity, a cyclic voltammogram of **2** was additionally performed in order to examine the differences between **2** and **5**. The cyclic voltammogram of **2** shows one quasi-reversible oxidation wave at a half-wave potential of −0.19 V.

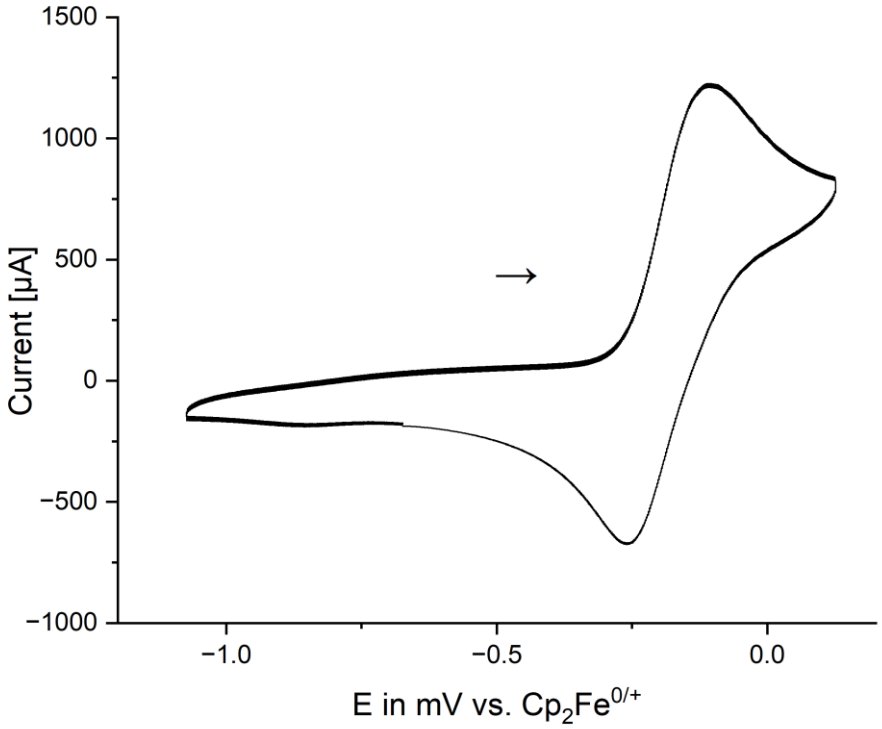

Figure S4.15: Full cyclic voltammogram of **2** in THF/ $^{n}Bu_4N^+[PF_6]^-$ at a scan rate of 100 mV/s showing one oxidation wave (c(**2**) = 10 mmol L^{-1}).

5 EPR Spectroscopy

EPR measurements were performed on an ElexSys E580 spectrometer (Bruker BioSpin) equipped with a MS3 split-ring resonator. The temperature was controlled with a helium gas flow cryostat CF935-O and an intelligent temperature controller ITC502 (both from Oxford Instruments). The samples were prepared inside a nitrogen-filled glovebox, filled into 3 mm Quartz tubes and immediately frozen in liquid nitrogen after removal from the glovebox.

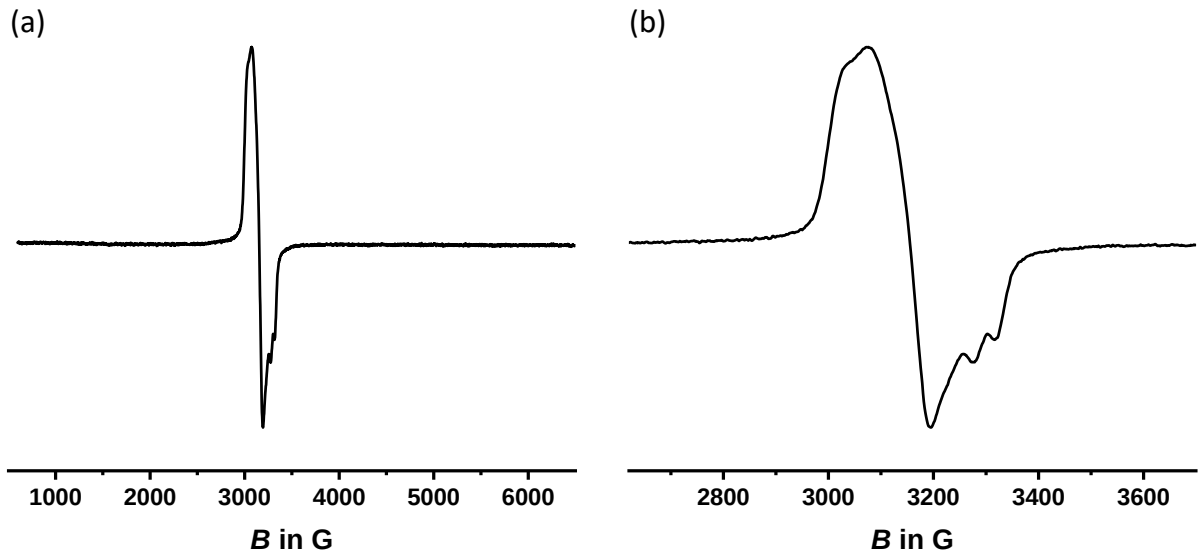

Figure S5.1: (a) Full-sweep X-band EPR spectrum of **7**, measured in CH_2Cl_2 at 10 K. (b) Zoom-in of the EPR signal.

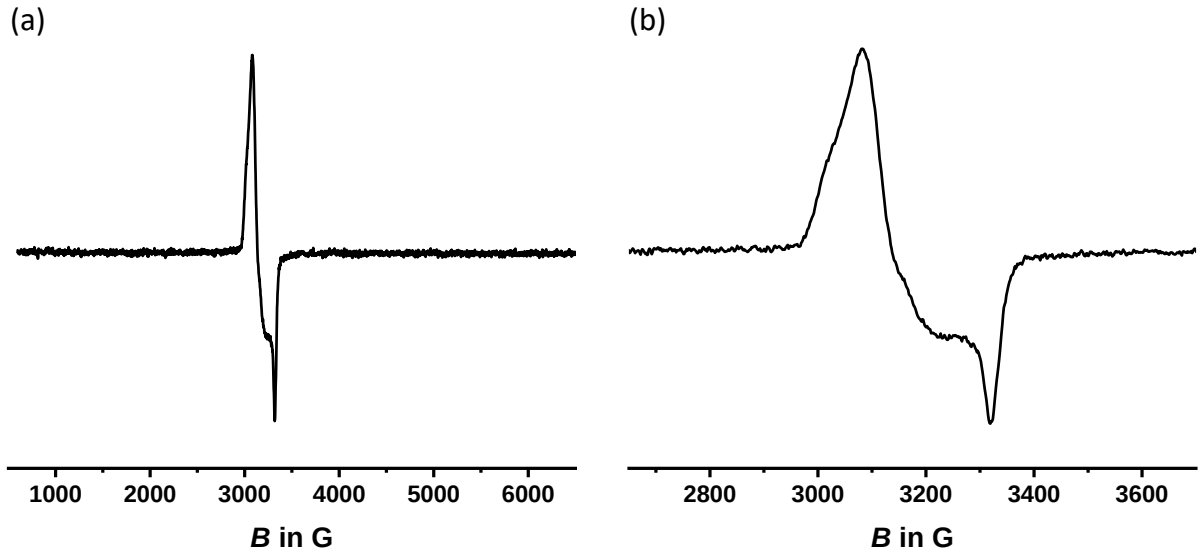

Figure S5.2: (a) Full-sweep X-band EPR spectrum of **5** after the addition of 1 eq. of [Thia][FAl], measured in CH_2Cl_2 at 10 K. (b) Zoom-in of the EPR signal.

The one- and two-electron-oxidized cations $\mathbf{5}^{+}$ and $\mathbf{5}^{2+}$ (**7**) were also investigated by X-band EPR spectroscopy at 10 K and 50 K in order to support the tentative attribution of redox sites based on our electrochemical studies. Ferrocenium radical cations usually exhibit axial EPR resonances with large *g*-anisotropies Δg of $\geq$ 2.2.[16] EPR spectra of the two cations in a matrix of frozen CH_2Cl_2 (see Figures S5.1–S5.2) are best described as being of the rhombic type with small *g*-anisotropy (g_x ca. 2.2, g_y ca. 2.1, g_z ca. 2.0) and either slightly different *g* values for the two termini, or only partially resolved hfs (e.g. to phosphine atoms) for the g_z-component. The differences in the spectra for the mono- and dioxidized species - one of the two peaks of the g_z-components of dication **7** is missing and a distinct shoulder in the g_x tensor component of **7** is less pronounced in the EPR resonance of $\mathbf{5}^{+}$ - make the first hypothesis more plausible.

The question remains whether the potential splitting for the oxidation of the peripheral units is merely due to electrostatic repulsion or whether some degree of electronic coupling between them exists. This can be conveniently probed by UV/Vis/NIR spectroelectrochemical experiments.

We hereby note at this point that the recorded EPR spectra of the isolated dication may contain traces of the presumed, but not isolable, monocation $\mathbf{5}^{+}$. It is assumed that the selective crystallization of **7** shifts the disproportionation equilibrium accordingly, which explains the appearance of this presumed trace amount of $\mathbf{5}^{+}$ on the EPR scale. According to the theoretical investigations of the dicationic **7** (*vide infra*), the two positive charges behave like two completely independent spins. Therefore, the simulation of the respective EPR spectra remains highly challenging. Up to this date, no completely satisfactory simulation of the EPR spectrum could be obtained up to this point. The best simulation obtained so far is depicted below in Figure S5.3, together with the respective g-tensors: g_x = 2.180; g_y = 2.109; g_z = 2.034.

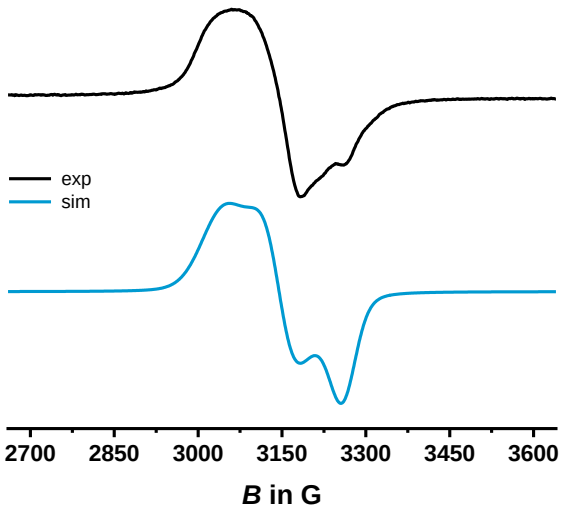

Figure S5.3: Experimental (top) and simulated (bottom) EPR spectrum of **7**. Measured in CH_2Cl_2 at 78 K.

In Scheme S5.1 the oxidation states of the respective Fe atoms in **5** and **7**, are formally calculated. In electronically neutral **5**, the outer lying Fe atoms possess the formal oxidation state of 0, due to the formally negatively charged Cp ligand and the positively charged [P_5MeR] phosphononium ligand. The resulting oxidation state distribution in **5** is therefore Fe^0 – Fe^{II} – Fe^0. During oxidation to the dicationic $\mathbf{5}^{2+}$ (**7**), a transition from Fe^0 to Fe^I occurs, due to formally one positive charge per {Cp*FeP_5Me} moiety. Therefore, the oxidation state distribution in **7** is Fe^I – Fe^{II} – Fe^I. Consequently, **7** behaves like a diradical species with two separated s = ½ spins, which is considered to be EPR active.

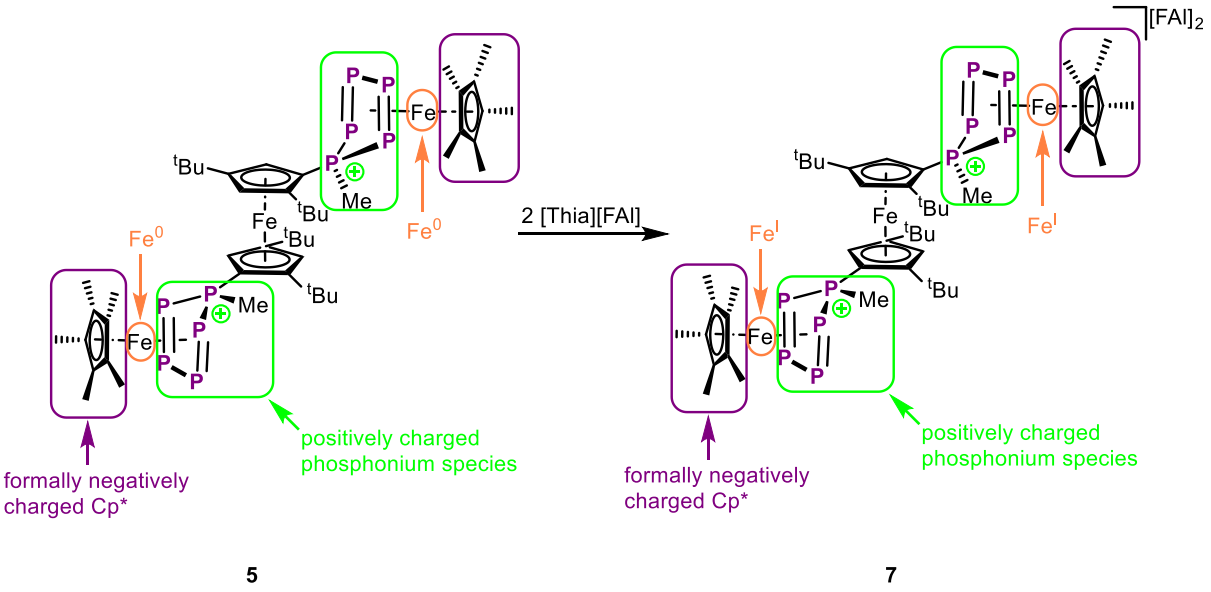

Scheme S5.1: Calculated Fe oxidation states in **5** and **7**.

6 UV/Vis/NIR Spectroscopy

UV/Vis/NIR spectra were recorded on a TIDAS fiber optic diode array spectrometer, consisting of a MCS UV/NIR and a PGS NIR instrument from J&M, in HELLMA quartz cuvettes with 0.2 cm optical path lengths and CH_2Cl_2 as solvent. Samples of air-sensitive compounds were prepared inside a nitrogen-filled glovebox.

For spectroelectrochemical (SEC) measurements, a custom-built Optically-Transparent-Thin-Layer-Electrochemical (OTTLE) cell based on the design by Hartl was used.[17] It consists of a standard liquid IR cell with CaF_2 windows and a Pt grid working and counter electrode and a Ag/AgCl silver plate (pseudo)reference electrode. The measurement was conducted under a blanket of dinitrogen in 1,2-$C_2H_4Cl_2$/ $^{n}Bu_4N^+$ BAr^{F24-} as supporting electrolyte. A Wenking POS 2 potentiostat from Bank Elektronik-Intelligent Controls GmbH was used for application of the required potential.

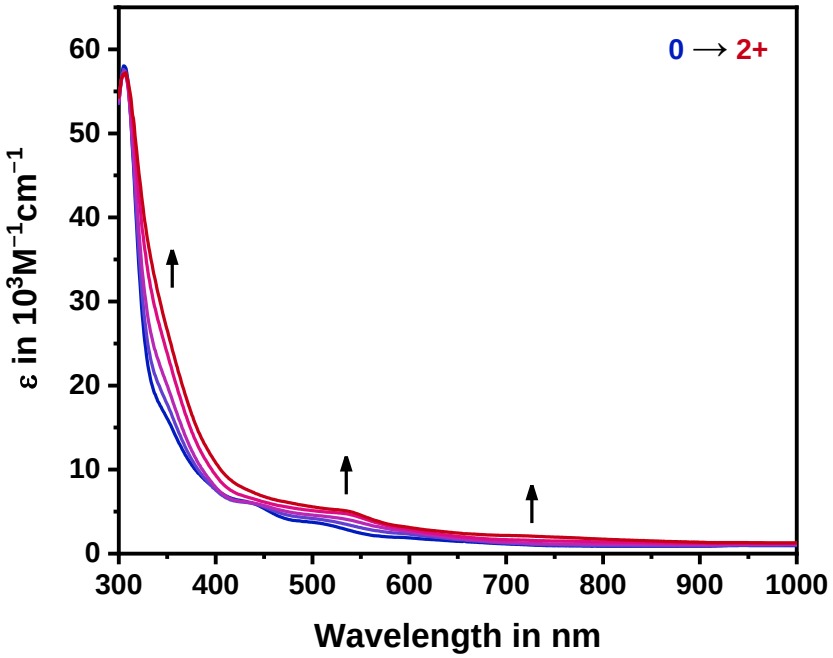

Figure S6.1: Changes in the UV/Vis/NIR absorption spectra of **5** during electrochemical oxidation to its dication **7**, measured in 1,2-$C_2H_4Cl_2$ / $^{n}Bu_4N^+$ BAr^{F24-} at r.t.

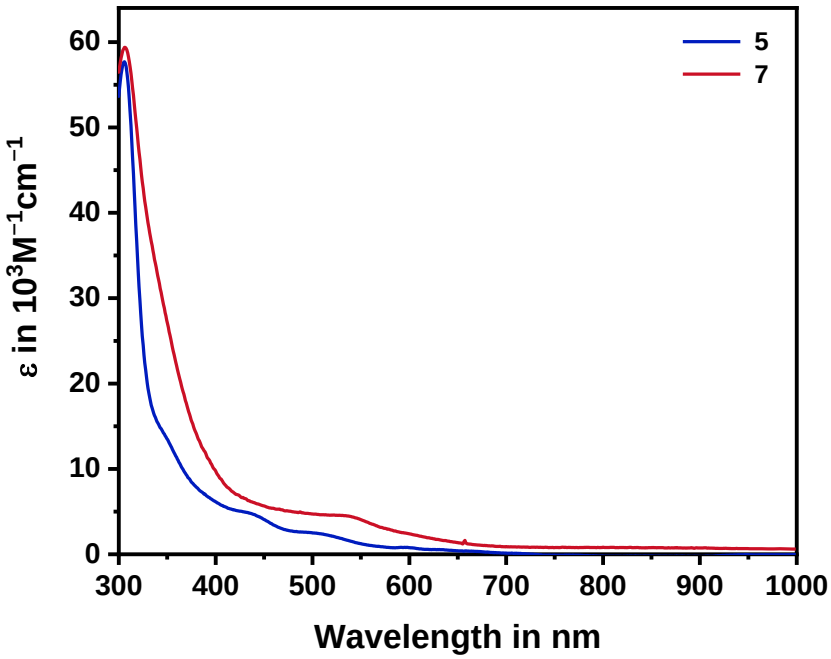

Figure S6.2: UV/Vis/NIR absorption spectra of pristine **5** and **7**, measured in CH_2Cl_2 at r.t.

As electronically coupled mixed-valent systems are expected to exhibit a so-called intervalence charge-transfer band originating from the intramolecular electron transfer from the remaining reduced to the already oxidized redox site. Spectra of dication **7** obtained under *in situ* conditions were well matched by those obtained from pristine samples of the chemically generated species and showed only small differences (compare the spectra in Figure S6.1 and in Figure S6.2). In particular we could not observe any intermittently formed electronic band, which, while slowly traversing over the closely spaced first two oxidation waves, would initially increase in intensity as the first Cp^*FeP_4 pendant is oxidized, and then decrease again during oxidation of also the second Cp^*FeP_4 to give dication **7**. Thus, mono-oxidized $\mathbf{5}^+$ is a valence localized mixed-valent system of class I according to the classification scheme of Robin and Day.[18]

7 Mössbauer Measurements

7.1 General Considerations

Zero-field ^{57}Fe-Mössbauer spectra were recorded on a WissEl Mössbauer spectrometer (MRG-500) at a temperature of 77 K in a constant acceleration mode. ^{57}Co/Rh was used as a γ-radiation source. WinNormos for Igor Pro software was used for the quantitative evaluation of the spectral parameters (least-squares fitting to Lorentzian peaks). The minimum experimental line width was determined at 0.21 mm s^{-1} (full width at half maximum, FWHM). The temperature of the sample was controlled by an MBBC-HE0106 Mössbauer He/N_2 cryostat with an accuracy of +/−0.3 K. Least-square fitting of the Lorentzian signals was carried out with the “Mfit” software, developed by Dr. Eckhard Bill (MPI CEC, Mühlheim/Ruhr).[19] The isomer shifts were reported relative to a α-iron reference at 300 K.

7.2 [{Cp*Fe(η^4-$P_5Me(C_5H_2{}^tBu_2)$}$_2$Fe]

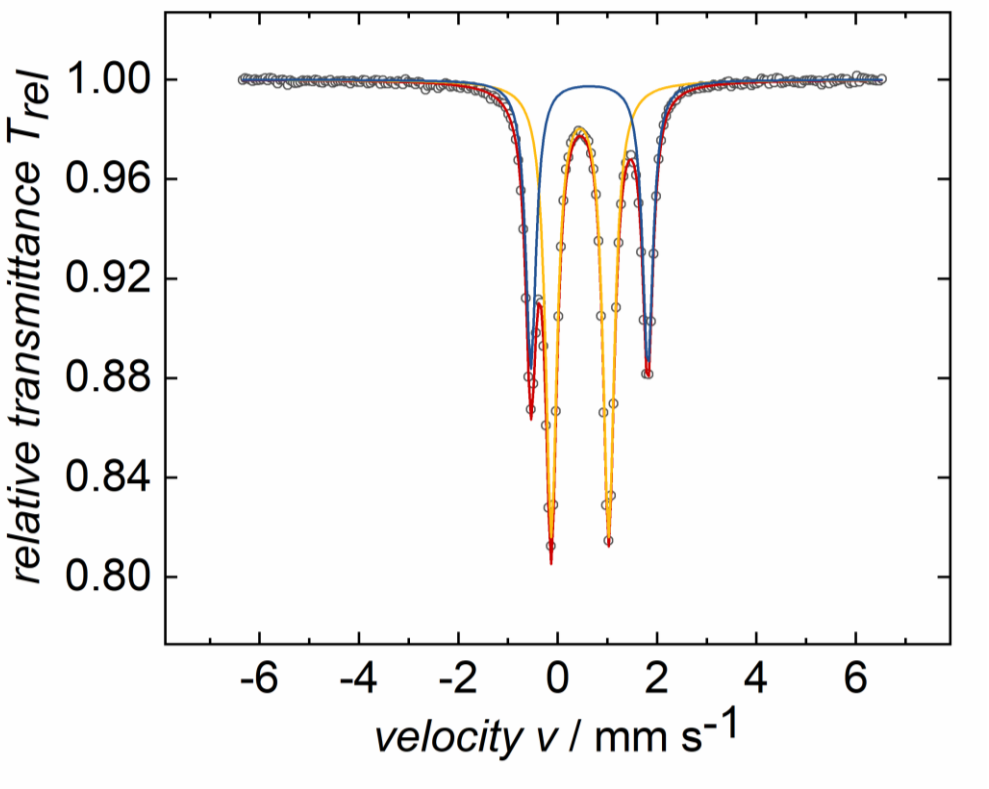

Figure S7.1: Zero-field ^{57}Fe-Mößbauer spectrum of **5**, recorded in solid-state at 77 K. The red trace represents the best fit obtained with the parameters given in the text, the yellow trace represents the best fit of species 1, and the blue trace represents the best fit of species 2. Collected data are represented by black circles.

Species 1: (yellow trace): δ = 0.45(1)mm s^{-1} and ΔE_Q = 1.16(1) mm s^{-1} with Γ_{FWHM} = 0.28 mm s^{-1}, spectral area = 63 %.

Species 2: (blue trace): δ = 0.64(1) mm s^{-1} and ΔE_Q = 2.35(1) mm s^{-1} with Γ_{FWHM} = 0.25 mm s^{-1}, spectral area = 37 %.

7.3 [{Cp*Fe(η⁴-P₅Me(C₅H₂ᵗBu₂)}₂Fe][FAl]

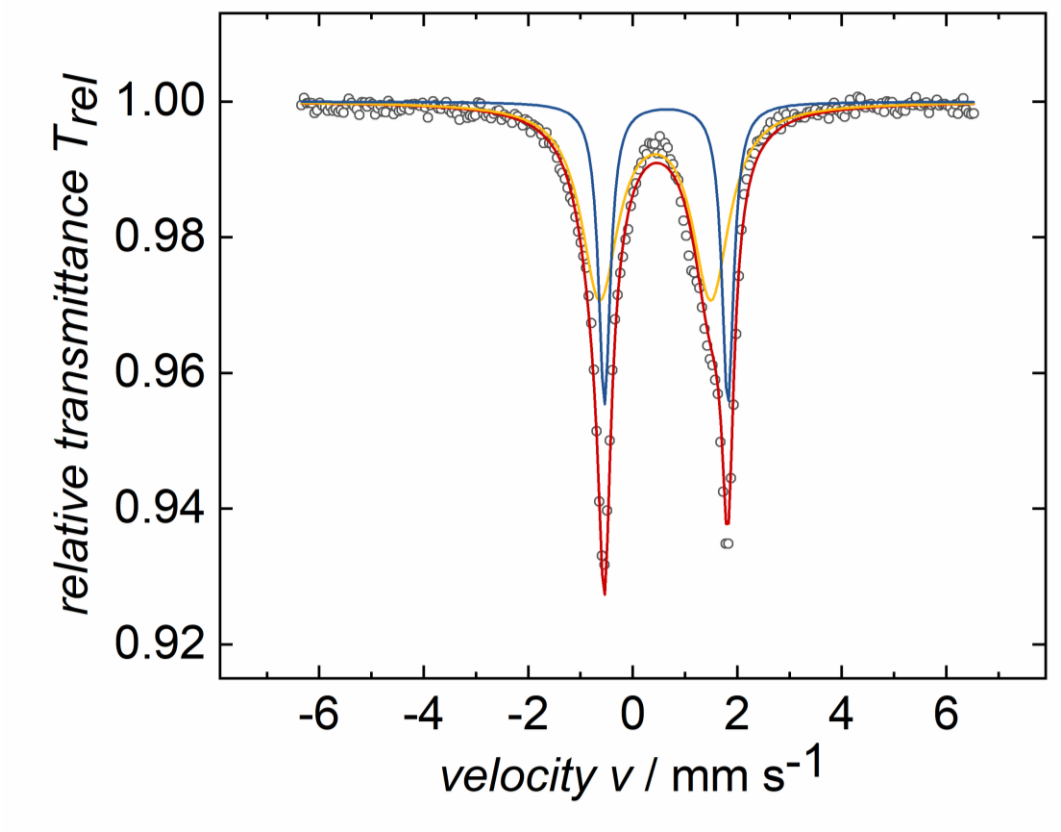

Figure S7.2: Zero-field ^{57}Fe-Mößbauer spectrum of **7**, recorded in solid-state at 77 K. The red trace represents the best fit obtained with the parameters given in the text, the yellow trace represents the best fit of species 1, and the blue trace represents the best fit of species 2. The collected data are represented by black circles.

Species 1: (yellow trace): δ = 0.43(1) mm s^{-1} and ΔE_Q = 2.13(1) mm s^{-1} with Γ_{FWHM} = 0.85 mm s^{-1}, spectral area = 66 %.

Species 2: (blue trace): δ = 0.64(1) mm s^{-1} and ΔE_Q = 2.36(1) mm s^{-1} with Γ_{FWHM} = 0.27 mm s^{-1}, spectral area = 34 %.

In both samples, two iron species with ratios of 1.7:1.0 (5) and 1.9:1 (respectively) are detected. The experimental results indicate that upon oxidation, the outside Fe atoms (yellow species) show an increase in quadrupole splitting (ΔE_Q = 1.16 to 2.23), while the isomer shifts remain almost the same. Conversely, the central Fe atom (blue species) does not change. Taking all these results into account, the data suggest that only the peripheral Fe atoms are involved in the oxidation process, changing from Fe(0) to Fe(I). The ferrocene building Fe atom, on the other hand, is unaffected by the oxidation process.

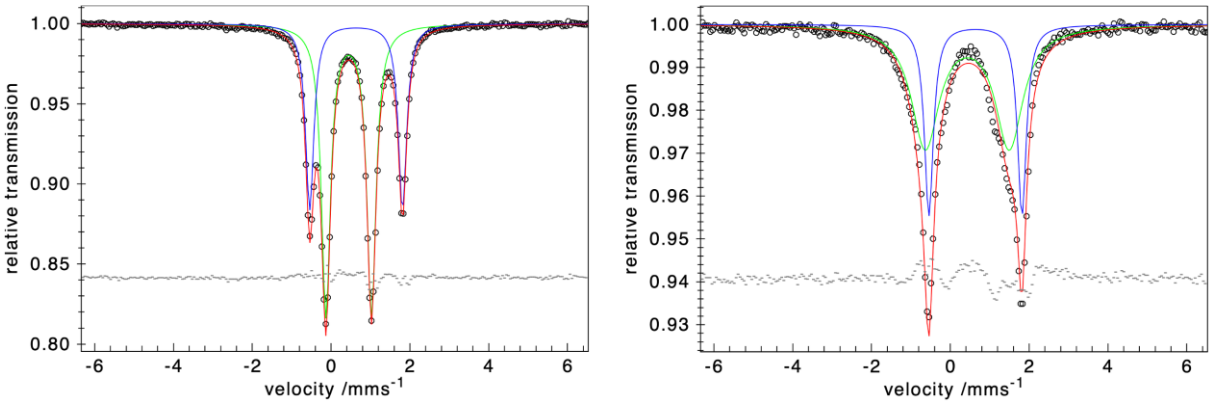

Figure S7.3: Simulated results for complex **5** (left panel) and **7** (right panel). The light-grey dots represent the error from data processing.

8 Computational Details

All calculations were performed with the ORCA 5.0 and ORCA 6.0 program.[20] The geometry was optimized starting from the X-ray coordinates using the r^{2}SCAN-3c composit method.[21] The relative energies of the different spin states of **7** were calculated as single point calculations on the r^{2}SCAN-3c optimised geometries with the ωB97X-D4[22] functional and def2-TZVPP basis set[23] in conjunction with the RIJCOSX approximation.[24]

The DFT calculations clearly show the diradical character of **7**. Two unpaired electrons are located on the two outer Fe atoms, with no coupling between the as shown by the broken symmetry calculations. The open shell singlet and the triplet spin states are degenerate, while the closed shell singlet spin state is considerably higher in energy.

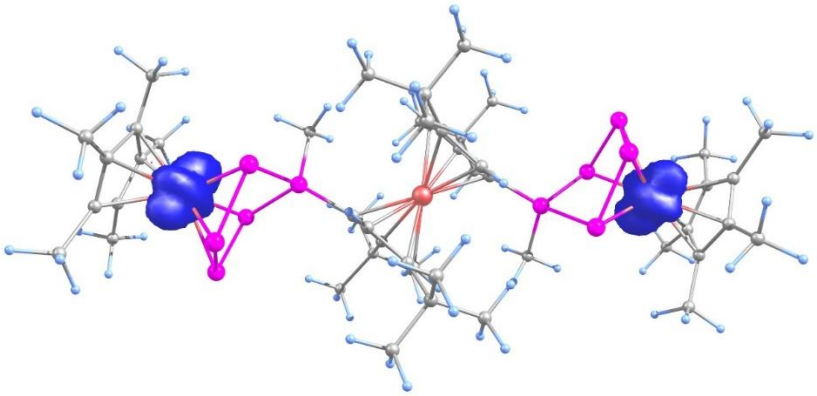

Figure S8.1: Spin density distribution in [{Cp*Fe(η^4-P$_5$Me(2,4-^{t}Bu$_2$C$_5$H$_2$))}$_2$Fe]$^{2+}$ (**7**) in the triplet spin state, at the r^{2}SCAN-3c level of theory.

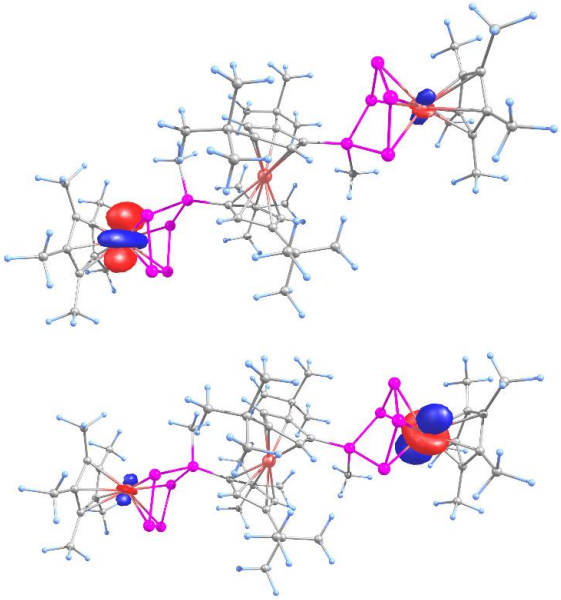

Figure S8.2: Isosurfaces of singly occupied, quasi restricted orbitals in [{Cp*Fe(η^4-P$_5$Me(2,4-^{t}Bu$_2$C$_5$H$_2$))}$_2$Fe]$^{2+}$ (**7**) in the triplet spin state, at the r^{2}SCAN-3c level of theory.

Table S8.1: Total SCF and relative energies of different spin states of [{Cp*Fe(η⁴-P₅Me(2,4-^{t}Bu₂C₅H₂))}₂Fe]²⁺ (**7**) at the ωB97X-D4/def2-TZVPP level of theory.

	Triplet spin state	Broken symmetry state	Open shell singlet	Closed shell singlet
SCF energy (Eha)	-9081.483823	-9081.483824	-9081.483818	-9081.330225
Rel. energy (kJ·mol^{-1})	0,00	0.00	0.01	403.27

Results of the broken symmetry state calculations for [{Cp*Fe(η⁴-P₅Me(2,4-^{t}Bu₂C₅H₂))}₂Fe]²⁺ (**7**) at the ωB97X-D4/def2-TZVPP level of theory.

```
----------------------------------------
BROKEN SYMMETRY MAGNETIC COUPLING ANALYSIS
----------------------------------------

S(High-Spin)      =   1.0
<S**2>(High-Spin) =   2.1484
<S**2>(BrokenSym) =   1.1485
E(High-Spin)      = -9080.965530 Eh
E(BrokenSym)      = -9080.965530 Eh
E(High-Spin)-E(BrokenSym)= 0.0000 eV 0.007 cm**-1 (ANTIFERROMAGNETIC cou-
pling)
```

Orbital energies of the open shell singlet spin state of [{Cp*Fe(η⁴-P₅Me(2,4-^{t}Bu₂C₅H₂))}₂Fe]²⁺ (**7**) at the ωB97X-D4/def2-TZVPP level of theory.

```
---------------
ORBITAL ENERGIES
---------------
                  SPIN UP ORBITALS
  NO   OCC          E(Eh)            E(eV)
 290   1.0000      -0.485328       -13.2064
 291   1.0000      -0.483632       -13.1603
 292   1.0000      -0.482328       -13.1248
 293   1.0000      -0.477438       -12.9918
 294   1.0000      -0.475863       -12.9489
 295   0.0000      -0.183581        -4.9955
 296   0.0000      -0.180247        -4.9048
 297   0.0000      -0.178403        -4.8546
 298   0.0000      -0.174575        -4.7504
                  SPIN DOWN ORBITALS
 290   1.0000      -0.485447       -13.2097
 291   1.0000      -0.483889       -13.1673
 292   1.0000      -0.482365       -13.1258
 293   1.0000      -0.477414       -12.9911
 294   1.0000      -0.475844       -12.9484
 295   0.0000      -0.183308        -4.9881
 296   0.0000      -0.180015        -4.8984
 297   0.0000      -0.178465        -4.8563
 298   0.0000      -0.174898        -4.7592
```

Table S8.2: Total Mulliken atomic charges and spin populations in [{Cp*Fe(η⁴-P₅Me(2,4-^{t}Bu₂C₅H₂))}₂Fe]²⁺ (**7**) in the open shell singlet spin state, at the ωB97X-D4/def2-TZVPP level of theory.

```
-------------------------------------------
MULLIKEN ATOMIC CHARGES AND SPIN POPULATIONS
-------------------------------------------
   0 Fe:    0.031515   -0.000069
   1 C :   -0.150767    0.000167
   2 H :    0.091839   -0.000002
   3 C :    0.110700    0.000832
   4 C :   -0.020661   -0.000865
```

5	C :	-0.168687	-0.000302
6	H :	0.094850	0.000010
7	C :	-0.102377	0.000771
8	H :	0.138069	-0.000086
9	C :	0.154397	0.000431
10	C :	0.139347	-0.000737
11	C :	0.029300	0.000047
12	C :	-0.012222	0.000909
13	C :	0.112214	-0.000713
14	C :	0.094601	-0.000035
15	C :	-0.101403	-0.000700
16	H :	0.139316	0.000126
17	C :	0.091430	0.000019
18	C :	-0.291962	-0.000273
19	H :	0.075993	-0.000048
20	H :	0.062387	0.000234
21	H :	0.119634	-0.000026
22	C :	-0.297609	0.000207
23	H :	0.057218	-0.000220
24	H :	0.121030	0.000029
25	H :	0.093720	0.000045
26	C :	0.055133	0.000008
27	C :	-0.300698	-0.000079
28	H :	0.120706	0.000002
29	H :	0.100516	0.000001
30	H :	0.044863	-0.000033
31	C :	-0.266316	-0.001062
32	H :	0.069176	0.000498
33	H :	0.102192	-0.000073
34	H :	0.111480	-0.000019
35	C :	-0.266890	0.001226
36	H :	0.103237	0.000077
37	H :	0.110922	0.000019
38	H :	0.066966	-0.000625
39	C :	-0.304877	0.000071
40	H :	0.056176	0.000036
41	H :	0.119860	-0.000001
42	H :	0.100746	-0.000001
43	C :	-0.311709	-0.000015
44	H :	0.088453	0.000005
45	H :	0.079650	0.000017
46	H :	0.116320	0.000000
47	C :	-0.286938	0.000139
48	H :	0.108068	-0.000003
49	H :	0.096557	0.000002
50	H :	0.090833	-0.000102
51	C :	-0.266548	-0.000507
52	H :	0.015191	0.000384
53	H :	0.087877	-0.000013
54	H :	0.114616	-0.000002
55	C :	-0.285323	-0.000180
56	H :	0.089812	0.000133
57	H :	0.107839	0.000001
58	H :	0.096897	-0.000002
59	C :	-0.267957	0.000491
60	H :	0.087368	0.000011
61	H :	0.114397	0.000000
62	H :	0.019071	-0.000353
63	C :	-0.311781	0.000016
64	H :	0.080100	-0.000019
65	H :	0.116329	0.000001
66	H :	0.088436	-0.000006
67	**Fe:**	**0.315488**	**-1.387745**
68	P :	0.207022	-0.005317
69	P :	-0.197239	0.068734
70	P :	-0.230101	0.067410
71	P :	-0.054935	0.031827
72	P :	-0.087162	0.035229
73	C :	0.075030	0.024084
74	C :	0.063747	0.039142
75	C :	0.149695	0.051125
76	C :	0.049024	0.026489
77	C :	0.128296	0.042388
78	C :	-0.304198	-0.002054
79	H :	0.148132	0.000129
80	H :	0.122719	0.000045
81	H :	0.134919	-0.000030
82	C :	-0.315775	-0.000673

83	H :	0.109763	0.000134
84	H :	0.143871	0.001871
85	H :	0.100730	0.000635
86	C :	-0.309024	-0.000906
87	H :	0.102476	0.000735
88	H :	0.142448	0.002147
89	H :	0.110209	0.000098
90	C :	-0.308491	-0.001577
91	H :	0.107602	0.000795
92	H :	0.143980	0.002538
93	H :	0.107519	0.000574
94	C :	-0.288735	-0.002324
95	H :	0.091450	0.000615
96	H :	0.143243	0.002137
97	H :	0.107289	0.000541
98	C :	-0.302299	-0.001563
99	H :	0.105398	0.000466
100	H :	0.143941	0.001191
101	H :	0.089160	0.000771
102	**Fe:**	**0.326589**	**1.387363**
103	P :	0.213650	0.005096
104	P :	-0.240539	-0.067977
105	P :	-0.192096	-0.068033
106	P :	-0.090823	-0.033241
107	P :	-0.056859	-0.032881
108	C :	0.108396	-0.041307
109	C :	0.087124	-0.040721
110	C :	0.051775	-0.024034
111	C :	0.148757	-0.052447
112	C :	0.069639	-0.024862
113	C :	-0.309323	0.002163
114	H :	0.137874	-0.000040
115	H :	0.147956	-0.000123
116	H :	0.124227	-0.000023
117	C :	-0.312207	0.000693
118	H :	0.110044	-0.000065
119	H :	0.143298	-0.001919
120	H :	0.100662	-0.000703
121	C :	-0.311034	0.000747
122	H :	0.102981	-0.000635
123	H :	0.143343	-0.002026
124	H :	0.109567	-0.000169
125	C :	-0.299259	0.001696
126	H :	0.090214	-0.000667
127	H :	0.143724	-0.001426
128	H :	0.107807	-0.000491
129	C :	-0.293560	0.002154
130	H :	0.104731	-0.000494
131	H :	0.143189	-0.001913
132	H :	0.091413	-0.000748
133	C :	-0.308139	0.001603
134	H :	0.107669	-0.000672
135	H :	0.144187	-0.002619
136	H :	0.107210	-0.000733

Sum of atomic charges : 2.0000000
Sum of atomic spin populations: 0.0000000

Table S8.3: Total Mulliken atomic charges and spin populations in [{Cp*Fe(η^4-P_5Me(2,4-^{t}Bu$_2$C$_5$H$_2$))}$_2$Fe]$^{2+}$ (**7**) in the triplet spin state, at the ωB97X-D4/def2-TZVPP level of theory.

MULLIKEN ATOMIC CHARGES AND SPIN POPULATIONS

0	**Fe:**	**0.031024**	**-0.000051**
1	C :	-0.149574	0.000120
2	H :	0.092161	0.000012
3	C :	0.110418	-0.000094
4	C :	-0.021397	0.000610
5	C :	-0.167791	0.000099
6	H :	0.094466	0.000010
7	C :	-0.101238	-0.000805
8	H :	0.138247	0.000101
9	C :	0.153990	0.000727

10	C :	0.138819	0.000932
11	C :	0.030148	0.000030
12	C :	-0.011920	0.000535
13	C :	0.110533	-0.000181
14	C :	0.093252	-0.000026
15	C :	-0.101423	-0.000776
16	H :	0.139253	0.000144
17	C :	0.090889	-0.000011
18	C :	-0.292030	-0.000282
19	H :	0.076438	-0.000037
20	H :	0.062238	0.000233
21	H :	0.119664	-0.000025
22	C :	-0.297455	-0.000213
23	H :	0.057277	0.000216
24	H :	0.121074	-0.000029
25	H :	0.093415	-0.000035
26	C :	0.054748	-0.000045
27	C :	-0.301086	-0.000099
28	H :	0.120712	0.000002
29	H :	0.100457	-0.000004
30	H :	0.045206	0.000009
31	C :	-0.266062	-0.001065
32	H :	0.068945	0.000493
33	H :	0.102215	-0.000073
34	H :	0.111454	-0.000021
35	C :	-0.266554	-0.001242
36	H :	0.103211	-0.000076
37	H :	0.110848	-0.000021
38	H :	0.066893	0.000634
39	C :	-0.304445	-0.000099
40	H :	0.056045	0.000003
41	H :	0.119859	0.000002
42	H :	0.100829	-0.000002
43	C :	-0.311651	-0.000009
44	H :	0.088500	-0.000009
45	H :	0.079671	0.000009
46	H :	0.116563	0.000001
47	C :	-0.286428	-0.000183
48	H :	0.107994	0.000002
49	H :	0.096512	-0.000002
50	H :	0.090837	0.000090
51	C :	-0.266603	-0.000506
52	H :	0.015382	0.000370
53	H :	0.087910	-0.000012
54	H :	0.114707	-0.000002
55	C :	-0.286144	-0.000225
56	H :	0.089900	0.000121
57	H :	0.107840	0.000001
58	H :	0.096929	-0.000002
59	C :	-0.267946	-0.000495
60	H :	0.087423	-0.000011
61	H :	0.114418	0.000002
62	H :	0.019077	0.000343
63	C :	-0.311377	-0.000012
64	H :	0.079962	0.000011
65	H :	0.116311	0.000001
66	H :	0.088312	-0.000009
67	**Fe:**	**0.313661**	**1.387582**
68	P :	0.207503	0.005437
69	P :	-0.197440	-0.068671
70	P :	-0.230128	-0.067334
71	P :	-0.054874	-0.031817
72	P :	-0.086804	-0.035183
73	C :	0.074232	-0.024200
74	C :	0.064092	-0.039261
75	C :	0.150101	-0.051077
76	C :	0.049663	-0.026523
77	C :	0.129254	-0.042239
78	C :	-0.304502	0.002044
79	H :	0.148123	-0.000130
80	H :	0.122718	-0.000048
81	H :	0.134986	0.000030
82	C :	-0.316016	0.000659
83	H :	0.109737	-0.000133
84	H :	0.143859	-0.001873
85	H :	0.100741	-0.000638
86	C :	-0.308970	0.000924
87	H :	0.102511	-0.000738

```
  88 H :    0.142425   -0.002150
  89 H :    0.110249   -0.000099
  90 C :   -0.308703    0.001580
  91 H :    0.107664   -0.000796
  92 H :    0.144072   -0.002544
  93 H :    0.107487   -0.000574
  94 C :   -0.288993    0.002314
  95 H :    0.091445   -0.000615
  96 H :    0.143254   -0.002130
  97 H :    0.107306   -0.000541
  98 C :   -0.301375    0.001583
  99 H :    0.105230   -0.000467
 100 H :    0.143982   -0.001198
 101 H :    0.089136   -0.000774
102 Fe:    0.325957    1.387184
 103 P :    0.212887    0.005113
 104 P :   -0.240627   -0.067926
 105 P :   -0.191433   -0.067932
 106 P :   -0.090543   -0.033207
 107 P :   -0.056700   -0.032883
 108 C :    0.109045   -0.041481
 109 C :    0.087895   -0.040590
 110 C :    0.051097   -0.023989
 111 C :    0.151574   -0.052459
 112 C :    0.066597   -0.024898
 113 C :   -0.309091    0.002153
 114 H :    0.137767   -0.000035
 115 H :    0.147924   -0.000123
 116 H :    0.124260   -0.000027
 117 C :   -0.312451    0.000711
 118 H :    0.110107   -0.000065
 119 H :    0.143261   -0.001921
 120 H :    0.100616   -0.000703
 121 C :   -0.311032    0.000743
 122 H :    0.103003   -0.000638
 123 H :    0.143336   -0.002023
 124 H :    0.109565   -0.000166
 125 C :   -0.298842    0.001699
 126 H :    0.090270   -0.000670
 127 H :    0.143677   -0.001420
 128 H :    0.107795   -0.000490
 129 C :   -0.293663    0.002157
 130 H :    0.104715   -0.000497
 131 H :    0.143193   -0.001919
 132 H :    0.091409   -0.000750
 133 C :   -0.308100    0.001606
 134 H :    0.107590   -0.000674
 135 H :    0.144322   -0.002624
 136 H :    0.107144   -0.000733
Sum of atomic charges         :    2.0000000
Sum of atomic spin populations:    2.0000000
```

Table S8.4: Total SCF and relative energies of selected conformers of [{Cp*Fe(η^4-P_5Me(2,4-^{t}Bu$_2$C$_5$H$_2$))}$_2$Fe] (**5**) at the r^{2}SCAN-3c level of theory.

Fc	Fc-I2	Fc-I3	Fc-I4
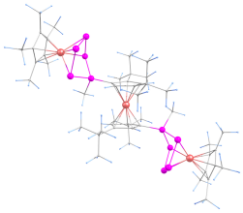	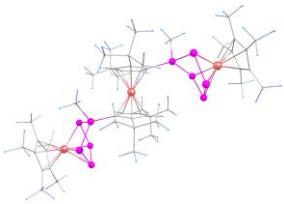	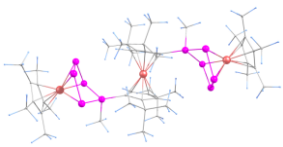	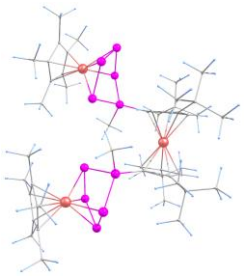
-9079.303064 Eh	-9079.299042 Eh	-9079.292641 Eh	-9079.293733 Eh
0.0 kJ·mol^{-1}	10.6 kJ·mol^{-1}	27.4 kJ·mol^{-1}	24.5 kJ·mol^{-1}

Table S8.5: Total SCF and relative energies of selected isomers of [Cp*Fe(η^4-P_5Me(2,4-^{t}Bu$_2$C$_5$H$_2$)]$^-$ (**2**$^-$) at the r^{2}SCAN-3c level of theory.

FeP5-Cp2-min	FeP5-Cp2-min-I2
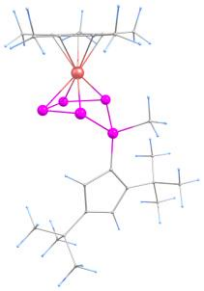	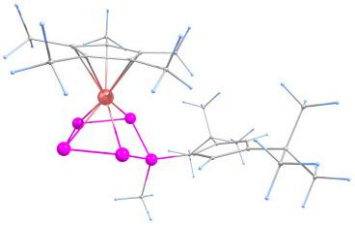
-3907.798974 Eh	-3907.803064 Eh
10.7 kJ·mol^{-1}	0.0 kJ·mol^{-1}

Table S8.6: Total SCF and relative energies of selected isomers of [Cp*Fe(η^4-P_5Me(2,4-^{t}Bu$_2$$C_5$$H_3$)] (**2**) at the r^{2}SCAN-3c level of theory.

FeP5-Cp2	FeP5-Cp2-I2	FeP5-Cp2-I3
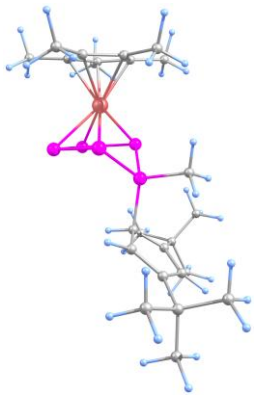	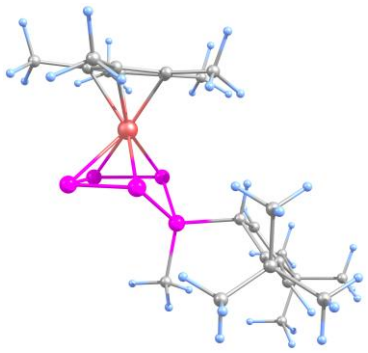	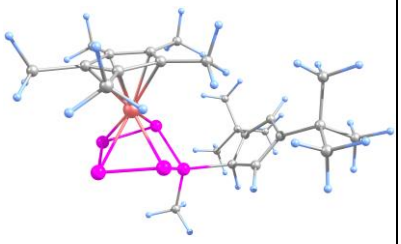
-3908.34245852156 Eh	-3908.342459 Eh	-3908.32751925357 Eh
0.0 kJ·mol^{-1}	8.9 kJ·mol^{-1}	39.22 kJ·mol^{-1}

Table S8.7: Optimized cartesian coordinates of **5**.

Fe	14.385180679	-18.908612663	17.672463149
C	16.235789025	-18.457330589	18.530607327
H	17.139273087	-18.186741497	18.005991438
C	14.134329391	-20.290453433	16.179520129
H	14.701847581	-21.204657689	16.070224556
C	12.888242164	-20.137634666	16.847507794
C	12.537763665	-18.763702659	16.718356949
H	11.643337665	-18.314380253	17.122048179
C	14.531100342	-19.024647705	15.610971148
C	15.867757334	-19.785925877	18.885009815
C	15.288574915	-17.511698851	19.021140013
C	13.492121300	-18.061078232	15.925393701
C	14.618607158	-19.682174002	19.557224953
H	14.042293668	-20.495217346	19.978451176
C	14.236582453	-18.292857793	19.646156208
C	16.803016522	-20.978134269	18.864365967
C	16.063994575	-22.314632457	18.783781020
H	15.350636148	-22.432426389	19.605466640
H	16.783447754	-23.137813385	18.852130039
H	15.527078633	-22.413332743	17.838087167
C	13.150063314	-16.739712226	15.252835995
C	11.939782516	-21.233977475	17.286898841
C	15.646460814	-16.041942040	19.190304921
C	14.362456971	-15.849456705	14.981675723
H	14.843581875	-15.550241515	15.915591712
H	14.045970198	-14.941254265	14.456983250
H	15.094644439	-16.345502815	14.338091788
C	12.124769930	-15.947000569	16.078233386
H	11.153451409	-16.450432137	16.109266309
H	11.966679476	-14.964357699	15.621644226
H	12.464827891	-15.794850649	17.104784969
C	14.443499257	-15.100425449	19.131790445
H	13.962063115	-15.141034613	18.152218054

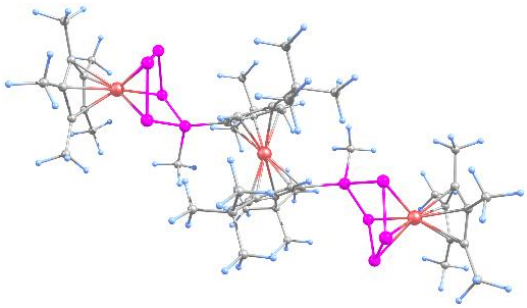

H	14.769570280	-14.069422425	19.307726977
H	13.708623510	-15.334970782	19.906950515
C	16.679118845	-15.599393565	18.142442790
H	17.645818704	-16.088941418	18.295984466
H	16.844286798	-14.519963335	18.222845311
H	16.341398586	-15.818002069	17.127461496
C	17.804431196	-20.890121380	17.709381193
H	17.293842453	-20.869593856	16.741461340
H	18.462346239	-21.765994999	17.716891692
H	18.443784942	-20.004453418	17.793357421
C	12.480096369	-17.102089391	13.907984861
H	13.169313762	-17.631089001	13.244466819
H	12.149105711	-16.188388301	13.400165340
H	11.607310336	-17.742495550	14.073792127
C	12.664480161	-22.477496434	17.803161991
H	13.368190192	-22.872519079	17.063756313
H	11.934431288	-23.265592693	18.017468045
H	13.210436140	-22.263725079	18.724594400
C	11.139533043	-21.619186373	16.022125173
H	10.600477747	-20.753740022	15.622012223
H	10.409029755	-22.399440661	16.265232447
H	11.803561861	-21.996911183	15.237241868
C	17.572323553	-20.920675109	20.203467877
H	18.123477818	-19.978859874	20.297984496
H	18.288765316	-21.748380531	20.260253193
H	16.884857171	-20.996432664	21.052705791
C	16.315604482	-15.916620374	20.577864992
H	15.621809155	-16.169752460	21.383729845
H	16.657653870	-14.886338438	20.732510709
H	17.180903650	-16.584004632	20.650498772
C	10.967240883	-20.740663549	18.361107643
H	11.502352401	-20.399331728	19.252620112
H	10.302212511	-21.555697751	18.666806504
H	10.333113520	-19.926478016	17.993101067
Fe	16.789546859	-20.350307050	11.743217847
P	15.908035539	-19.042258698	14.416771536
P	15.678198760	-18.413570140	12.338453069
P	16.731463219	-21.002594939	13.968514073
P	14.464570528	-20.035109294	11.588451304
P	15.172012663	-21.772107363	12.682885189
C	18.098979272	-21.753791229	10.918384405
C	18.855042356	-20.673037780	11.476954911
C	17.448795039	-19.792781706	9.858705501
C	18.455563669	-19.464795712	10.827524161
C	17.222719297	-21.210582052	9.919559920
C	17.320295484	-18.047201311	15.049740180
H	18.051751917	-17.949071023	14.242005880
H	17.779488552	-18.558157264	15.898190673
H	16.981522278	-17.057553482	15.362150549
C	16.300182155	-21.992323952	9.044020592
H	15.906173564	-22.868554039	9.565795476
H	16.822536887	-22.339871246	8.142971579
H	15.446113472	-21.387547056	8.728768226
C	18.246658110	-23.196036795	11.276477773
H	18.463193627	-23.324200571	12.341381526
H	19.070018221	-23.652757947	10.711359207
H	17.334292388	-23.755873836	11.057593749
C	19.931231912	-20.798833559	12.504845555
H	19.982982092	-19.912934559	13.143803103
H	20.909141027	-20.921445139	12.020294534
H	19.766175476	-21.662890858	13.152758935
C	19.053111742	-18.113617936	11.045159541
H	18.319051659	-17.319084132	10.888436419
H	19.885106230	-17.946499547	10.347766989
H	19.448645204	-18.009533346	12.059304216
C	16.805284738	-18.834774768	8.911477084
H	15.803665324	-19.168418944	8.627792979
H	17.401764185	-18.734432270	7.994979599
H	16.707823473	-17.839816007	9.355755775
Fe	11.957682347	-18.135187370	23.726749447
P	12.865644832	-17.871509289	20.772203528
P	13.132225665	-16.566560892	22.503119025
P	11.988561138	-19.526720861	21.873795414
P	14.293793150	-17.863683825	23.781331139
P	13.523840336	-19.849199439	23.360622791
C	9.882891058	-18.066843073	24.010312240
C	11.409221062	-17.053058495	25.429602412
C	10.453757522	-16.813426925	24.390372701

C	11.430969143	-18.463670920	25.695203485
C	10.479662295	-19.091106934	24.820259097
C	11.461386043	-17.132276619	19.840177049
H	10.739824456	-16.755286491	20.571100179
H	10.987599582	-17.899605763	19.224332921
H	11.804943633	-16.315433865	19.202842572
C	8.787163904	-18.264569063	23.014586266
H	8.816506965	-17.502988124	22.230606031
H	7.806410371	-18.198370106	23.504749284
H	8.856181569	-19.242098232	22.530988214
C	12.191161014	-16.003496899	26.148750053
H	13.096783513	-16.418905079	26.596930287
H	11.589542973	-15.555915429	26.951049041
H	12.497938517	-15.198206626	25.474302557
C	10.061576171	-15.472759968	23.862940678
H	10.896106821	-14.767979044	23.897503493
H	9.241616746	-15.054443088	24.461938466
H	9.719450741	-15.530031328	22.825969483
C	10.124439542	-20.541009126	24.795545471
H	9.833130734	-20.862848703	23.791368645
H	9.282912997	-20.747432118	25.470069623
H	10.968339917	-21.161614894	25.108364240
C	12.240732589	-19.144867375	26.747915827
H	12.446669748	-20.183636164	26.477846177
H	11.709550707	-19.141563008	27.708856640
H	13.203502615	-18.647073598	26.892234624

Table S8.8: Optimized cartesian coordinates of **5**-I2.

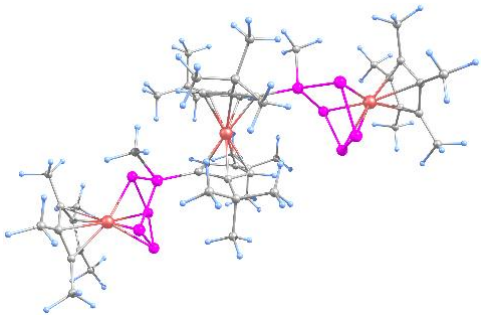

Fe	16.455132054	-18.446720624	19.951174276
C	15.632259805	-19.165928509	18.179518200
H	16.131532880	-19.793533715	17.457894851
C	18.308721287	-17.559763632	20.014797913
H	18.751851588	-16.953659761	19.236477998
C	17.579262296	-17.089246552	21.138588063
C	17.201798590	-18.244494822	21.882453291
H	16.590797867	-18.233459984	22.776187499
C	18.439943251	-18.993502196	20.090413864
C	15.647095293	-17.742641407	18.157571746
C	14.832676123	-19.663055460	19.251150918
C	17.759760593	-19.422714603	21.298083621
C	14.894317512	-17.322632334	19.296525821
H	14.715805660	-16.300512535	19.608600781
C	14.380946030	-18.492879324	19.978960005
C	16.081114877	-16.921571516	16.959536641
C	16.469270881	-15.488792674	17.321975204
H	15.675630572	-14.984162925	17.882831842
H	16.645484530	-14.910494543	16.408282287
H	17.384494884	-15.466280405	17.916537453
C	17.856029404	-20.733922733	22.050985776
C	17.554305143	-15.663809007	21.655747026
C	14.269506902	-21.084163398	19.245984533
C	17.957749668	-21.939557263	21.111237673
H	17.173854554	-21.915007633	20.351064741
H	17.861652222	-22.872295783	21.677473920
H	18.933492551	-21.968021841	20.614896306
C	16.666773076	-20.882277147	23.014696464
H	16.757181643	-20.191851923	23.858743016
H	16.638703457	-21.896674582	23.426236325
H	15.712318593	-20.679746168	22.527191811
C	14.258486815	-21.793310482	20.601725042
H	15.260716024	-22.097654234	20.902370829
H	13.637239611	-22.694063999	20.536557044
H	13.839903217	-21.166165643	21.390280514
C	15.032013138	-21.968703850	18.247092946
H	14.891026335	-21.635035870	17.213557824
H	14.659776790	-22.995940431	18.318051719
H	16.104194307	-21.986074579	18.462078913
C	17.248821776	-17.582318288	16.218403467
H	18.118518090	-17.705794712	16.871699794
H	17.556099361	-16.958508308	15.371888009
H	16.971052439	-18.562018905	15.814987154
C	19.143605037	-20.667009400	22.903040755
H	20.034951953	-20.558344404	22.277978341
H	19.245068780	-21.587449145	23.490555472
H	19.102671527	-19.819365411	23.595075660

C	17.679553745	-14.623165190	20.542417674
H	18.573216420	-14.783345565	19.930082722
H	17.759468509	-13.624025655	20.984452040
H	16.801005948	-14.634607870	19.893700287
C	18.796248733	-15.556448644	22.571018195
H	18.732185221	-16.271101370	23.397889486
H	18.863686257	-14.546111245	22.990901305
H	19.714965824	-15.764085518	22.011493745
C	14.854551375	-16.877912679	16.020554687
H	14.539208904	-17.889409427	15.742649570
H	15.098226449	-16.327956049	15.104141227
H	14.008470503	-16.379835503	16.506882827
C	12.812568938	-20.969448503	18.741376260
H	12.166768508	-20.520044487	19.501851561
H	12.415740839	-21.968288945	18.526285976
H	12.758119629	-20.369666288	17.825739958
C	16.301449994	-15.366036384	22.475505090
H	15.399204635	-15.452380722	21.864640438
H	16.346466479	-14.345930098	22.873507679
H	16.191221391	-16.048724003	23.322796836
Fe	22.715739921	-19.562697550	18.336299829
P	19.684938422	-19.756828219	19.000279196
P	21.425267130	-20.791977035	19.808994922
P	20.807558973	-18.381723821	17.744134748
P	22.494724290	-19.105549733	20.633724651
P	22.088593013	-17.488891600	19.241327610
C	24.084215761	-18.946157510	16.882986883
C	23.311354007	-20.038577378	16.372082253
C	24.397799202	-20.771390801	18.283762112
C	23.501323651	-21.162512269	17.233375338
C	24.754130016	-19.395756304	18.070473909
C	18.921841130	-20.938341032	17.815523273
H	19.731421674	-21.377382700	17.224356275
H	18.237881478	-20.401854754	17.154122781
H	18.385420454	-21.728650742	18.342852838
C	25.709719475	-18.595381543	18.891878428
H	25.437613470	-17.536431980	18.894111021
H	26.730316803	-18.683358465	18.496778211
H	25.717327573	-18.932750454	19.931269250
C	24.212484044	-17.599358888	16.250727509
H	23.276265428	-17.288740145	15.777118590
H	24.991458681	-17.607417142	15.476728031
H	24.476017784	-16.837558400	16.988313963
C	22.511331959	-20.027740352	15.111110446
H	21.658433767	-20.709489711	15.169632088
H	23.133563864	-20.341833275	14.262307032
H	22.122168670	-19.030551276	14.891501355
C	22.946780531	-22.532706924	17.022632760
H	22.776041349	-23.048075990	17.971134944
H	23.642903051	-23.140776555	16.429113859
H	21.995294388	-22.502706604	16.484430687
C	24.915868542	-21.662771341	19.364020568
H	25.192098434	-21.090662232	20.253564855
H	25.804713554	-22.210133688	19.023182990
H	24.166344869	-22.400174141	19.666457629
Fe	11.578553059	-18.065717211	23.910320549
P	13.001666206	-18.242585813	21.165073574
P	13.035929387	-16.727022825	22.725526355
P	11.887694739	-19.715068667	22.337653073
P	13.869451205	-17.834666987	24.379317806
P	13.093800069	-19.844816291	24.123197249
C	9.484234535	-17.939145098	23.791407714
C	10.768287450	-16.701963214	25.272255931
C	10.026692830	-16.642354460	24.048073778
C	10.687881108	-18.044409612	25.774013827
C	9.887764832	-18.809131324	24.858555682
C	11.714982609	-17.583962143	20.008291999
H	10.791606653	-17.418886253	20.569002304
H	11.540706849	-18.299392433	19.200471298
H	12.061339482	-16.640620481	19.577306729
C	8.567971277	-18.304426239	22.669849094
H	8.706935704	-17.648140844	21.806540722
H	7.520624535	-18.212337771	22.987317065
H	8.728181900	-19.333358941	22.337277432
C	11.448816317	-15.547916204	25.931999785
H	12.240145949	-15.885042337	26.605758596
H	10.730881170	-14.959566504	26.518798150
H	11.906001059	-14.877336429	25.197752878

C	9.789182421	-15.412790670	23.234947683
H	10.629244092	-14.717424825	23.305978495
H	8.888561797	-14.891834912	23.586483963
H	9.644688785	-15.649620696	22.177267704
C	9.484651586	-20.237931441	25.018153277
H	9.353481771	-20.726505981	24.048122229
H	8.533600779	-20.314588576	25.561784032
H	10.237433329	-20.803787353	25.573391133
C	11.269905882	-18.537925140	27.057013451
H	11.496115010	-19.605848070	27.003048820
H	10.570101898	-18.379062850	27.887916812
H	12.201655971	-18.017749900	27.294862426

Table S8.9: Optimized cartesian coordinates of **5**-I3.

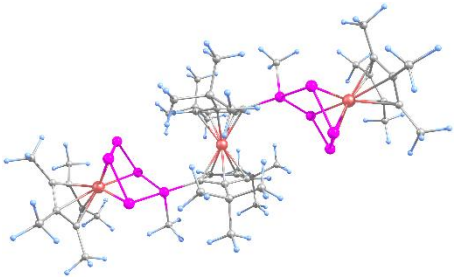

Fe	16.273505829	-18.680100943	19.940939038
C	15.354076812	-19.353524928	18.198845531
H	15.836197193	-19.990545216	17.469019591
C	18.195018806	-17.989066238	19.864701891
H	18.628828381	-17.483113184	19.010629533
C	17.572617800	-17.369263549	20.987846398
C	17.115327698	-18.426385965	21.824557526
H	16.546219215	-18.290009250	22.734986788
C	18.194408114	-19.424400854	20.054268283
C	15.384592400	-17.929896444	18.176359695
C	14.589768314	-19.830196859	19.312719832
C	17.526199157	-19.694286339	21.309468453
C	14.718992694	-17.498214444	19.360194834
H	14.573253966	-16.471977927	19.675820484
C	14.206266396	-18.652187316	20.062765406
C	15.692458734	-17.072169574	16.963454592
C	16.250778429	-15.697945684	17.327793871
H	15.604985156	-15.169576789	18.036965654
H	16.328495273	-15.078409904	16.427258118
H	17.248814642	-15.789152456	17.761550270
C	17.484540419	-20.956029655	22.150993466
C	17.707004053	-15.927217609	21.444171240
C	13.987025122	-21.231893203	19.340632106
C	17.437964955	-22.233601516	21.305084463
H	16.794935973	-22.118630550	20.431596458
H	17.073696866	-23.078519618	21.899100636
H	18.431656056	-22.503470718	20.940526622
C	16.299765347	-20.893232925	23.129319799
H	16.467928729	-20.152717420	23.917652635
H	16.163885904	-21.863004758	23.618897140
H	15.368450176	-20.627965630	22.626309633
C	13.918586979	-21.893902454	20.718294706
H	14.904396310	-22.178371766	21.079805362
H	13.310217294	-22.803183316	20.649732252
H	13.451154629	-21.249434398	21.466193533
C	14.743256468	-22.160853644	18.378965244
H	14.607035161	-21.865154687	17.333438226
H	14.367402646	-23.183722400	18.485839541
H	15.817944574	-22.174529363	18.581536577
C	16.659121016	-17.758629638	16.000073865
H	17.619156949	-17.966529634	16.479966323
H	16.842447915	-17.111366492	15.135002184
H	16.262353748	-18.706816737	15.624818340
C	18.781187953	-20.984493704	22.991119575
H	19.664634756	-21.074284096	22.350401598
H	18.767028598	-21.850270978	23.663719612
H	18.878733467	-20.077313694	23.596934646
C	17.985831889	-14.947586455	20.304278446
H	18.827838412	-15.265482523	19.679728403
H	18.237496372	-13.966545315	20.721822053
H	17.106871898	-14.824406482	19.670975255
C	18.927313161	-15.928860084	22.394819294
H	18.757598034	-16.595388938	23.246571104
H	19.106812934	-14.917273255	22.776903993
H	19.829322276	-16.266590834	21.872077826
C	14.333094387	-16.880028998	16.251860707
H	13.895189913	-17.846841370	15.981848191
H	14.469802480	-16.294682624	15.335242416
H	13.622692319	-16.351543653	16.897304697
C	12.539113848	-21.083074367	18.816669005

H	11.898966386	-20.602393659	19.564211384
H	12.117823695	-22.074490507	18.614366046
H	12.509127981	-20.498626204	17.890219891
C	16.478380366	-15.448493087	22.218716281
H	15.584139830	-15.457718682	21.590134459
H	16.636370634	-14.423234308	22.572742678
H	16.271481850	-16.072406880	23.092693952
Fe	20.368058369	-21.965555073	16.546241157
P	19.374987729	-20.356835174	19.002404722
P	19.641962574	-19.799127892	16.918112884
P	19.724395117	-22.494682871	18.686466832
P	18.264515066	-21.137351423	15.929523386
P	18.314448679	-22.949174592	17.121484300
C	21.560062448	-23.612517248	16.137380101
C	22.377778244	-22.561786755	16.672780802
C	21.388766955	-21.775818777	14.729131616
C	22.272141329	-21.432589039	15.803202989
C	20.942515700	-23.123984634	14.935844964
C	20.967012646	-19.811487670	19.772143559
H	21.796696425	-20.259402785	19.219772131
H	21.003890234	-20.129908004	20.817208042
H	21.034792106	-18.720765892	19.732646754
C	20.054318400	-23.901744213	14.022132219
H	19.507721974	-24.676369417	14.565946744
H	20.640812945	-24.388519647	13.231960601
H	19.314140396	-23.254015005	13.544557265
C	21.436902223	-24.991305372	16.697269118
H	21.516037874	-24.988499770	17.788518124
H	22.231394084	-25.641173071	16.306835264
H	20.475175992	-25.441724615	16.438103746
C	23.266651774	-22.676193071	17.867155031
H	23.481127435	-21.698067728	18.305795044
H	24.227739651	-23.127896223	17.586645481
H	22.817985329	-23.300470952	18.644555962
C	23.018071735	-20.146136989	15.938947440
H	22.458396089	-19.310735537	15.511248929
H	23.982605613	-20.208576584	15.417456183
H	23.221505601	-19.905006259	16.985890409
C	21.045180300	-20.897617691	13.571113490
H	20.083594756	-21.176169433	13.133805285
H	21.810823345	-20.972283021	12.787457276
H	20.977912781	-19.847590485	13.871506849
Fe	11.611773573	-17.814793577	24.053039377
P	12.894279193	-18.295614602	21.292459634
P	13.110475782	-16.667721716	22.713159031
P	11.765947354	-19.615496817	22.615979839
P	13.927683793	-17.691255444	24.428870055
P	13.017747382	-19.659515998	24.372669646
C	9.518837855	-17.599221308	24.006138798
C	10.927570196	-16.278108938	25.287106593
C	10.131577492	-16.312204829	24.095686764
C	10.807802374	-17.552947856	25.936557185
C	9.931110330	-18.369146893	25.144372936
C	11.583586086	-17.653880386	20.151482474
H	10.689344966	-17.422475398	20.734642151
H	11.352748924	-18.405886151	19.392680641
H	11.947656247	-16.751031316	19.653716836
C	8.534558857	-18.038468738	22.972589883
H	8.664401563	-17.493593575	22.033839178
H	7.509246225	-17.853855323	23.320431684
H	8.627516339	-19.105698528	22.755194865
C	11.694064483	-15.097700887	25.785987965
H	12.503681070	-15.402852216	26.453360248
H	11.036687614	-14.413726795	26.339165378
H	12.141344987	-14.534540378	24.961283100
C	9.913746115	-15.165700568	23.163522779
H	10.783312402	-14.504556284	23.132885931
H	9.049010750	-14.570631643	23.486777278
H	9.719765307	-15.503348562	22.141651623
C	9.469520162	-19.751145511	25.470440645
H	9.312499796	-20.342967137	24.563605348
H	8.518895957	-19.724077278	26.019593657
H	10.200753490	-20.280559601	26.086544685
C	11.423552008	-17.935208723	27.241350040
H	11.601603979	-19.012364384	27.294391067
H	10.767362157	-17.657272498	28.076563957
H	12.386144099	-17.437512816	27.386942982

Table S8.10: Optimized cartesian coordinates of **5**-I4.

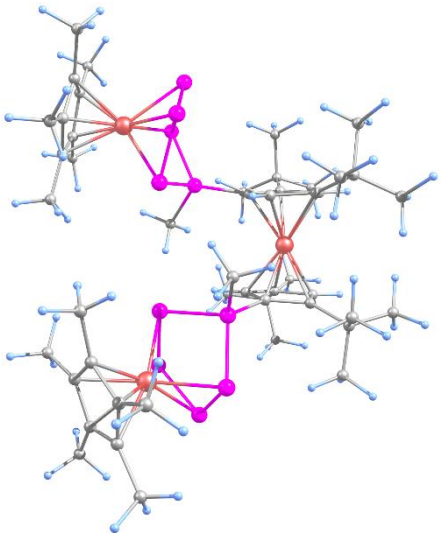

Fe	14.291114039	-18.697759993	17.726124845
C	14.305074770	-17.715445205	19.566069623
H	13.508140930	-17.114875720	19.983563778
C	13.902337994	-20.137754339	16.288957518
H	14.342566094	-21.121271678	16.228969912
C	12.649319513	-19.822129010	16.869157483
C	12.488968910	-18.413327454	16.719555489
H	11.635664756	-17.848727761	17.070362821
C	14.483472000	-18.957455670	15.703088699
C	15.414565339	-17.203005289	18.831657522
C	14.451245719	-19.121555108	19.782106875
C	13.554649912	-17.866414862	15.939579734
C	16.194314336	-18.326475859	18.466156323
H	17.113253684	-18.297994402	17.901355436
C	15.632882165	-19.522825620	19.037959499
C	15.928829936	-15.773823785	18.916995763
C	17.168730839	-15.546496890	18.044386894
H	17.991257276	-16.205395134	18.341976784
H	17.512574249	-14.512843629	18.157807196
H	16.964562430	-15.711753883	16.984028145
C	13.420231153	-16.536847625	15.222415096
C	11.508318271	-20.804497117	17.083013640
C	13.733576547	-19.832284317	20.914747722
C	14.764515993	-15.866872471	14.938850196
H	15.343773914	-15.744440874	15.855545079
H	14.607619135	-14.877943880	14.494285696
H	15.352432803	-16.447896053	14.220728652
C	12.501060345	-15.589396682	16.012302102
H	11.458315890	-15.917220240	15.955883222
H	12.547414743	-14.581324590	15.587052276
H	12.782329282	-15.535427335	17.066264162
C	13.544290164	-21.329768394	20.671809558
H	12.991229430	-21.513079196	19.749117745
H	12.985863111	-21.777376052	21.501329286
H	14.507437104	-21.847709744	20.622144275
C	12.380306744	-19.160796779	21.205589141
H	12.519744991	-18.186035931	21.683549557
H	11.797167351	-19.779510982	21.895799375
H	11.794787599	-19.011074945	20.295585102
C	14.871298230	-14.708214170	18.620156062
H	14.631932345	-14.665271479	17.556703895
H	15.245502341	-13.722743201	18.919798362
H	13.945678533	-14.894184364	19.175394284
C	12.735292372	-16.843562674	13.870589237
H	13.353961954	-17.500079916	13.250790354
H	12.565263708	-15.910484352	13.320133332
H	11.768983136	-17.333694095	14.029600050
C	11.993207856	-22.256061213	17.166440583
H	12.522894793	-22.552994782	16.255061650
H	11.132945385	-22.923855545	17.283588903
H	12.656541698	-22.421805251	18.018333445
C	10.654936043	-20.675740859	15.795770116
H	10.205889377	-19.680020958	15.721046528
H	9.849168686	-21.418805214	15.807359056
H	11.268412314	-20.840879569	14.903608445
C	16.371346503	-15.621472664	20.394499808
H	15.512241465	-15.680082540	21.070846671
H	16.858440067	-14.650109483	20.538976883
H	17.078815685	-16.410532215	20.671141084
C	14.627213074	-19.653804799	22.164405401
H	15.598877485	-20.139729421	22.031602612
H	14.136192369	-20.098150339	23.038477794
H	14.800762194	-18.591595711	22.366658826
C	10.618189322	-20.474358356	18.283232367
H	11.122544053	-20.682534204	19.227907813
H	9.707790219	-21.083517850	18.247793717
H	10.312441164	-19.422569992	18.280919726
Fe	16.811751145	-20.911894591	12.192715185
P	15.910361034	-19.224391042	14.603783249
P	15.770484751	-18.857629629	12.461280929
P	16.593303739	-21.280268996	14.475623652
P	14.515262715	-20.503947069	11.851256869

P	15.065536747	-22.119394294	13.191912580
C	18.063525452	-22.485247840	11.613227824
C	18.862041902	-21.409561288	12.119886693
C	17.640589674	-20.603025472	10.322218499
C	18.602375870	-20.248695544	11.328203063
C	17.302724236	-21.987983554	10.502453414
C	17.393728616	-18.272220327	15.129014757
H	18.074587184	-18.232971716	14.273804015
H	17.887706392	-18.788501720	15.957369781
H	17.118671415	-17.260680670	15.428332946
C	16.382460982	-22.788341930	9.641386368
H	15.871892009	-23.563408769	10.219524272
H	16.936959543	-23.278460941	8.830311931
H	15.612619009	-22.155304921	9.193207218
C	18.074038773	-23.888911623	12.122434216
H	18.196450324	-23.920072670	13.209863918
H	18.902708911	-24.455970507	11.677693115
H	17.141842561	-24.405926029	11.882759681
C	19.848405066	-21.508744533	13.237816221
H	19.936165147	-20.567073779	13.786688231
H	20.842029037	-21.767578683	12.847940318
H	19.557724988	-22.278386986	13.957264750
C	19.288867554	-18.928056770	11.451660598
H	18.616524730	-18.100700574	11.209328702
H	20.145697109	-18.876558595	10.766210544
H	19.670626831	-18.767123366	12.463507653
C	17.140876089	-19.703963034	9.240417484
H	16.135364480	-19.988323072	8.918756100
H	17.801200765	-19.745566073	8.363945410
H	17.098025979	-18.663585987	9.575882901
Fe	19.546264044	-21.948465176	19.611352451
P	16.681165173	-21.010370359	18.978606347
P	17.553573846	-21.835291005	20.796250739
P	18.535428502	-20.781422421	17.876189057
P	19.030892457	-20.326309607	21.244104817
P	19.690098027	-19.627986758	19.297663234
C	20.175794072	-23.596245823	18.476569319
C	20.630669764	-23.329954549	20.733839950
C	19.813636736	-24.031271502	19.788179019
C	21.504537117	-22.455883815	20.002500539
C	21.226488688	-22.625914655	18.603306680
C	15.833109112	-22.430729181	18.171664579
H	16.317770527	-23.350024684	18.512640821
H	15.941005474	-22.346958505	17.085862883
H	14.776812465	-22.449156048	18.439534974
C	19.620814402	-24.119318668	17.191839675
H	18.580049725	-24.436453388	17.300442782
H	20.201040731	-24.986382600	16.848135429
H	19.649762137	-23.360082036	16.405959898
C	20.611221282	-23.528934109	22.213587915
H	20.981325488	-22.645037234	22.738655503
H	21.240726074	-24.382434253	22.498731496
H	19.598123388	-23.726964435	22.576691642
C	18.822548361	-25.097581508	20.118679089
H	18.336440624	-24.912490349	21.079901922
H	19.321590010	-26.074316866	20.176310992
H	18.039574610	-25.172037162	19.359105194
C	21.933445634	-21.959101511	17.469849103
H	21.256624653	-21.786004801	16.626816421
H	22.763819004	-22.580332589	17.108602997
H	22.341045860	-20.990153183	17.769896460
C	22.565234933	-21.585403170	20.590476240
H	22.759933974	-20.715798568	19.957591577
H	23.505176442	-22.141501507	20.703888494
H	22.271679395	-21.213322676	21.575733731

Table S8.11: Optimized cartesian coordinates of **2**-min.

Fe	9.505617711	9.909442773	11.167369239
P	9.736183838	10.086966349	7.975036818
P	9.146434049	8.468573565	9.381772461
P	10.346334655	11.419586773	9.600926835
P	11.769507925	10.201970795	10.664875947
P	10.955789986	8.186124259	10.500787516
C	10.698089555	9.357720965	5.277092294
C	12.148911954	10.398783408	6.765403314
H	12.520408175	10.873289449	7.663855323

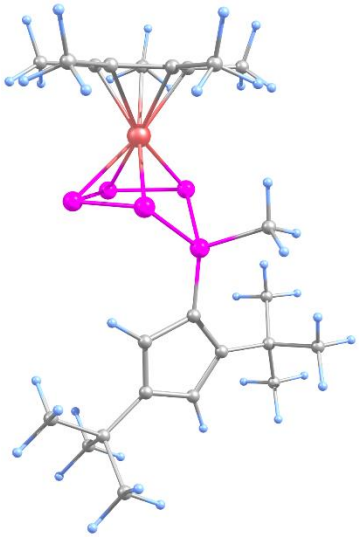

C	8.041370899	11.164885925	11.993331082
C	10.788771332	9.963682903	6.585648314
C	9.486859799	9.825650250	13.222193786
C	12.858603026	10.121567840	5.610052110
C	9.236397428	11.172062817	12.788672012
C	8.439120878	8.993119376	12.699518355
C	11.963613944	9.478972787	4.705096518
H	12.233427177	9.126251111	3.715834014
C	8.063366797	10.775697498	7.563994476
H	7.473091343	10.071882148	6.973065489
H	8.185977751	11.708509050	7.005988430
H	7.546167982	10.969073056	8.509055050
C	9.501283828	8.713436494	4.599934921
C	14.312331862	10.431616008	5.324758555
C	7.551695328	9.824242740	11.939258520
C	9.943106973	7.913629249	3.362394283
H	10.402900115	8.563532826	2.610459948
H	9.073596115	7.428134354	2.901195441
H	10.669291772	7.140909924	3.636314943
C	8.507699810	9.789796312	4.116380534
H	8.177761965	10.425931489	4.939789118
H	7.621234277	9.334905001	3.651219716
H	8.995318098	10.437524961	3.379509004
C	8.793695283	7.726479222	5.543743091
H	9.493847938	6.952604580	5.876123399
H	7.946181106	7.241701518	5.040049622
H	8.409618558	8.208631148	6.445980259
C	7.383560778	12.371816124	11.407171974
H	8.123399744	13.097125710	11.057645188
H	6.745608270	12.867959810	12.152988765
H	6.751465692	12.110590615	10.553563228
C	10.043381232	12.382481100	13.128318299
H	11.082261106	12.116073743	13.341378095
H	9.634404063	12.901380385	14.007138078
H	10.055911201	13.091038245	12.294010839
C	6.292270412	9.370604907	11.276093828
H	6.059072440	9.977545268	10.396213792
H	5.440574656	9.439348468	11.968230979
H	6.373843703	8.333601136	10.939765129
C	10.604843086	9.377635947	14.106032750
H	10.910122735	8.355607104	13.863275524
H	10.313368953	9.406716911	15.165599558
H	11.484462395	10.014038114	13.975600375
C	15.069971746	9.129419675	5.003017261
H	15.013979246	8.439904724	5.852289801
H	16.127619773	9.331689598	4.781753015
H	14.628107122	8.626219144	4.136343972
C	14.979609190	11.100622483	6.532354427
H	14.482821212	12.045474315	6.778825036
H	16.035293213	11.311712462	6.318644568
H	14.927872432	10.454417651	7.415340816
C	8.266708239	7.527629995	12.933712987
H	7.884223129	7.026301697	12.038764616
H	7.562145270	7.336793036	13.756065681
H	9.219475423	7.054140891	13.184968899
C	14.420108290	11.380131096	4.114986026
H	13.963828935	10.929677630	3.226892685
H	15.469699624	11.612214262	3.884191822
H	13.890911711	12.316824008	4.321840518

Table S8.12: Optimized cartesian coordinates of **2**-min.

Fe	9.535918863	10.004729558	11.048758517
P	9.964397048	10.636297013	8.017737248
P	8.993009429	8.965110216	9.041988459
P	10.854531607	11.475765566	9.826476676
P	11.850934291	9.776714705	10.713624692
P	10.585513105	8.083038588	10.204425292
C	7.610714899	11.733867908	6.611662996

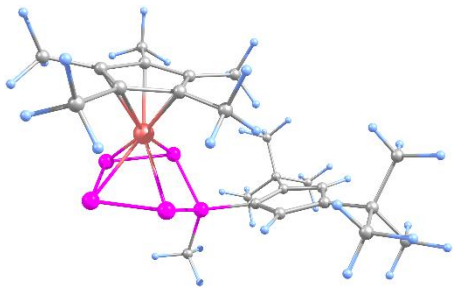

C	8.903676567	13.176420206	7.889271145
H	9.711660092	13.552317304	8.503051765
C	8.516202278	11.562015142	12.038134037
C	8.795166177	11.820466918	7.426489937
C	9.098821953	9.534168488	13.003816566
C	7.833588850	13.905614156	7.387136646
C	9.444018321	10.925495996	12.924598770
C	7.947476316	9.318162542	12.168798569
C	7.047711759	13.015592844	6.608726648
H	6.147356837	13.296054999	6.073374215
C	11.234949675	10.158372648	6.758940797
H	10.772865511	9.670559920	5.897340375
H	11.952138492	9.480593017	7.232589293
H	11.742538018	11.072076120	6.431472712
C	6.972190610	10.541106812	5.912922766
C	7.539298340	15.375064467	7.602312869
C	7.598833634	10.576254905	11.563358166
C	6.159121973	11.011812844	4.692226410
H	5.321999505	11.651393892	4.988231226
H	5.743254772	10.144953353	4.162351901
H	6.790577201	11.578513028	3.998982297
C	6.010082780	9.809072385	6.870464723
H	6.556852313	9.408346303	7.729078212
H	5.504246908	8.974638913	6.363378729
H	5.251796224	10.505916254	7.244890547
C	8.017427926	9.539637211	5.400684662
H	8.740683825	10.041483918	4.747944763
H	7.530584766	8.738412831	4.828934566
H	8.554016787	9.061010030	6.225541985
C	8.457046906	13.015556236	11.698927119
H	9.434966027	13.493455367	11.802708302
H	7.751226240	13.533581016	12.363967933
H	8.129895186	13.165961093	10.664590287
C	10.553753623	11.610145127	13.654146706
H	11.345892130	10.905051139	13.919108925
H	10.189702164	12.081752407	14.578032662
H	11.006909868	12.391085452	13.035578435
C	6.454793448	10.850814436	10.640675944
H	6.748380808	11.532892873	9.834824571
H	5.615056269	11.304399945	11.186835659
H	6.096376164	9.931489895	10.171599115
C	9.777667727	8.510390216	13.854537635
H	9.669153641	7.510475292	13.425804409
H	9.360093236	8.494925926	14.871449309
H	10.849913248	8.713636284	13.931026817
C	7.502252141	16.109444550	6.248539714
H	8.466923357	16.009188812	5.738998126
H	7.283044767	17.178670138	6.380760460
H	6.736137630	15.679386258	5.594769579
C	8.609784177	16.029462027	8.484111269
H	8.661671406	15.540705888	9.463707304
H	8.380195392	17.091059004	8.641682009
H	9.599081731	15.956462190	8.018962053
C	7.213741462	8.029103664	11.992814671
H	6.779368058	7.957681530	10.991026760
H	6.397367724	7.933038613	12.722637700
H	7.884074860	7.173402074	12.117136836
C	6.171830757	15.536196616	8.293851202
H	5.376277400	15.087629522	7.689520828
H	5.929173001	16.596348431	8.454556852
H	6.178183829	15.026753682	9.264190331

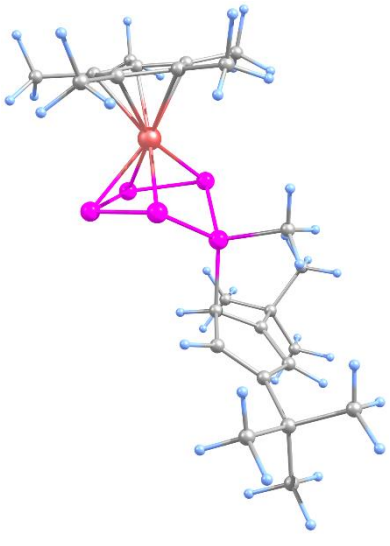

Table S8.13: Optimized cartesian coordinates of **2**.

Fe	8.453332232	11.727663070	10.340205207
P	9.786816203	11.265316890	7.614219498
P	8.033072802	10.357978424	8.514408294
P	10.431102900	12.412036024	9.330544883
P	10.571101608	10.812476859	10.778415914
P	8.977106081	9.438082364	10.230044776

C	10.780284437	9.760733415	5.373579699
C	12.246660952	11.226024221	6.529495677
H	12.744520887	11.748319621	7.335666370
C	7.466105381	13.552684037	10.478056738
C	11.136606679	10.249954225	6.753214192
H	11.368467523	9.455202839	7.474032738
C	7.838005949	12.132431732	12.279086455
C	12.454770801	11.363034325	5.198454645
C	8.294845693	13.330237493	11.632346671
C	6.721594262	11.627477815	11.535457400
C	11.553032082	10.450510421	4.497657365
H	11.539766593	10.323151453	3.421155470
C	9.217024977	12.471414450	6.351984588
H	8.594268302	11.977591442	5.603280405
H	10.090637487	12.914178769	5.865334283
H	8.639802062	13.249481520	6.858637597
C	9.799713091	8.648622614	5.052999236
C	13.446628098	12.260673767	4.498353343
C	6.494197840	12.503634170	10.428393678
C	10.229871749	7.930853568	3.762825277
H	10.180498273	8.595761779	2.894410686
H	9.558891133	7.086979568	3.568910907
H	11.252480410	7.548850822	3.846283092
C	8.381461814	9.212970566	4.837876330
H	7.983777117	9.663069991	5.753092385
H	7.697073030	8.407074545	4.547653376
H	8.382916743	9.965633273	4.041747964
C	9.764671830	7.625143621	6.199521352
H	10.756919983	7.192844539	6.370701457
H	9.076955802	6.809287478	5.951644201
H	9.416468117	8.076681264	7.134711627
C	7.533574073	14.728427511	9.559343099
H	8.561709083	15.075548258	9.427322146
H	6.943742071	15.565599617	9.956856956
H	7.131823829	14.483780647	8.572190074
C	9.389999150	14.222715258	12.115274072
H	10.194890839	13.647004145	12.581629506
H	9.011247018	14.936242749	12.858827285
H	9.828559000	14.796073477	11.294178020
C	5.381621591	12.384788076	9.439923667
H	5.661113574	12.795863553	8.466261701
H	4.498158128	12.931334865	9.795896512
H	5.090891208	11.342615645	9.285551005
C	8.373503783	11.558111188	13.548982542
H	8.314847027	10.466231105	13.547668353
H	7.801885641	11.926434664	14.411077861
H	9.421592471	11.829626149	13.694857919
C	14.399015314	11.396293879	3.651145624
H	14.942229060	10.686777340	4.283904837
H	15.130065497	12.031719877	3.138197546
H	13.857139625	10.824917730	2.890507958
C	14.267710158	13.069497949	5.507620537
H	13.624116811	13.703829661	6.126734997
H	14.976180616	13.718006409	4.981096213
H	14.839612651	12.411204181	6.170122203
C	5.894637794	10.434632870	11.887481459
H	5.534747937	9.916177817	10.994091490
H	5.016830139	10.736131473	12.474463742
H	6.465558810	9.714461386	12.477663948
C	12.683584030	13.230398289	3.576184721
H	12.079537748	12.692242190	2.838135281
H	13.387736421	13.872087240	3.034112432
H	12.014387977	13.874061829	4.157692517

Table S8.14: Optimized cartesian coordinates of **2**.

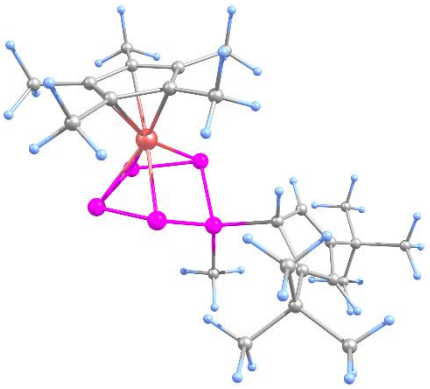

Fe	8.662597217	11.385297942	10.412853803
P	9.412830258	11.714845048	7.425259641
P	10.146305073	12.723193305	9.204682875
P	7.837301540	10.577201248	8.399031928
P	6.758929112	12.210984272	9.315341823
P	8.305312367	13.638745400	9.866621581
C	10.620920286	9.891123047	5.542379676
C	11.998799554	11.475832090	6.659146864

H	12.407782034	12.108100799	7.435791176
C	9.360031516	9.614591559	11.250082295
C	10.811844771	10.581688561	6.879245139
H	10.944976848	9.878159990	7.713124668
C	7.893475080	11.073274236	12.309814580
C	12.391955231	11.392026041	5.370072952
C	7.978970633	9.834675520	11.587626528
C	9.219636525	11.605785890	12.430849952
C	11.545438487	10.405495569	4.697965219
H	11.684123316	10.097426058	3.668244128
C	9.023396131	12.737065096	5.949706495
H	8.497710004	12.137730922	5.202122461
H	9.953166670	13.129540925	5.525687028
H	8.383933821	13.560288980	6.279445079
C	9.663856863	8.751060662	5.246546565
C	13.515805007	12.132606536	4.686273624
C	10.119515571	10.704968774	11.779568969
C	10.174346938	7.934730850	4.047909354
H	10.178363948	8.527576215	3.127345610
H	9.514560448	7.076380171	3.882268658
H	11.188659413	7.561932627	4.224938682
C	8.257350585	9.275286244	4.894794052
H	7.800064065	9.814524679	5.729354981
H	7.597097087	8.435149021	4.649742703
H	8.301634663	9.938807291	4.024093774
C	9.571604999	7.818049330	6.466300028
H	10.558824023	7.421638735	6.730855286
H	8.912052412	6.972144372	6.243003646
H	9.158276884	8.336530221	7.337131994
C	9.917771819	8.407388104	10.570514719
H	9.187896980	7.957918992	9.892481717
H	10.204901980	7.644950174	11.307594578
H	10.809121402	8.652577674	9.985638122
C	6.846398707	8.904892049	11.301001530
H	5.909443157	9.451117287	11.158845386
H	6.703046855	8.198098557	12.129007814
H	7.028168413	8.323485420	10.392791579
C	11.605597035	10.842196926	11.730161989
H	12.024101299	10.376978592	10.833567419
H	12.060118106	10.358365290	12.605031189
H	11.911642814	11.891315639	11.730070998
C	6.659253350	11.663659179	12.907915377
H	6.690936213	12.756560556	12.887252719
H	6.548385410	11.348780478	13.954066376
H	5.765041465	11.351351602	12.363256482
C	14.537162008	11.111910606	4.150313742
H	14.954353671	10.516450621	4.969121720
H	15.360364390	11.630028256	3.645258453
H	14.079976481	10.425589196	3.430226542
C	14.219002361	13.086123976	5.656922849
H	13.522434487	13.830556289	6.057793299
H	15.025231175	13.619879598	5.142472828
H	14.658895168	12.540140540	6.498380127
C	9.606437256	12.850115226	13.160639770
H	10.461771535	13.342395120	12.688990472
H	9.884008711	12.618045962	14.197552074
H	8.784211161	13.568910057	13.181890644
C	12.938868896	12.941080922	3.509178845
H	12.435908525	12.291906333	2.784683220
H	13.741415385	13.473096814	2.985572988
H	12.212861533	13.680949458	3.863351405

Table S8.15: Optimized cartesian coordinates of **2**-I3.

Fe	8.571943009	11.398424648	10.497474930
P	9.797058274	11.502675732	7.645102563
P	10.327130453	12.540380543	9.477340282
P	8.038350565	10.483136829	8.412957692
P	6.931820223	12.230848520	9.042663352
P	8.467120778	13.612614574	9.747306157
C	12.409807089	10.069529154	7.731849139
C	10.490462440	8.828657516	7.072936508
H	9.524331570	8.583121746	6.653506202
C	8.917335037	9.631479562	11.541503272
C	11.063464634	10.217784696	7.049641142
H	11.238268313	10.526270886	6.005914607
C	7.552189853	11.354302626	12.290004450

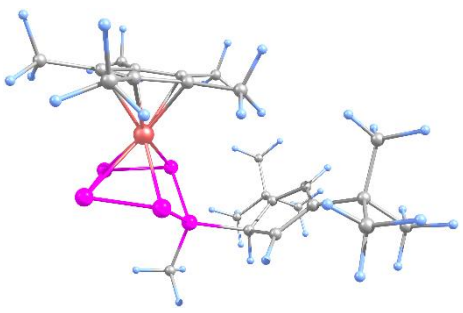

C	11.365165539	7.988629656	7.666698031
C	7.550614009	10.051685013	11.680885730
C	8.917061933	11.723199310	12.539446924
C	12.535139152	8.767188648	8.076142665
H	13.420506425	8.332171918	8.528218002
C	9.526341290	12.539021388	6.145322790
H	9.166407162	11.905711738	5.326572031
H	10.456111696	13.036048823	5.850409535
H	8.768002015	13.289224222	6.383278417
C	13.529353731	11.099200801	7.783205296
C	11.280024797	6.481844905	7.766698510
C	9.753594614	10.658777313	12.076614365
C	14.761001396	10.519327524	7.054235653
H	15.126069787	9.614376247	7.548629700
H	15.575158386	11.253581669	7.046912381
H	14.516751573	10.263204686	6.017558442
C	13.916310909	11.392998192	9.244180422
H	13.076243387	11.833348988	9.788655267
H	14.758146752	12.094697936	9.278939644
H	14.215485032	10.473767902	9.758735410
C	13.150418234	12.411668023	7.084663766
H	12.894876625	12.245519206	6.031271326
H	14.003085498	13.098806293	7.108519039
H	12.316403054	12.915831246	7.582518166
C	9.402774722	8.331272311	10.996307940
H	8.683025693	7.894973671	10.298827484
H	9.576559484	7.607889982	11.805309531
H	10.341495034	8.467804539	10.452823933
C	6.345674715	9.250803106	11.312043617
H	5.505100895	9.896962662	11.044375044
H	6.029802350	8.612861399	12.148041925
H	6.547341506	8.601948815	10.454809845
C	11.240563853	10.589406118	12.195670968
H	11.681917139	10.030208522	11.365520058
H	11.522751292	10.087119365	13.130873533
H	11.693295719	11.584455255	12.201880255
C	6.348441852	12.151010496	12.670960879
H	6.539783499	13.224287645	12.585866027
H	6.055125796	11.940536268	13.707976541
H	5.499013224	11.917827554	12.024251039
C	12.306067888	5.891077554	6.777208101
H	12.090470219	6.220006292	5.755350431
H	12.271583966	4.795650278	6.805386624
H	13.325442127	6.205009448	7.026692396
C	9.879136160	5.985586701	7.394874988
H	9.118947590	6.429795300	8.046814025
H	9.825404807	4.896449791	7.498672591
H	9.629212037	6.234871366	6.358180099
C	9.385785950	12.968513219	13.217133024
H	10.336366704	13.318811134	12.803526619
H	9.535085088	12.790584729	14.290510613
H	8.661434595	13.778803808	13.106183318
C	11.627227912	5.996933116	9.184118316
H	12.609114208	6.356726483	9.508654290
H	11.650757464	4.901503134	9.206024074
H	10.883784915	6.332621531	9.911604697

Table S8.16: Optimized cartesian coordinates of [{Cp*Fe(η^4-P_5Me(2,4-*t*$Bu_2C_5H_2$))}$_2$Fe]$^{2+}$ (**7**) in the singlet spin state, at the r^{2}SCAN-3c level of theory.

Fe	5.522197446	11.139072403	0.870865058
C	5.227668111	11.190036158	-1.215345826
H	4.861627931	12.028940854	-1.787137904
C	4.409331458	12.116085367	2.441460450
C	6.600621904	10.916017761	-0.968815063
C	5.252819733	11.093347140	2.964704918
H	4.890357943	10.257996632	3.544004719
C	6.628563810	9.737941841	-0.177750245
H	7.513710530	9.247437424	0.203905413
C	5.296201195	13.018399016	1.724893002
C	5.280264925	9.259925107	0.016660538
C	2.991874219	12.313242173	2.961409689

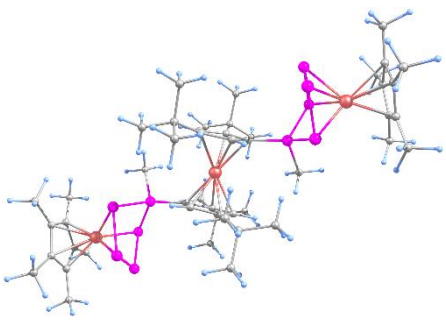

C	6.623189214	11.359835881	2.698454860
C	4.387332782	10.168198412	-0.684141881
C	7.762340272	11.571616586	-1.684882686
C	6.645475559	12.535492963	1.903235697
H	7.527349484	13.022534058	1.509706204
C	7.791903935	10.701578484	3.400737784
C	2.061553632	13.030650115	1.983584565
H	1.911256020	12.443263749	1.075290996
H	2.431532475	14.025153699	1.716654705
H	1.082453241	13.180819808	2.449139678
C	2.042134881	9.267424222	-0.189325674
H	2.411810144	8.272217894	0.075279280
H	1.055761306	9.120311065	-0.640310295
H	1.907699339	9.858456977	0.718989233
C	2.961179163	9.978553071	-1.182266869
C	2.356100521	10.971776815	3.356871175
H	1.308615874	11.130003563	3.629933641
H	2.847363888	10.522152886	4.225097677
H	2.385708444	10.257723045	2.531774296
C	3.123556436	13.158711209	4.249312532
H	3.530782304	14.151046395	4.041201832
H	3.776564203	12.665055494	4.976154411
H	2.136017399	13.286383487	4.705459029
C	3.068025751	9.132235342	-2.471699047
H	3.712799594	9.621543056	-3.208779684
H	2.072880438	9.010349173	-2.912590068
H	3.472352358	8.137546477	-2.269222627
C	2.326837325	11.323648224	-1.567114812
H	2.372963193	12.036276456	-0.741310720
H	1.274387608	11.171732056	-1.824200960
H	2.807421432	11.771766841	-2.442064951
C	9.071818936	11.496796749	-0.898159586
H	9.340518800	10.465388384	-0.649706901
H	9.018625724	12.075267403	0.027127284
H	9.886449205	11.906438817	-1.503387259
C	7.925519517	10.766049096	-2.995781350
H	8.738294712	11.192689077	-3.592600682
H	7.009425252	10.791900755	-3.594934564
H	8.167190857	9.719151665	-2.784485513
C	7.460844691	13.031679347	-2.032439318
H	7.290881289	13.626272805	-1.128326142
H	6.591585774	13.125720487	-2.691880392
H	8.313291901	13.471744091	-2.559104278
C	7.970219997	11.504005810	4.711509433
H	8.208974786	12.551495994	4.499869046
H	8.790466572	11.076462071	5.297345963
H	7.061414522	11.476361966	5.321652632
C	7.493356956	9.240800357	3.748095598
H	6.628849098	9.145329294	4.413593460
H	8.349673754	8.800496887	4.268329556
H	7.317940198	8.647616369	2.844098659
C	9.092654086	10.776816756	2.599768757
H	9.028316260	10.200358921	1.673918926
H	9.913573716	10.365024419	3.194904220
H	9.359300686	11.808565131	2.350597908
Fe	5.879702944	4.697210329	0.037198851
P	5.065926718	7.575091433	0.685068426
P	4.071259780	6.047080016	-0.540158700
P	6.942675166	6.510294559	1.045719028
P	5.592426654	5.790643437	-2.041517307
P	7.473260261	6.090221830	-1.006120876
C	7.163341596	2.992036456	0.066991473
C	5.171413690	3.138300194	1.245476183
C	6.081890244	2.765148162	-0.849955800
C	4.850032514	2.852019342	-0.120449552
C	6.602847970	3.232770793	1.362097459
C	4.183905369	7.601859090	2.292638687
H	3.252316751	8.165236675	2.210578481
H	4.825754815	8.062065975	3.046863000
H	3.963869140	6.569773473	2.582492120
C	8.615091848	2.875982570	-0.245536098
H	8.827230523	3.111872082	-1.290221244
H	8.945342158	1.845382924	-0.061913201
H	9.221966463	3.533397201	0.381543719
C	3.492375871	2.597131877	-0.678504868
H	2.709915921	3.068417344	-0.079906275
H	3.294974204	1.517986915	-0.694709020
H	3.400446795	2.961824245	-1.705383961

C	6.224953729	2.370284045	-2.279016853
H	5.339157288	2.622896941	-2.865116235
H	6.366894827	1.283492745	-2.340133479
H	7.090573491	2.841993061	-2.750067995
C	4.196325416	3.280881566	2.363033170
H	4.583453610	3.922097098	3.158790163
H	3.998073697	2.296682389	2.808481723
H	3.238915077	3.681999494	2.021206334
C	7.376104035	3.405791447	2.625296427
H	8.327651711	3.913488993	2.451115534
H	7.599186527	2.422934228	3.059088108
H	6.818989366	3.978801436	3.369728510
Fe	5.938190123	17.577559732	1.723192622
P	5.080778710	14.704722691	1.061605589
P	6.953850944	15.764623524	0.668471828
P	4.125055655	16.240120783	2.308995414
P	7.533139620	16.155901725	2.713713279
P	5.673149634	16.463274996	3.789147006
C	6.693371064	19.053754044	0.426472999
C	5.260963703	19.153171926	0.520945059
C	7.233328926	19.277433408	1.733045679
C	6.137982328	19.500213558	2.634939278
C	4.917970637	19.425764005	1.885121328
C	4.167306268	14.688764510	-0.528742889
H	3.949000093	15.723542422	-0.810329627
H	3.233338308	14.131964328	-0.430824588
H	4.790803630	14.227387698	-1.297657921
C	8.679990408	19.386286657	2.071359766
H	8.875108192	19.126846174	3.113776203
H	9.012182959	20.420967105	1.916566120
H	9.296917731	18.743247069	1.439491809
C	3.553336463	19.685138958	2.424381852
H	2.776604206	19.227728428	1.807933144
H	3.364515244	20.765565483	2.451102419
H	3.442053874	19.308534669	3.445061315
C	4.303679552	19.024651520	-0.613550406
H	4.696272091	18.379909169	-1.403831620
H	4.125245604	20.012152300	-1.060189042
H	3.335706098	18.634990958	-0.288835239
C	7.487309077	18.888865103	-0.824873326
H	8.426766784	18.361885879	-0.641877071
H	7.735320944	19.874721264	-1.237735073
H	6.934451158	18.337873379	-1.588762111
C	6.259929588	19.882002818	4.069423487
H	5.364835735	19.625978964	4.639726774
H	6.402604984	20.968036980	4.142073563
H	7.117518789	19.404795375	4.549338925

Table S8.17: Optimized cartesian coordinates of [{Cp*Fe(η^4-P_5Me(2,4-*t*$Bu_2C_5H_2$))}$_2$Fe]$^{2+}$ (**7**) in the triplet spin state, at the r^{2}SCAN-3c level of theory.

Fe	5.552391153	11.143532526	0.857043885
C	5.214691253	11.205159518	-1.209955014
H	4.844596468	12.043570473	-1.780000500
C	4.451674282	12.106002312	2.421593102
C	6.590604407	10.929848343	-0.975618365
C	5.307372525	11.092297128	2.938983399
H	4.956261513	10.261849168	3.531982110
C	6.625748632	9.747450134	-0.188150674
H	7.513477423	9.250617842	0.179111932
C	5.324764334	13.016334217	1.697144509
C	5.273042074	9.273995208	0.018713353
C	3.033260353	12.285848362	2.941991367
C	6.673126250	11.357831396	2.644462674
C	4.374551282	10.190923290	-0.667943590
C	7.742005483	11.580436239	-1.714869143
C	6.681503037	12.535116027	1.848540810
H	7.555396697	13.026475450	1.442900839
C	7.851280418	10.706006101	3.338809015
C	2.101258277	12.994711688	1.959626783
H	1.998259430	12.425863496	1.033242049
H	2.445314198	14.007232574	1.725385643
H	1.105932888	13.102496656	2.402123761
C	2.012519532	9.322860818	-0.167973054
H	2.398335559	8.358679252	0.177840419

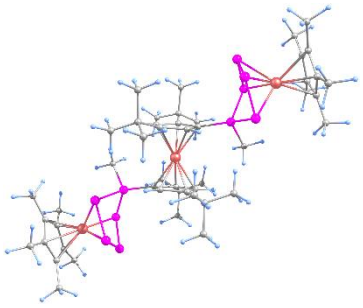

H	1.047531846	9.118135112	-0.642593899
H	1.829430534	9.966210914	0.695059245
C	2.949738108	9.993343858	-1.172023657
C	2.418899955	10.929861582	3.322170469
H	1.360531713	11.058687049	3.568220795
H	2.901887888	10.494652068	4.202396575
H	2.494660250	10.218844903	2.497304234
C	3.139048056	13.125668628	4.234519535
H	3.530184481	14.126436082	4.033678434
H	3.797311076	12.640981797	4.962648568
H	2.146803754	13.234904478	4.685704999
C	3.060001501	9.105681410	-2.432841916
H	3.732465792	9.555491628	-3.170401234
H	2.071434557	8.992761645	-2.890974858
H	3.435323378	8.107762885	-2.193555901
C	2.325847322	11.326604302	-1.614598258
H	2.374199254	12.076541668	-0.822734573
H	1.272736304	11.171036316	-1.867623424
H	2.814087482	11.730286578	-2.506655941
C	9.068479313	11.488702036	-0.959520057
H	9.333179784	10.452607279	-0.726103480
H	9.039978946	12.057602426	-0.027393153
H	9.873353756	11.897028424	-1.578882699
C	7.870980690	10.792654823	-3.039101958
H	8.673073203	11.219061868	-3.650783410
H	6.940697243	10.833018693	-3.615180889
H	8.108230686	9.741001852	-2.846296133
C	7.444438248	13.047379804	-2.037940122
H	7.289120527	13.629277288	-1.122957495
H	6.565140630	13.154026368	-2.682087251
H	8.290849303	13.491311260	-2.571467513
C	8.037508939	11.498905413	4.653011667
H	8.269861374	12.548860843	4.445507413
H	8.863646811	11.072569162	5.231829992
H	7.132527359	11.464660842	5.268623562
C	7.563287592	9.241113813	3.678860547
H	6.705635926	9.137732280	4.352148673
H	8.426639831	8.799075482	4.186230216
H	7.377896877	8.656022648	2.771693829
C	9.145823078	10.790377060	2.529194117
H	9.077429761	10.216954843	1.601825788
H	9.974121235	10.382264142	3.117008153
H	9.403620738	11.824692291	2.280781379
Fe	5.862125613	4.659929691	0.027443952
P	5.055328372	7.602124799	0.682338881
P	4.052097389	6.049165869	-0.510271419
P	6.925777062	6.507616975	1.019789872
P	5.546473091	5.758168019	-2.038332671
P	7.442142940	6.057066504	-1.027071049
C	7.122249601	3.046430192	0.686020523
C	4.798750716	3.018720414	0.801531456
C	6.613486101	2.715765383	-0.610903431
C	5.179763539	2.709761748	-0.545675772
C	6.003678797	3.231055329	1.563103017
C	4.204555144	7.595610509	2.306805292
H	3.251861432	8.125791026	2.250414022
H	4.848035680	8.077859074	3.045953769
H	4.027129991	6.556325702	2.600620189
C	8.556783603	3.117088371	1.079929027
H	9.198396667	3.367070455	0.232179960
H	8.884075589	2.145020538	1.470073472
H	8.723655243	3.858077832	1.866267857
C	4.249125214	2.349264681	-1.651098735
H	3.303419783	2.893046974	-1.578636806
H	4.016379581	1.277744613	-1.605522783
H	4.685896761	2.553439009	-2.630825299
C	7.428895022	2.389931334	-1.813425056
H	6.924397980	2.678295158	-2.738420392
H	7.599074125	1.306223185	-1.852499889
H	8.405211467	2.878228508	-1.788350368
C	3.410980022	2.982070058	1.346659610
H	3.290435618	3.651107158	2.202008875
H	3.179948287	1.965461682	1.689660724
H	2.669766429	3.254014909	0.592225106
C	6.077380057	3.472793244	3.033004418
H	6.981879794	4.017223042	3.311821153
H	6.091220298	2.510547992	3.560930778
H	5.212215070	4.030898520	3.398981665

Fe	5.951880654	17.610294275	1.758046578
P	5.084451202	14.692230808	1.055741709
P	6.944668718	15.784335742	0.658897603
P	4.146765946	16.224552811	2.326052727
P	7.555936024	16.160484379	2.696093406
P	5.708044368	16.447063930	3.797743076
C	6.185206407	19.091905067	0.286344957
C	4.934099448	19.276824335	0.977871279
C	7.243821798	19.245217507	1.240614813
C	6.650216913	19.533440310	2.513806132
C	5.225435469	19.542207886	2.355648752
C	4.156275976	14.717234988	-0.525264263
H	3.954794833	15.758946538	-0.794203082
H	3.212838403	14.176900801	-0.425727317
H	4.764586677	14.251952515	-1.304162083
C	8.701132960	19.198686505	0.936394220
H	9.290945189	18.935493971	1.816906710
H	9.039938041	20.182520593	0.588018349
H	8.925625071	18.476408673	0.146940088
C	4.222985527	19.851217079	3.412919019
H	3.278844441	19.328871932	3.238612253
H	4.007391004	20.927227934	3.417922678
H	4.584845171	19.580768778	4.407409834
C	3.583914287	19.318666208	0.345412807
H	3.528787430	18.681737269	-0.540597224
H	3.362720366	20.344517915	0.023935677
H	2.798149466	19.012175565	1.038905196
C	6.352115389	18.911322162	-1.184800686
H	7.283018161	18.395241667	-1.428169715
H	6.376822296	19.893723389	-1.673597855
H	5.524251616	18.349078283	-1.623611122
C	7.388469069	19.818629064	3.774785019
H	6.811058949	19.536031964	4.657581814
H	7.590114643	20.895682179	3.839991344
H	8.348843440	19.299936423	3.810321682

9 References

1 *omics.pnl.gov/software/molecular-weight-calculator*.

2 O. J. Scherer and T. Brück, *Angew. Chem. Int. Ed. Engl.*, 1987, **26**, 59.

3 C. Riesinger, G. Balázs, M. Bodensteiner and M. Scheer, *Angew. Chem. Int. Ed.*, 2020, **59**, 23879.

4 L. Dütsch, M. Fleischmann, S. Welsch, G. Balázs, W. Kremer and M. Scheer, *Angew. Chem. Int. Ed.*, 2018, **57**, 3256.

5 *CrysAlisPRO, Oxford Diffraction /Agilent Technologies UK Ltd, Yarnton, Oxfordshire, England*, 2014.

6 O. V. Dolomanov, L. J. Bourhis, R. J. Gildea, J. A. K. Howard and H. Puschmann, *J. Appl. Crystallogr.*, 2009, **42**, 339.

7 G. M. Sheldrick, *Acta Cryst. A*, 2015, **71**, 3.

8 G. M. Sheldrick, *Acta Cryst. C*, 2015, **71**, 3–8.

9 D. F. Evans, *J. Chem. Soc.*, 1959, 2003.

10 G. A. Bain and J. F. Berry, *J. Chem. Educ.*, 2008, **85**, 532.

11 A. S. Baranski, W. R. Fawcett and C. M. Gilbert, *Anal. Chem.*, 1985, **57**, 166.

12 a) F. Barrière, N. Camire, W. E. Geiger, U. T. Mueller-Westerhoff and R. Sanders, *J. Am. Chem. Soc.*, 2002, **124**, 7262; b) F. Barrière and W. E. Geiger, *J. Am. Chem. Soc.*, 2006, **128**, 3980; c) A. Hildebrandt, D. Miesel and H. Lang, *Coord. Chem. Rev.*, 2018, **371**, 56; d) A. Hildebrandt, D. Miesel, Q. Yuan, J. Freytag, J. Mahrholdt and H. Lang, *Dalton Trans.*, 2019, **48**, 13162;

13 P. Sahay, E. Crovini, K. Stavrou, Z. Zhang, B. M. Nguyên, D. Wagner, P. Strohriegl, S. Bräse, A. Monkman, E. Zysman-Colman and W. Brütting, *J. Mater. Chem. C*, 2024, **12**, 11041.

14 J. H. L. Ong, C. Nataro, J. A. Golen and A. L. Rheingold, *Organometallics*, 2003, **22**, 5027.

15 a) G. Pilloni, B. Longato and B. Corain, *J. Organomet. Chem.*, 1991, **420**, 57; b) C. Nataro, A. N. Campbell, M. A. Ferguson, C. D. Incarvito and A. L. Rheingold, *J. Organomet. Chem.*, 2003, **673**, 47;

16 a) R. Prins and A. R. Korswagen, *J. Organomet. Chem.*, 1970, **25**, C74-C76; b) W. H. Morrison and D. N. Hendrickson, *Inorg. Chem.*, 1975, **14**, 2331;

17 M. Krejčik, M. Daněk and F. Hartl, *J. Electroanal. Chem.*, 1991, **317**, 179.

18 M. B. Robin and P. Day, *Adv. Inorg. Chem. Radiochem.*, 1967, **10**, 247-422.

19 a) E. Bill, 2019; b) E. Bill, 2019;

20 a) F. Neese, *WIREs Comput. Mol. Sci.*, 2012, **2**, 73; b) F. Neese, *WIREs Comput. Mol. Sci.*, 2018, **8**, e1327; c) F. Neese, *WIREs Comput. Mol. Sci.*, 2022, **12**, e1606;

21 S. Grimme, A. Hansen, S. Ehlert and J.-M. Mewes, *J. Chem. Phys.*, 2021, **154**, 064103.

22 a) A. Najibi and L. Goerigk, *J. Chem. Theory Comput.*, 2018, **14**, 5725; b) A. Najibi and L. Goerigk, *J. Comput. Chem.*, 2020, **41**, 2562;

23 a) F. Weigend and R. Ahlrichs, *Phys. Chem. Chem. Phys.*, 2005, **7**, 3297; b) F. Weigend, *Phys. Chem. Chem. Phys.*, 2006, **8**, 1057; c) A. Hellweg, C. Hättig, S. Höfener and W. Klopper, *Theor. Chem. Acc.*, 2007, **117**, 587;

24 B. Helmich-Paris, B. de Souza, F. Neese and R. Izsák, *J. Chem. Phys.*, 2021, **155**, 104109.